The Dissertation Committee for Wesley Joseph Cole certifies that this is the approved version of the following dissertation:

Dynamic Modeling, Optimization, and Control of Integrated Energy Systems in a Smart Grid Environment

Committee:

Thomas Edgar, Supervisor

Michael Baldea

Roger Bonnecaze

Gregor Henze

David Morton

Atila Novoselac

Dynamic Modeling, Optimization, and Control of Integrated Energy Systems in a Smart Grid Environment

by

Wesley Joseph Cole, B.S.

Dissertation

Presented to the Faculty of the Graduate School of

The University of Texas at Austin

in Partial Fulfillment

of the Requirements

for the Degree of

Doctor of Philosophy

The University of Texas at Austin

May 2014

Dedication

To my beautiful wife Cassie

Acknowledgements

My primary thanks goes to my wife, Cassie, for her unfailing support, encouragement, and skill. She made it possible for me to balance work and home life, and she serves as a magnificent mother to our three little boys. She has also been incredibly valuable in teaching me to be a better writer. We spent many long hours in front of the computer while she patiently taught me how my writing could be improved.

I have been tremendously blessed to have worked under my adviser, Dr. Thomas Edgar. He is a man of integrity, and he values people for who they are and what they can become. He has been very generous to me in terms of both support and opportunity, and my graduate education would not be what it is without that generosity. Because one of my primary modes of learning is observation, watching him interact with other in both professional and personal settings was an education in its own right.

My Ph.D. committee members have been very helpful. I have done collaborative work with most of the members of my committee, and received valuable input from all of them.

Though not a member of my committee, Dr. Michael Webber has enhanced my education as well. Like with Dr. Edgar, observing him has taught me to think more broadly and to invest in those things that matter most.

My research group has been instrumental in helping me bounce around ideas and solve research issues. I was fortunate enough to join the Edgar group a year after Kody Powell. His friendship and expertise were invaluable as I progressed through my graduate studies. Jong Kim, Krystian Perez, Kriti Kapoor, Matt Walters, Abby Ondeck, Bo Lu, Shu Xu, Akshay Sriprasad, and Cara Touretzky have been valuable associates and friends. I'm grateful to have worked with them.

The IGERT research group provided an interdisciplinary environment that helped me learn and develop new ideas. I am grateful to have been an affiliate, and I developed collaborations that would never have happened without the IGERT program. This program connected me with Josh Rhodes, Charlie Upshaw, Robert Fares, and Dave Tuttle. All of these people have provided me with ideas, sounding boards, and examples of high quality research work. Special thanks go to Josh and Dave for bouncing around ideas, providing extra insights, and showing examples of integrity and hard work.

Elaine Hale served as my mentor during my internship at NREL. She continued to support my research work after I left NREL, and has been supportive in helping to prepare me for postdoctoral opportunities.

Sarah De Berry-Caperton, and more recently Kristine Poland, have made the graduate experience much smoother. Their work allowed me to focus more time on my education.

My work would not have been possible without the financial support provided by the Cockrell School of Engineering, Pecan Street, Inc. (through a grant from the Department of Energy), and the National Science Foundation.

Dynamic Modeling, Optimization, and Control of Integrated Energy Systems in a Smart Grid Environment

Wesley Joseph Cole, Ph.D.

The University of Texas at Austin, 2014

Supervisor: Thomas F. Edgar

This work considers how various integrated energy systems can be managed in order to provide economic or energetic benefits. Energy systems can gain additional degrees of freedom by incorporating some form of energy storage (in this work, thermal energy storage), and the increasing penetration of smart grid technologies provides a wealth of data for both modeling and management.

Data used for the system models here come primarily from the Pecan Street Smart Grid Demonstration Project in Austin, Texas, USA. Other data are from the Austin Energy Mueller Energy Center and the University of Texas Hal C. Weaver combined heat and power plant. Systems considered in this work include thermal energy storage, chiller plants, combined heat and power plants, turbine inlet cooling, residential air conditioning, and solar photovoltaics. These systems are modeled and controlled in integrated environments in order to provide system benefits. In a district cooling system with thermal energy storage, combined heat and power, and turbine inlet cooling, model-based optimization strategies are able to reduce peak demand and decrease cooling electricity costs by 79%.

Smart grid data are employed to consider a system of 900 residential homes in Austin. In order to make the system model tractable for a model predictive controller, a

reduced-order home modeling strategy is developed that maps thermostat set points to air conditioner electricity consumption. When the model predictive controller is developed for the system, the system is able to reduce total peak demand by 9%.

Further work with the model of 900 residential homes presents a modified dual formulation for determining the optimal prices that produce a desired result in the residential homes. By using the modified dual formulation, it is found that the optimal pricing strategy for peak demand reduction is a critical peak pricing rate structure, and that those prices can be used in place of centralized control strategies to achieve peak reduction goals.

Table of Contents

List of Tables

List of Figures

Chapter 1: Introduction

In 2008 the National Academy of Engineering announced fourteen grand challenges for engineering for the 21st century. The first three grand challenges dealt directly with sustainable energy: solar, fusion, and carbon sequestration [1]. Clearly, the need to manage energy systems in a sustainable manner will be an important part of the development of future energy systems.

In the electrical system, one of the challenges is the constant need to match supply with demand. Engineers have largely been successful in addressing this challenge, but new difficulties relating to sustainability have arisen. For example, renewable energy systems such as wind and solar are intermittent and nondispatchable. Additionally, climate science has shown how the fossil fuel backbone of the electric grid might be driving significant and costly climate changes. The smart grid aims to provide a platform for addressing these and other issues through enhanced communication, information, and control.

Because of the new information available through the smart grid infrastructure, facilities that were once reactive can become proactive. For example, buildings have traditionally been blind consumers of electricity, but with smart grid technologies, they can now respond to signals to improve overall grid management. The smart grid provides additional degrees of freedom for managing energy systems, and data made available through smart meters make it easier to create accurate models of grid systems. This combination provides a rich environment for model-based optimization and control of energy systems that are connected to the grid.

The work presented here focuses on how energy systems with thermal energy storage (TES) technologies can be harnessed in a smart grid environment to provide grid

benefits. As the name implies, TES stores thermal, rather than electrical or chemical energy. By so doing, it can integrate with cooling systems, such as chiller networks, to manage electricity consumption. Thermal storage has become an increasingly popular technology. For example, the utility that provides power to New York City, Consolidated Edison (or ConEdison), recently proposed new incentives for TES. ConEdison is offering $2600/kW for TES, which is more than for batteries ($2100/kW), demand response ($800/kW), equipment improvements ($800-1250/kW), or combined heat and power plants ($1150-2150/kW) [2].

Incorporating storage into an energy system increases the degrees of freedom of that system. By implementing optimization or advanced control schemes, such as model predictive control, those extra degrees of freedom can be utilized to improve the economic or energetic performance of the system. This work investigates how the integration of energy systems with thermal energy storage can be managed by predictive, optimization-based control schemes in order to provide grid benefits.

Because this work considers various configurations of thermal energy storage, Chapter 2 will provide an introduction and literature review of the optimization and control of thermal storage systems. Chapter 3 investigates how chilled water thermal energy storage can enhance the flexibility of a small campus in meeting its cooling loads. Chapter 4 considers a larger campus of buildings, and integrates a combined heat and power plant with turbine inlet cooling, as well as thermal energy storage. Chapter 5 presents a method for developing a linear, reduced-order model for residential homes, and demonstrates how the model can be used in a model predictive control framework. Chapter 6 extends the work in Chapter 5 to a community of 900 residential homes and investigates how the thermal mass of the homes can be used as thermal storage to shape the community's energy consumption. Chapter 7 builds on Chapter 6 by considering the

combined effects of air conditioning thermostat control with solar photovoltaic generation. Chapter 8 uses the community model presented in Chapter 6 to find the optimal electricity prices that lead to peak demand reduction.

Each chapter contains its own introduction and conclusion. Chapter 9 then summarizes the conclusions of the entire work and presents some directions for future research.

Elements of Chapters 2-8 have been published or submitted for publication. Chapter 2 was published in *Reviews in Chemical Engineering* [3], Chapters 3 and 7 were presented as conference papers in the American Control Conference [4], [5], Chapter 4 was published in the *International Journal of Energy Research* [6], initial concepts for Chapter 5 were presented at the American Control Conference [7], and later developments of the chapter were published in *Energy & Buildings* [8], and Chapters 7 and 8 have been submitted to *Applied Energy* and *Journal of Process Control*, respectively [9], [10].

Chapter 2: Optimization and Advanced Control of Energy Systems with Thermal Energy Storage[1]

INTRODUCTION

Rising energy prices and the possibility of greenhouse gas emission regulations have made energy efficiency essential to all industries. The electric power sector has historically dealt with rising demand for electricity by building new power plants. Because this demand fluctuates on a daily basis, however, much of the installed power capacity goes unused because it is sized to meet peak electrical loads. Therefore, during off-peak hours, this equipment might sit idle. Furthermore, "peaking" power plants are usually inefficient because they are designed to have low capital costs as they will only be used a fraction of the time. However, the paradigm of building new generation capacity to meet peak demand might be changing. Energy storage technologies could help electric utilities level their electric demand by allowing consumers (or suppliers) of energy to shift the times that electricity is used. For instance, energy can be stored during off-peak times and dispatched during peak times, thereby reducing the peak generation that a utility must have. In order for energy storage to make a significant impact, inexpensive storage technologies, which can be implemented on a large scale, must be developed. Thermal energy storage (TES), the storage of heat or cooling, has the potential to make such an impact.

Because TES stores energy in one of its basest forms, it is a relatively simple technology. It is this simplicity that gives TES the potential to be a very inexpensive, yet impactful, technology. For example, TES can have an immediate impact on capital costs

[1] This chapter was included in W. J. Cole, K. M. Powell, and T. F. Edgar "Optimization and advanced control of thermal energy storage systems," *Reviews in Chemical Engineering*, vol. 28, no. 2–3, pp. 81–99, 2012. Powell's contributions included a review of TES for solar thermal applications (not included in this chapter) and Edgar contributed general advising and editing.

by replacing expensive chilling or power generation equipment with a much less expensive storage tank. TES will also provide ongoing operating cost savings by allowing the system to shift times of consumption (production) of energy to off-peak (on-peak) times. Therefore, TES systems can dramatically reduce payback periods in addition to improving the project's return on investment.

Many of the benefits of TES could also be realized in the chemical industry. A key to energy efficiency in the chemical industry is waste heat recovery, wherein waste heat is extracted from one process and delivered to another in an effort to reduce energy consumption. With TES, heat integration can be done dynamically, where excess heat can be stored at one time and delivered at another. Because chemical processes are typically energy intensive (many even have their own electricity and heat generation facilities), TES has significant potential to improve energy efficiency and provide great cost savings in the chemical industry.

Because systems that use energy storage and the storage itself are inherently transient, it is critical to develop effective operating strategies for using TES technologies. This chapter provides a review of research that has taken place in TES with a particular emphasis on modeling, optimization, and control. It is focused on two main areas in which TES has found widespread use: combined heat and power systems and building systems.

OVERVIEW OF TES

TES is the storage of heat or cooling for later use. Because TES involves storing energy in one of its most primitive forms, it is a technology that has been used for centuries. Its simplicity has allowed it to become a successful energy storage technology. TES is typically a very cost-effective method of storing energy, especially when

compared to storage technologies that rely on expensive, sometimes exotic materials, such as battery storage. As a consequence of its simplicity, however, TES is not as versatile. Therefore, intelligent ways to use TES must be developed so that this promising, cost-effective technology is effectively applied.

Thermal energy can be stored as sensible heat (where heat is stored simply by changing a material's temperature), latent heat (where heat is stored by changing a material's phase), or chemical heat (where heat is stored in reversible, endothermic reactions and recovered by the corresponding exothermic reaction). TES can be classified as active or passive. In active systems, a fluid is circulated in order to collect and distribute heat (e.g., hot water flowing from a tank to heat a building). In passive systems, the storage medium and delivery system are stationary and are built into the system (e.g., the thermal mass of a building).

TES systems can use any phase (solid, liquid, or vapor) as a storage medium. Often, multiple phases might be used, such as in pebble bed storage where a fluid passes through a packed bed of solid particles in order to transfer heat to the particles. Latent heat storage also uses the transformation of the medium between phases so that energy can be stored using the material's heat of fusion (solid to liquid) or heat of vaporization (liquid to vapor). The development of phase change materials (PCMs) for heat storage is an active research field. PCMs are materials designed to change phase at a specified temperature. For example, one application of PCMs is embedding such materials into a building to increase the building's thermal mass so it can be used for passive heat storage.

TES can be used to shift electrical, heating, and cooling loads and has found popularity in a wide variety of applications. TES is widely used in district cooling, where multiple buildings in a region share a cooling loop and a central chilling station. This setting, which takes advantage of economies of scale, uses a central TES system

(typically with chilled water or ice as a storage medium) to lower electricity costs by chilling the water during off-peak hours. This stored energy is then used to offset peak cooling loads the following day by using the stored energy, rather than the chiller. Combined heat and power (CHP) systems, where electric power and heat are generated simultaneously, are frequently used in district heating or cooling, making these applications a good candidate for TES as well. If cooling, heat, and electrical loads do not coincide, TES can be used to store the heat or cooling, to help better align these loads. TES has also found application in solar energy. TES can be used to store the sun's energy as heat, which can be used for space or water heating in buildings. TES can be used in solar thermal power applications, taking an intermittent source of energy, such as the sun, and converting it into power that can be readily dispatched as needed [11], [12]. Thus, TES can be an effective technology, which has proven valuable in a wide variety of applications. For further reading regarding TES overview, see Dincer and Rosen [13].

OVERVIEW OF CONTROL STRATEGIES

Because systems that require storage exhibit transient behavior and the storage processes themselves are transient, selection of appropriate control strategies is critical. In some cases, single-input-single-output (SISO) control can be used. SISO systems use only one input to manipulate a corresponding output. SISO control can be done using measurements of the process output (feedback) and using that output in an algorithm to determine the prescribed input. The most common algorithm is the proportional-integral-derivative (PID) controller (or variants thereof), where the magnitude, integral, and derivative of the error between the measured output and its desired set point are used to determine the input. For processes where inputs and outputs are highly coupled, multiple-input-multiple-output (MIMO) controllers can be used. Feedback control can also be

implemented on a MIMO basis, although the PID algorithm will no longer be valid. MIMO controllers take a more holistic approach where a combination of output signals is used to determine the prescribed inputs. If disturbances to the system can be measured, feedforward control can be added to give the system the ability to reject measured disturbances in advance, without having to rely entirely on feedback measurements.

When system dynamics are too complex for a simple feedback control algorithm to be adequate or when there are process operating constraints, advanced control methods are needed. These advanced control methods often use optimization in order to handle the additional complexity and constraints [14]. Much research has been done in the field of advanced process control, resulting in a wide variety of control techniques. Among these techniques, model predictive control (MPC) has found widespread use. In MPC, a model of the system is used to make predictions of system performance and determine the inputs that result in optimal performance. Many variants of MPC exist, based on the type of model used, performance index, etc. Because MPC is the most widely used advanced control technique for systems with TES, it is highlighted in this chapter. However, other optimization and control topics are also covered including optimal system design and dynamic optimization.

COMBINED HEAT AND POWER AND TES SYSTEMS

Introduction

Combined heat and power (CHP), also known as cogeneration, is the concurrent production of electricity and thermal energy from a single energy source. In a conventional system electricity is generated at a power plant (usually operated by the local utility) and the waste heat from the system is vented via cooling towers or ponds. Facilities that get electricity from these power plants then must use additional energy to

provide their heating or cooling. Thus CHP has a major advantage over the traditional systems because it can utilize the waste heat from the electricity generation to meet the heating and cooling loads (via absorption chillers) of the facility (Figure 2.1). There are many variations of CHP such as trigeneration or CCHP (combined cooling, heating, and power), and BCHP (building combined heat and power) [15], but for this chapter all variants of CHP will be grouped into the general CHP category.

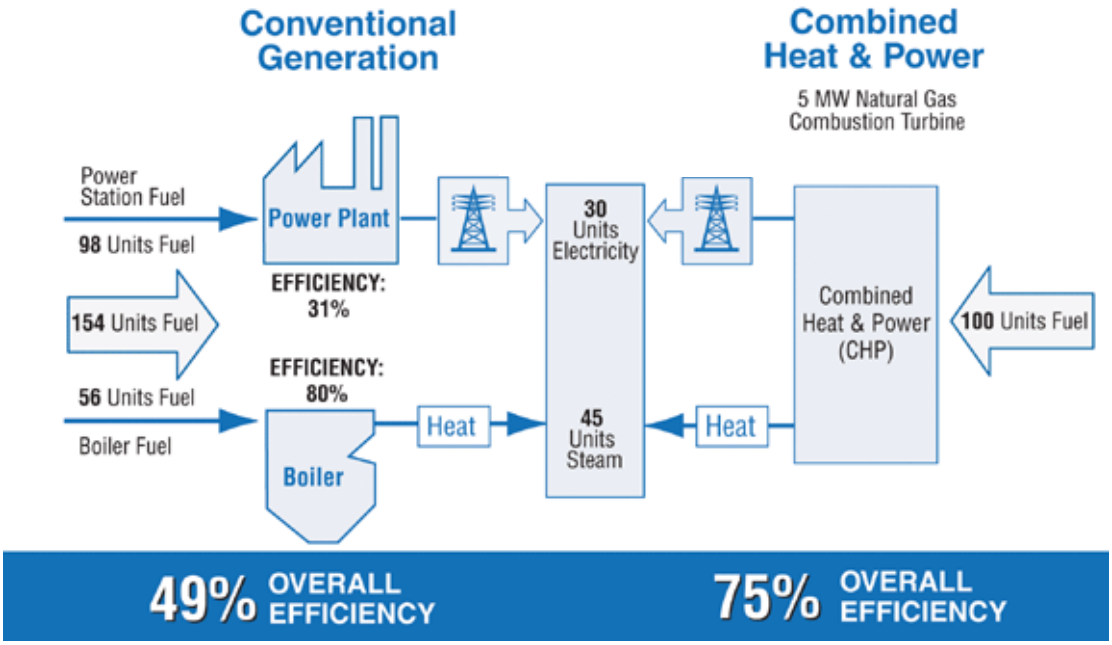

Figure 2.1: Conventional energy supply system (left) vs. combined heat and power system (right) [16]. The combined heat and power system has a much higher efficiency because it is able to utilize the waste heat from the electricity generation process.

Combined heat and power is not a new technology in the manufacturing industries. In paper manufacturing, for example, over 40% of the required electrical power was generated using CHP as of 2006 (see Figure 2.2). In other industries, however,

CHP is far less prevalent. CHP coupled with TES is even less common. Therefore, there is significant potential for further adoption of CHP and TES to increase the energy efficiency of manufacturing plants.

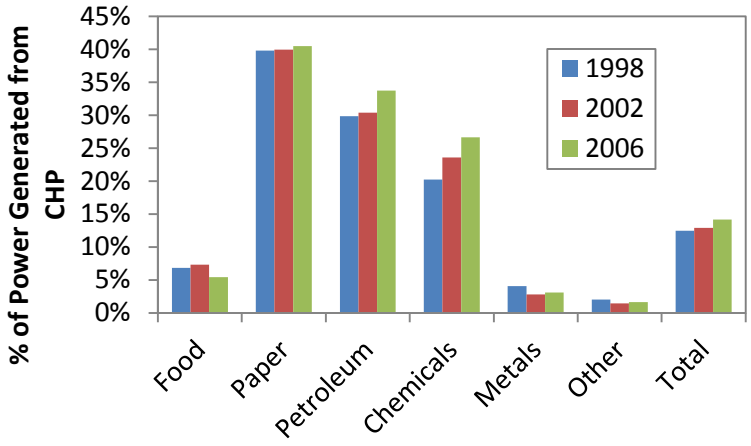

Figure 2.2: Percent of total electrical power usage that was generated from CHP, by industry [17]–[19].

In many cases, CHP potential is limited because of the difficulty of matching electrical and thermal demands. Thermal energy storage can be coupled with CHP to provide economic and energy savings, system flexibility, and system feasibility (see Figure 2.3 and Figure 2.4) [20]. These systems will be referred to as CHP-TES systems. Thermal and electrical loads can be decoupled to some extent by adding TES to a CHP system. This has grown increasingly important as peak loads have grown, increasing the gap and variation in on-peak and off-peak electricity market prices. Proper design and control is necessary to realize the maximum value of a CHP-TES system. A review of optimization in CHP systems without thermal storage was recently published [21]. This section focuses solely on CHP-TES systems.

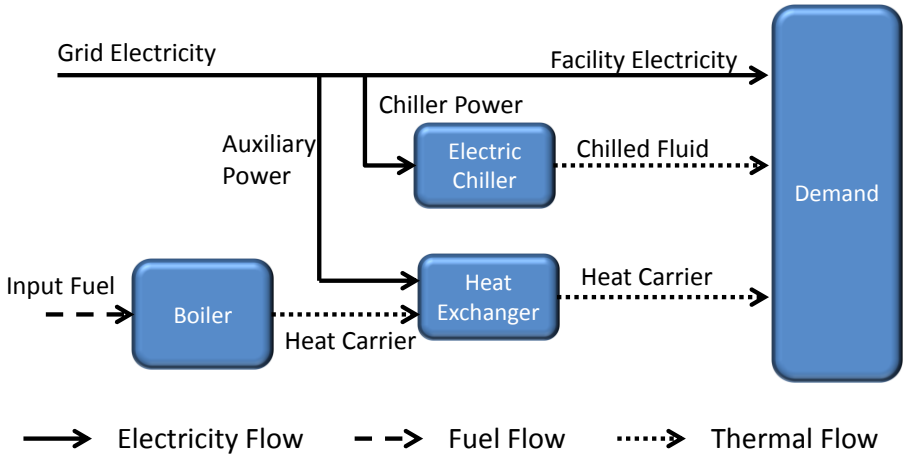

Figure 2.3: A typical configuration for a conventional system. Adapted from [22].

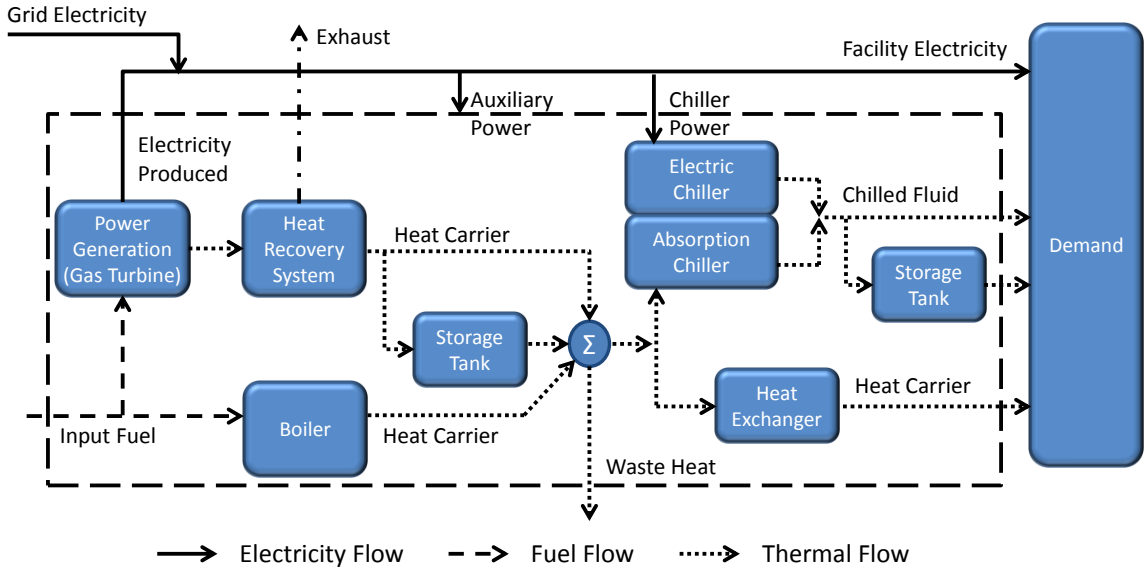

Figure 2.4: CHP-TES system. The power generation is typically a gas turbine, but it could be a fuel cell, steam turbine, or other device that generates both heat and electricity. Adapted from [22].

Modeling of CHP systems has been performed using a variety of methods and a plethora of software packages. Hinojosa et al. [23] reviewed some of those software packages, both commercial and custom, that are commonly used for modeling CHP-TES

systems. CHP models can be as simple as a model of the CHP prime mover (typically a gas or steam turbine) to meet required electrical and heat demands for a few design days or as complex as a large system model that describes not just the prime mover, but also electrical and thermal loads, thermal storage, chillers and boilers, and the distribution systems. Other considerations in CHP-TES models include an appropriate time step, the ability to export electricity, the ability to model the utility rate structure, CO_2 saving projections, the ability to calculate required financial indicators (e.g., NPV, IRR, payback period), and the ability to accept different fuels. It is important to choose a model with the appropriate complexity for the project requirements. CHP systems that will be providing relatively constant electrical or thermal loads do not require as extensive of a model as a system with many integrated components that have significant interdependence and fluctuating demands.

The design and operation of a CHP-TES system is often sufficiently complex that researchers apply optimization in order to maximize project economics [24]. Henning [25] discussed a number of optimization models that have been created for handling CHP systems with storage. Numerous researchers have investigated the best ways to address the optimization problem, which is generally formed as a mixed integer linear programming problem [26]–[32], though it has been formed as a linear programming problem [25], [33], a nonlinear programming problem [34], and a mixed integer nonlinear programming problem [35]. Sancho-Bastos and Perez-Blanco [36] formed a linear quadric (LQ) problem with the solution provided by a linear quadratic regulator (LQR). CHP-TES optimization focuses on two aspects: the optimal CHP-TES operation and the optimal CHP-TES design (with emphasis on equipment capacity). Both aspects are highly dependent on the requirements of the system and on the electricity rate structure. If the electricity rate structure is not defined (such as with electricity spot

market prices), this requires the prediction of the electrical prices [29]. Because there will always be model uncertainties and errors in predicted values (in the case of Rolfsman there was a 35% decrease in system value because of imperfect predictions), it is important that optimal controllers are closed-loop [37].

Conventional Operation Strategies

Ristic et al. [38] described the following conventional operation strategies for CHP systems with or without TES.

1. **Electricity base load:** In the design phase the CHP unit is scaled to only meet the base electrical load. The CHP unit then runs at full capacity all the time. This has the advantage of operating the equipment at its most efficient operating point. However, it cannot take advantage of changing electricity prices or variations in thermal loads.
2. **Heat demand following:** The CHP system follows the heat demand and electricity is treated as a beneficial by-product. This strategy might reduce auxiliary boiler requirements and ensures that there is never surplus heat that must be wasted. It cannot take advantage of changing electricity prices, and might in fact be negatively impacted by the price variation (if heat production is high when electricity prices are low it might be more economical to operation a boiler to meet the heat load).
3. **Electricity demand following:** The CHP system follows the electricity demand and the heat is treated as a beneficial by-product. This strategy is typical when electricity export is not allowed. It also allows the facility to "island" (i.e. operate independent of the power grid), because all electricity can be produced on-site.

Objective Function

The objective functions used for CHP-TES optimization vary considerably, but most objective functions follow the standard "costs minus revenue" form. The variation between objective functions generally comes about with which specific costs are considered as part of the objective function. In general the problem is formed as

$$J = \min\left\{C_{fuel} + C_{elec,pur} - C_{elec,sold}\right\} \tag{2.1}$$

where C_{fuel} is the cost of fuel consumed by the CHP unit and any auxiliary boilers or electricity-only generation units, $C_{elec,pur}$ is cost of any purchased electricity (which might include demand charges as in [35]), and $C_{elec,sold}$ is the revenue generated from selling electricity to the grid. The objective function is minimized subject to constraints such as heating or cooling loads, equipment capabilities (such as maximum or minimum capacities), and in some cases legal constraints (e.g., [31]). Constraints can be imposed as equality or inequality constraints. A requirement that electricity production matches demand would be an equality constraint while an inequality constraint would be, for example, the operating range for specific equipment.

Simple variations to the objective function given in Equation 1 include adding the cost of water [35], adding a penalty term for violating space heating or cooling comfort rules [39], including staff and maintenance costs [32], adding an electrical standby cost (a cost paid to the utility for providing permanent backup power) [35], including a cooling tower heat rejection cost [31], including a plant energy self-consumption term [40], adding a static transmission efficiency term for electricity exchanged with the grid [41], and including a cost relating to storing energy [29]. In some cases the capital costs of the CHP-TES system are considered along with the operating costs. Lozano et al. [31] used

an objective function that included the fixed costs plus variable costs, or in other words the equipment amortization and maintenance costs plus a modified operating cost function as given in (2.1). Bruno et al. [42] maximized return on investment (ROI) and thereby included both fixed and variable costs. Piacentino and Cardona [43] formed a similar objective function, only they maximized rather than considering ROI. Note that constants added to the objective function (e.g., fixed capital cost) do not affect the optimal solution.

Wang et al. [22] used the following for their objective function

$$J = \max\left\{\omega_1 R_{energetic} + \omega_2 R_{economic} + \omega_3 R_{environmental}\right\} \tag{2.2}$$

where $R_{energetic}$ is the ratio of energy savings compared to a conventional system, $R_{economic}$ is the ratio of economic savings compared to a conventional system, $R_{environmental}$ is the ratio of environmental savings (measured as CO_2 emissions) compared to a conventional system, and ω_1, ω_2, and ω_3 are weighting factors. The authors used an equal weight method (i.e., $\omega_1 = \omega_2 = \omega_3 = 1/3$). In this way Wang et al. were able to optimize their system based on all three conditions. Shifting the weights to give one factor preference gives the user more flexibility in examining the "what-if's" of a system. Using weights in the objective function was also performed by Rolfsman [29]. He used the inverse of the equipment efficiencies as weighting terms for the fuel consumption of each unit.

Kostowski and Skorek [44] introduced two objective functions, thermodynamic and economic. The thermodynamic optimum was defined as the lowest peak boiler usage, so the objective function minimized the peak boiler usage. The economic objective function was to maximize the change in net present value, or the increase in net present value from adding TES versus the no storage case. The economic optimal TES volume

was 38% smaller than the optimal thermodynamic volume with a 27% shorter payback period.

In the majority of cases reviewed the objective function was applied to an entire year, but the way the year's data were compiled varied significantly. As little as three days were used to represent a year, one day for each of the three relevant seasons [40], while others used 365 distinct days [29]. The climate affects the choice of the appropriate number of unique days. For example, Azit and Nor [35] stated that in Malaysia the annual facility load can be represented by a single week of typical hourly loads since the climate is fairly constant year round.

Optimization Techniques

Optimal solutions to both the design and operation problems have been found using dynamic programming [45], [46], Lagrangian relaxation [47], evolutionary programming [41], branch and bound method [39], sequential quadratic programming [37], particle swarm algorithm [48], decomposition method [28], Simplex method [49], reduced-gradient algorithm combined with a quasi-Newton algorithm [24], generalized reduced gradient method (via Microsoft Excel's Solver) [40], and Newton-Raphson combined with the conjugate method [35]. The optimization technique used might influence the optimal solution, but if the optimization problem is convex then an optimum is guaranteed and will be global. In that case the choice of the optimization technique will largely be affected by computation time, ease of implementation, ability to handle required constraints, etc. For solving nonconvex problems, the choice of a solver might be more important. In some cases, however, the quality of the solution might be largely independent of the algorithm used. For example, Wang et al. [22] showed that the optimal solution from particle swarm algorithm produce 1% greater savings than using a

genetic algorithm. More information on optimization techniques is readily available in a variety of textbooks and other material (e.g., [14], [50]).

Applications

Because the design and considerations of a CHP-TES system are dependent on the specific application, the most common CHP-TES applications will be reviewed separately. They include district heating and cooling, building heating and cooling, and integration with renewable energies. These three applications tie directly into chemical process facilities: plants often have some sort of district heating or cooling system to integrate heating and cooling streams, plants contain buildings which are heated or cooled, and introducing renewable energies correctly into plants is a valuable energy sustainability measure.

District Heating and Cooling

There is more attention given in literature to CHP-TES systems in district heating and cooling networks than any other CHP-TES system, nearly all of which emanates from Europe. In district heating and cooling networks that incorporate CHP, the CHP units produce electricity and use the waste heat from the electricity production to meet heating or cooling loads. Typical standalone CHP units are generally operated using the heat demand following strategy. This means that CHP units might be producing large amounts of electricity (because thermal loads are high) during off-peak hours when electricity prices are low thus reducing revenues. It also means that during on-peak hours, when electricity prices are highest, CHP units might either have to run at partial capacity (because of low thermal loads) or run at full capacity and waste the excess heat. Additionally, because the CHP units are required to follow a changing thermal load, they will not always be operating in their most efficient operating region (i.e., at or near full

capacity). Thermal energy storage, almost exclusively in the form of chilled or hot water, has been applied to address these issues.

Thermal energy storage has been shown to add significant economic savings to a CHP plant by taking advantage of the electricity rate structure. Bogdan and Kopjar [40] modeled the addition of a hot water TES to a CHP system on a district heating network in Croatia and found that TES increased the plant's net income by 17% compared to the CHP-only system under a dual-time electricity tariff (i.e., where different rates apply for on-peak and off-peak times). The savings came from maximizing electricity production during peak electrical times (thus garnering the higher electricity market price) and storing the excess heat in the TES. At night with the low electricity prices, the CHP system would shut down and thermal loads would be met by the TES. This resulted in a net decrease in annual fuel consumption and electricity production as compared to the CHP-only case (i.e., the increase in on-peak production was less than the decrease in off-peak production). The decrease was allowed because the CHP-TES unit was not contracted to supply a set amount of heat or electricity.

Fragaki et al. [51] found that for the United Kingdom, with a large difference between night and day electricity rates, TES can more than double the return on investment of CHP plants when measured in terms of net present value. They also determined that TES is still economical even if the electricity or gas prices change. In a sensitivity analysis they found that TES is economical up to a 15% reduction in average electricity prices or a rise in natural gas prices by more than 15%, although optimal size of the TES and the resulting NPV varied as prices changed.

Streckiene et al. [52] found that TES allowed the CHP units to run at full load for longer amounts of time, thus increasing system efficiency (a finding also pointed out in [53]). They also found that the more variation there is in electricity spot market prices

(e.g., the more the price changes), the more favorable CHP-TES systems are. Strekiene et al. reported more sensitivity of CHP-TES plants to fuel and electricity prices than did Fragaki et al., even to the point of the TES becoming uneconomical with a 10% increase in fuel prices. The added sensitivity can in part be explained by the differences between the energy markets (Strekiene et al. in Germany and Fragaki et al. in the United Kingdom). For example, Fragaki et al. used a two-tariff electricity rate structure, while Strekiene et al. used an electricity spot market. However, Strekiene et al. did point out that as long as electricity prices and natural gas prices move in the same direction then the negative impact on the economic analysis is limited. Adding TES gives the operator more market opportunities and more security because fluctuations in heat demand can be dealt with more easily, but these benefits come with additional operating risks of price sensitivity.

Pagliarini and Rainieri [54] modeled a CHP-TES system for the University of Parma Campus in Parma, Italy. In their analysis they identified a range for the optimal TES size and found that by including a TES tank in that range the annual income increased by 48% and the overall simple payback period of the system was reduced from 4.4 to 3.5 years.

Rolfsman [29] focused on the optimal operation of CHP-TES systems in a district heating network. Like Lin and Yi [55], he included not just hot water TES, but also passive TES from raising building temperatures in the heating district by 1-2°C. He found that proper operation of the TES was able to keep the most expensive equipment from coming online in order to meet short spikes in heat demand. He also showed that optimal operation allowed the CHP units to work at full capacity when electricity prices are high, storing the excess heat in the TES units. The TES would then be discharged at night when it was no longer cost effective to produce electricity.

The optimal TES capacity in a district heating network is a function of the CHP system selected. For example, Lund and Andersen [56] demonstrated that as the engine or turbine size increased (e.g., from 2 MWe to 4 MWe) the optimal size of the TES also increased. This can also be seen in the work done by Verda & Colella [57]. They found that including a second CHP system increased optimal TES size (see Figure 2.5). However, Fragaki et al. [51] found that if multiple small engines or turbines were selected (e.g., two 2 MWe vs. one 4 MWe) then the optimal TES size decreased because during low heat demand and low electricity prices only one engine or turbine needed to run.

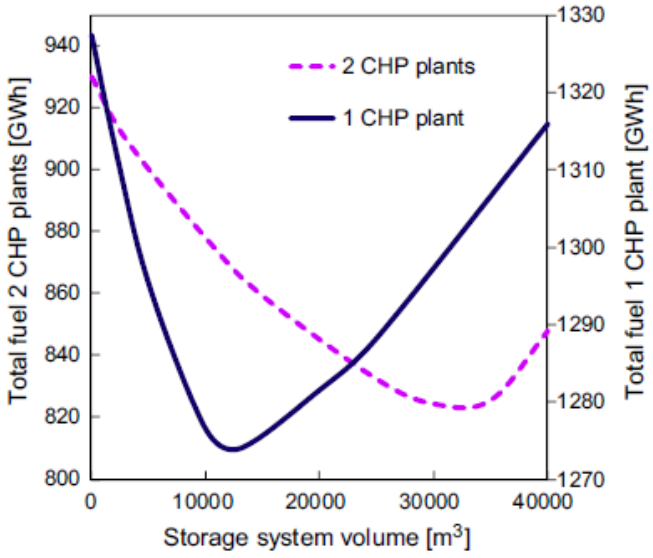

Figure 2.5: Fuel requirements for 1 and 2 CHP plants versus TES volume. Note that the optimum value increases as a second CHP plant is added [57].

The work by Urbaneck et al. [58]–[60] is interesting in that it focuses on a strictly cooling network, and that it includes CHP capacity fired by brown coal instead of natural gas. They emphasize that the optimal CHP-TES solution for one system cannot be transferred to another system without adaptation.

Bruno et al. [42] demonstrated why ice TES is rare compared to chilled water in district energy systems. In performing their optimization of a CHP system with ice storage they found that the optimal TES size was zero while the optimal chilled-water TES size was 47.4 MWh. They suggested that ice TES is only suitable for CHP-TES district energy applications where there are significant space limitations.

As an interesting side note, the idea extending a CHP's district heating network to outlying residences using mobile-TES has been examined by Wang, Hu, et al. [61]. They considered four different options for removing heat (either via steam or hot water) from the CHP plant in order to charge the mobile-TES for distribution.

Building Heating and Cooling

For actively cooling buildings in CHP-TES systems, chilled water and ice are the most common forms of TES, although phase change materials (PCMs) embedded into buildings to increase thermal mass have also been explored [62], [63]. Except for the rare case of aquifer and borehole TES [64], heating buildings in CHP-TES systems uses hot water tanks.

In the case of meeting building cooling loads, one of the major benefits of coupling TES with CHP is that it allows the equipment to be downsized. Air conditioning equipment is sized based on peak cooling demand requirements, so by incorporating TES, air conditioning equipment can be downsized which greatly reduces capital costs. For example, Ehyaei et al. [65] looked at using micro gas turbines coupled with ice TES to meet the heating, cooling, and hot water needs for a 40-unit residential building in three different cities in Iran. The electricity from the CHP micro turbines was used to meet building electricity demands and to run mechanical chillers while the waste heat was used to run absorption chillers. In two of the cities, 21 micro turbines were required

when no TES was used, but only 11 micro turbines were required when TES was incorporated. The reduction came because the TES could discharge to meet the peak demand, eliminating the need for peaking equipment that only ran during the hot afternoon periods. This resulted in a reduction in investment costs by 27.5% and 29.5%, respectively. In the third city, the ice TES reduced the required number of micro turbines from 75 to 40, resulting in a 14% savings in investment costs. The lower investment cost reduction for the third city was attributed to the hot and humid nature of its climate, while the other two cities were mild and semi-hot.

Similarly, Liu et al. [66] examined a hybrid heating, ventilation, and air conditioning (HVAC) system that included a CHP unit, liquid desiccant, vapor compression and absorption chillers, gas boilers, and hot water and desiccant storage tanks for application in a 10-story building. During the summer the excess heat recharged the desiccant and ran the absorption chiller. In the winter the CHP unit provided space heating. The addition of TES lengthened the operating hours of the CHP system and significantly decreased the capacity of the auxiliary boiler and compression chiller. The system had a payback period of two years and reduced CO_2 emission by 40%.

Somcharoenwattana et al. [67] performed two case studies, one of an airport and the other of a government office building, both located in Bangkok, Thailand. In the airport case study they demonstrated the importance of using high efficiency equipment. The most optimal economical solution was not to incorporate TES, but to replace the 20-year-old low efficiency gas turbines with new, high efficiency models. In the office building case study the CHP plant was designed to meet the cooling load and the electricity production was supplemental. Incorporating cold TES reduced the simple payback period of the CHP plant from 17.8 years to 9.2 years. The TES allowed the CHP to run more continuously, and decreased the size of needed equipment. The authors

pointed out that the longer the operating hours of the CHP plant the better the economic outlook of CHP-TES system. A similar investigation with similar findings was reported by Ziher & Poredos [68].

Khan et al. [69] investigated energy conservation for the buildings of the Asian Institute of Technology in Bangkok, Thailand. They compared a CHP-only system and a CHP-TES system to a system where all electricity is purchased from the national grid. They included a thorough economic analysis, including installation and maintenance costs. The savings from incorporating the TES are shown in Table 2.1.

	Peak-Demand Reduction	**Energy Reduction**	**Internal Rate of Return (IRR)**
CHP only	13%	16%	21%
CHP with TES	23%	21%	25%

Table 2.1: Savings from including CHP and CHP-TES vs. purchasing all electricity from the national grid.

McNeill et al. [70] found that incorporating a hybrid CHP-TES system that included desiccants for humidity control in a given building brought the same amount of savings regardless of location. They regressed the cost savings of the CHP-TES system in five different US cities and found that their regression coefficients were nearly identical. For a more standard CHP-TES system, however, Wang et al. [48] found that climate influenced system energy usage and economic outlook (though they did use the non-standard objective function given in Equation 8). They examined four building categories (hotel, office hospital, school) and five climates. In some of the cases with a high summer cooling load, the CHP-TES system used more energy than the conventional system during the summertime, though in only one case was the CHP-TES system less economical than the conventional system.

Other researchers have investigated CHP-TES systems for single-family residential buildings. Houwing et al. [30] showed that using MPC on a single-family CHP-TES system brought 2-6% savings in operational costs versus the heat demand following control strategy. One of the primary benefits of adding TES to these small-scale CHP units was that the TES allowed the CHP unit to operate more continuously and for more hours out of the year. Because of this benefit, a CHP system with an optimally-sized TES reduces CO_2 emissions by almost three times compared to a CHP-only system [71].

The type of TES model used in a building CHP-TES simulation has been shown to affect the results. Campos Celador et al. [72] looked at the effect of how a hot water TES tank is modeled on the overall energy and exergy (the maximum useful work possible) efficiency of a CHP facility. Energy and exergy efficiency differences between perfectly stratified and fully mixed were 2% and 0.7%, respectively. However, this small difference translated into a 12% difference in annual net savings between the two tank models.

Integration with Renewable Energies

When there is a large penetration of intermittent renewable energies such as wind and solar power in the electricity sector, there needs to be some "balancing" system that can handle the intermittency. CHP-TES is an ideal candidate for balancing intermittent renewable energy sources because CHP units are often tied to thermal loads rather than electrical loads [73]. This allows the CHP to balance an intermittent electrical load while using the TES to meet thermal demands. The incorporation of energy storage is key to increasing the system's ability to balance renewable energies [74]–[77]. Adding TES to CHP systems improves flexibility to maximize profit [20].

In places such as Denmark there are large amounts of electricity production coming from both wind and CHP. Because of the large penetration of wind, electricity prices are largely a function of the amount of wind: when there is an abundance of wind power, electricity prices are lower and when there is little or no wind electricity prices are higher. This decreases the marginal value of building additional wind turbines. However, this also allows for distributed CHP-TES systems to take a larger part in the electricity system. When there is lots of wind, CHP-TES facilities can stop producing power and meet thermal loads by discharging their TES, or in very high wind scenarios, they can even purchase cheap power for running heat pumps to meet thermal loads. During low wind scenarios, the CHP units can run at full capacity, the heat pumps can be shut off, and the thermal loads can be met by a combination of waste heat and discharging the TES. In this way TES increases the flexibility of CHP to deal with the intermittency of wind [78], [79].

Other Investigations

Caldon et al. [34] discussed virtual power plants, which is an aggregation of distributed CHP facilities treated as a single facility. They showed that incorporation of TES in the virtual power plants reduced operation costs. Collazos et al. [39] showed that a model predictive controller applied to CHP-TES systems in a virtual power plant setting reduced operating costs by 13% versus using a boiler and purchasing all required electricity from the grid. Wille-Haussmann et al. [32] demonstrated that TES gives more flexibility to a virtual power plant of five CHP units. Optimal control led to a 10% cost reduction over heat demand following CHP by allowing the CHP units to actively participate in the spot market.

Ryu et al. [80] reported on a hybrid CHP-TES system that can be applied to military-type or disaster recovery applications where the ability to island is of high priority. The system could provide all the heating, cooling, and fresh water needs of a facility (it condenses water from the air). Ryu et al. discussed the importance of selecting the appropriate heat recovery capacity as that would determine strongly influence the selection of other components such as TES size and chiller capacity.

Several additional investigations on CHP have been published in the literature that include, but do not focus on, interaction with TES. They include [81]–[91].

Implications for Chemical Industries

Combined heat and power systems currently produce over 25% of electrical power for chemical industries [92]. Coupling thermal storage to CHP has been shown to increase CHP operating hours, economics, and flexibility. When proper optimization and control are applied, CHP-TES units have been shown to operate effectively in district heating/cooling scenarios, building heating and cooling situations, and areas with significant renewable energy penetration. Because chemical industries can be viewed as district heating/cooling networks and often contain buildings that are heated and cooled, the principles reviewed can be directly applied. Applications from using CHP-TES to deal with intermittent renewable energy show that CHP-TES is flexible to meet plant loads that might be intermittent or uncertain. TES augments the potential of CHP to be a cost-effective and sustainable technology for the chemical industries. This might become especially valuable in smart grid environments where pricing signals to curb electricity demand (or increase electricity production) might vary hourly. TES enables the production of CHP electricity on demand without underutilizing waste heat.

BUILDINGS AND TES (WITHOUT CHP)

More work has been done concerning the control and optimization of TES in the buildings sector than for any other sector. This is only logical considering the number of large-scale buildings throughout the world. Buildings are also an enormous energy sink, as 40% of all energy in the U.S. is consumed in buildings [93], [94]. Due to the volume of work in this area, building energy systems coupled with TES provides insight into the benefits of proper control of TES systems. The building sector has also showcased the power of model predictive control (MPC). For that reason, MPC in buildings is given special attention to demonstrate that MPC is capable of controlling complex systems while generating cost and/or energy savings.

Thermal energy storage is primarily applied to shift electrical loads from high-cost peak times to low-cost off-peak times by shifting the building's thermal load (see Figure 2.6). In doing so, it provides extra degrees of freedom for sizing and operating heating and cooling equipment. For example, in traditional heating and cooling systems equipment is sized to meet the peak demand for the year. For the majority of the year the equipment is not operating at peak conditions and is therefore oversized. Adding TES reduces the peak load that a chiller or boiler must meet thereby allowing it to operate closer to its design points where its efficiency is higher [95]. Other advantages of incorporating TES include using cool nighttime air to precool building mass (given the appropriate climate) and operating the system's chillers at improved ambient conditions [96]. Conditions that tend to favor the implementation of TES include high utility demand costs, high utility on-peak rates, high daily load variations, short duration loads, infrequent or cyclical loads, insufficient capacity of cooling equipment to handle peak loads, and rebates for shifting peak loads [97].

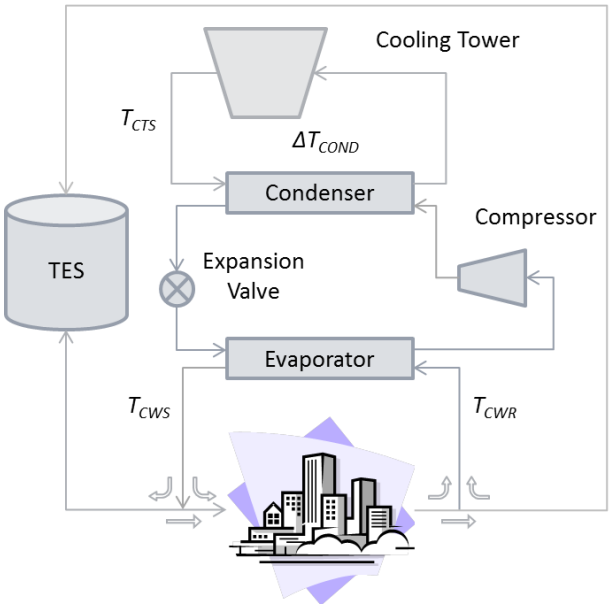

Figure 2.6: Building TES cooling system. Cooling fluid from the TES flows counterclockwise during discharge and clockwise when recharging.

The TES in buildings systems can be active or passive. Active TES is typically ice or chilled water for cooling system and hot water for heating systems. Passive TES is most commonly sensible heat storage in the building material (i.e., the concrete, steel, etc. that make up the building), but might also include engineered phase change materials (PCM). PCM's have been reviewed extensively (e.g., [98]), so specific information about PCM's will not be included here. Most of the literature on active TES control systems focuses on ice TES, though chilled water is very common in actual TES applications [99]. Modeling and control of ice TES is more challenging because of the variety of the ice-making devices and the difficulty of capturing the dynamic heat transfer characteristics as ice is formed or melted [100]. Passive TES has gained popularity in the optimal control field because, other than the controller, it can require no system changes.

TES Control Strategies

Most of the recent investigations in literature center on how the TES should be used. Determining how the TES system will be used also specifies, to some extent, the size of the required size of the system.

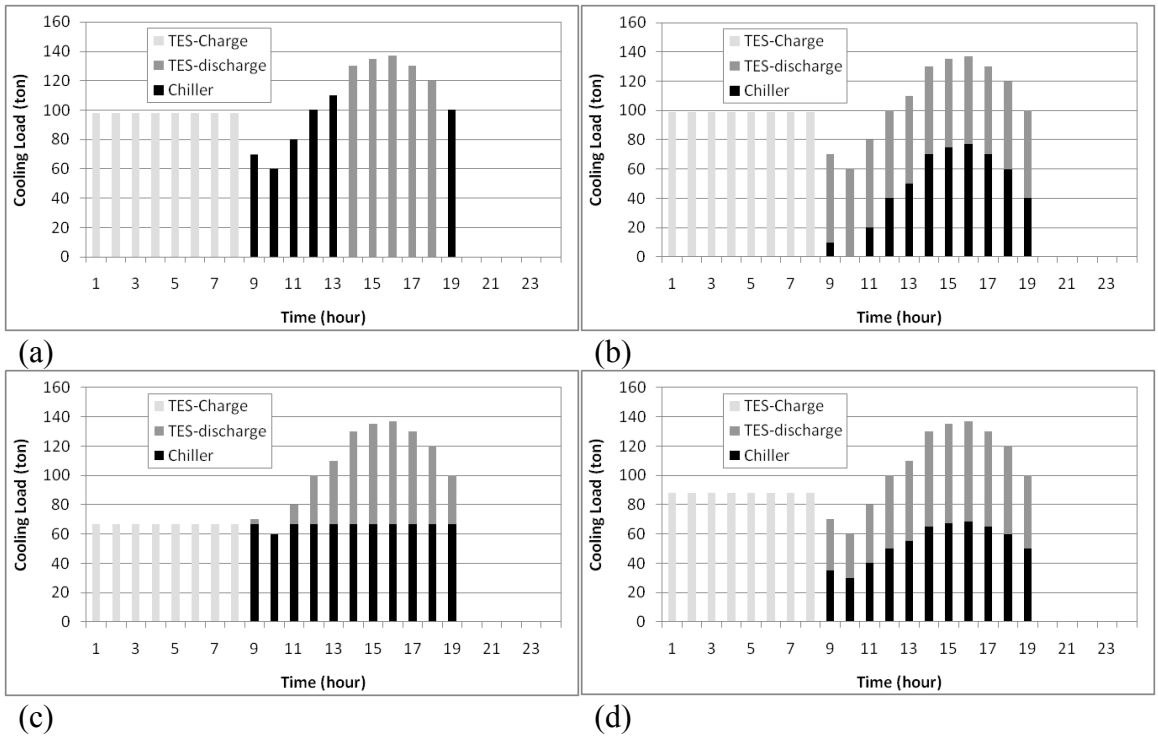

Figure 2.7: Conventional active TES control strategies. Full-storage (a), demand-limiting (b), chiller-priority (c), and constant-proportion (d). Full-storage and demand limiting are both storage priority control methods.

Conventional TES control strategies include storage-priority, chiller-priority, and constant-proportion control [101]–[105]. Storage-priority control can be further subdivided into full-storage and demand-limiting control, though in some senses full-storage control can be seen as a special case of demand-limiting control [106]. Results from applying these different control strategies for TES are shown in Figure 2.7. The only difference between the control techniques is the rate and time of the TES discharge.

Chiller-priority and constant-proportion control are fairly simple to implement and might require no more than an on/off schedule. Storage-priority control is somewhat more difficult since it requires load forecasting. These control strategies are used as a metric for comparing for more advanced control schemes.

Model predictive control (MPC) is a more advanced control strategy in which a model of the building and appropriate systems (e.g., chiller, ice storage tank, etc.) is generated. The controller uses the model along with weather, occupancy, and energy price predictions to determine the optimal trajectory of the planning horizon (typically 24 hours, though 48 hours has been used Henze et al. [107]), but it only takes an action for the first time step (see Figure 2.8). For the following time step the planning horizon is shifted forward, the optimal trajectory is recalculated, and the first action is again taken. In this way the controller is always using the model to predict behavior over the next sampling period, e.g., 24 hours, but it only implements the first control action in that planning horizon. The models are often created using popular building modeling and simulation software such as EnergyPlus or TRNSYS. These modeling tools are able to capture the dynamics of a complicated building system without spending excessive amounts of time generating a model. These models can even be coupled with tools such as MATLAB to further increase user flexibility [108].

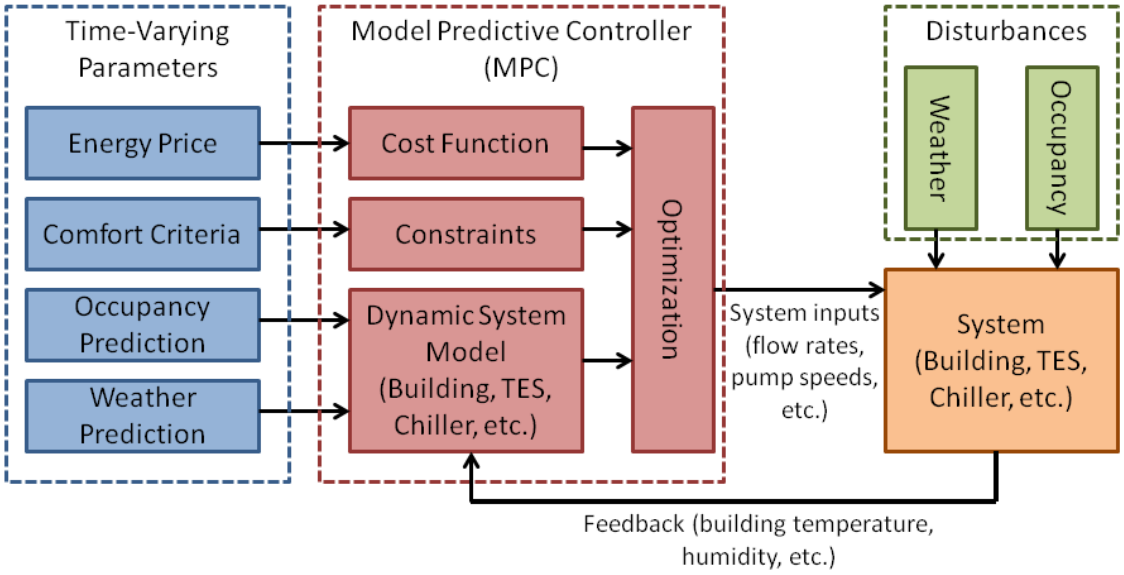

Figure 2.8: Model predictive controller for building energy systems. Adapted from [109].

Most researchers selected 1 hour as their time step (e.g., Henze et al. [110]) but some chose smaller time steps [100], [104]. Ma et al. [111] showed that the choice of the time step is important. They found that by choosing too coarse of a time step (they used 1 hour), the MPC was not able to take full advantage of the system because the optimal time of many of the decisions occurred between the 1 hour decision periods. The drawbacks of MPC include the potential high cost of generating an accurate model for the controller, unavoidable mismatch between the model and the actual environment, and the difficulty of appropriately predicting future conditions such as weather and electricity price.

Because energy systems using TES depend so heavily on environmental conditions in order to make accurate predictions and decisions about how the system operates, it is very useful to incorporate weather forecasts so that the ambient conditions and projected loads can be anticipated. Henze et al. [102] and Henze et al. [112]

examined various weather prediction methods for MPC's, including random walk, 30- and 60-day bin predictors, harmonic predictor, autoregressive neural network, and same-as-yesterday predictor. They found that the 30- and 60-day bin predictors were the best weather predictors and that they led to cost savings that were only marginally worse than the perfect prediction scenarios.

Model predictive controllers have been used for passive TES (e.g., [107]), active TES (e.g., [113]), and simultaneous active and passive TES (e.g., [114]). Interest in MPC for passive TES has increased because one of the benefits of using MPC is that it can take advantage of the building's thermal mass under a variable electricity rate structure [109], [115]. A general solution for passive TES using MPC is shown in Figure 2.9. The controller takes advantage of the thermal mass by precooling the building before the occupancy period begins and then gradually increases the room temperature set points during times when electricity is most expensive to allow the building mass to absorb the heat. Use of PCM's with MPC can further increase the potential of passive TES since temperature levels could be kept perpetually within the comfort range. Use of MPC with passive TES does not guarantee savings, however. Oldewurtel et al. [116] found that in some cases a variable rate structure under optimal MPC can still increase overall energy costs versus an average, flat-rate structure because some loads such as lighting cannot be shifted to off-peak hours.

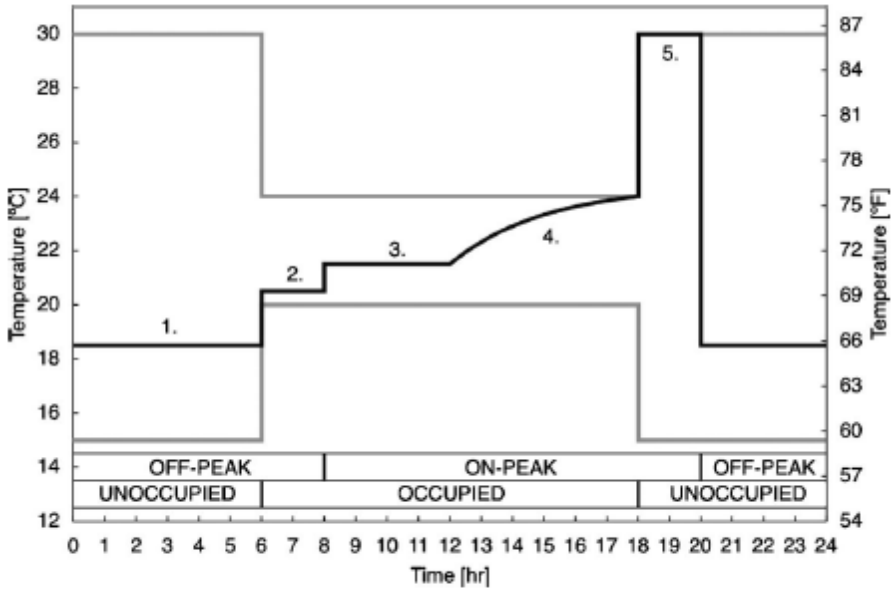

Figure 2.9: Set points for optimal control of passive TES. The black line is the control path and the gray lines are upper and lower control limits. [117].

Zhou et al. [118] developed a MPC for an active chilled water TES system. The MPC operated differently than typical MPC's in that instead of changing equipment set points it functioned more as an equipment scheduler. The MPC predicted the campus load over the planning horizon and then determined the best time to discharge the TES, the number of chillers that must operate at each time step to meet the remainder of the load, and the start and stop times of each chiller.

Henze, Kalz, et al. [112], Henze, Felsmann, et al. [119], and Henze et al. [110] applied MPC to a system with both active and passive TES. They solved the passive TES problem first and the active thermal storage problem second. This led to the same results as solving both problems simultaneously but took significantly less computation time and reduced the risk of landing in a local optimum. They also used the optimal solution from the previous time step as a guess value for future time steps.

Liu and Henze [120] analyzed the effects of mismatch between a model and an actual system when using a MPC. Incorrectly modeled building construction characteristics negatively affected the MPC's ability to fully utilize passive TES. Zone temperature set points and TES performance were strongly affected if the model contained improper internal heat gains, especially when those heat gains were underestimated. Relative efficiencies between chillers were also quite important as they determined the order in which chillers were put on-line.

By using a fractional factorial analysis Cheng et al. [121] found that the four factors that most influence the effectiveness and cost using passive TES with MPC were utility rate structure, internal load levels, building mass level, and equipment efficiency. In a follow-up study Henze et al. [117] performed a full factorial analysis on four parameters found by Cheng et al. They considered four cities, each with its actual rate structure. They found that cost savings from passive TES were limited by the available storage capacity and that more savings could generally be achieved when the system has lower efficiency equipment because more energy usage can be shifted from on-peak to off-peak. Control strategies were simplified by applying the average of the four optimization variables, and nearly all building achieved equal savings as using the MPC. Savings from passive TES were most sensitive to utility rates (which was also demonstrated by [96]), followed by building mass and then internal heat gains. Relative savings due to passive TES were fairly insensitive to climate. Incorporation of PCM's might change the impact of climate, though. Corgnati et al. [122] found that the influence of PCM's was very climate dependent, but that using building thermal mass provided benefit regardless of climate.

Touretzky and Baldea [123] used nonlinear models to develop a MPC for a small building with energy recycle. They provided theoretical justification for the multiple

timescale dynamics in buildings with energy recovery and presented methods for developing controllers based on decomposing those time scales to the one most relevant for control.

Seo and Krarti [124] considered the influence of building shape on TES MPC operation. They found that it had a small impact on TES performance (<5% difference in savings potential for a square building versus rectangular building). They also found that optimal control led to 15% higher savings than chiller priority.

Other controllers such as learning controllers [125], fuzzy logic controllers [126], heuristic controllers [100], and weight priority method controllers [127] have also been used for buildings that include TES with varying levels of success. However, I believe that MPC is the most versatile control type for the operation of TES.

Implications for Chemical Industries

TES and MPC have only been examined together in building heating and cooling environments, demonstrating the potential of model-based predictive controllers in TES systems. TES in buildings brings many benefits, such as reducing cycling or the size of heating and cooling equipment, but that TES with MPC amplifies the benefits of TES, including enhanced economics and flexibility. TES in building systems has also shown how advanced control can take advantage of the utility rate structures to bring significant cost savings. Deployment of TES in the chemical industries would be similarly benefited if advanced controls such as MPC are applied [128].

CONCLUSIONS

There are many benefits and challenges to integration of TES in an energy system. Adding TES to a CHP system can improve overall system efficiency and economics, and provide some degree of independence from an external utility. TES used

in building heating and cooling systems can shift peak loads and reduce the size and cost of peaking equipment or peaking energy. TES allows users to take advantage of time-of-use rates, operating equipment during times of lowest cost. Buildings with TES demonstrate that MPC is a viable control strategy to manage complicated systems in a variety of utility rate structures and that MPC amplifies the cost-effectiveness of TES systems.

In summary, when TES is properly designed and controlled it can:

- Increase system flexibility
- Improve system efficiency
- Reduce energy consumption
- Reduce equipment costs
- Increase independence from utilities
- Reduce emissions
- Manage intermittency from an energy source or sink

Because chemical processes are often heavily integrated with significant thermal and electrical loads, thermal energy storage, especially when coupled with CHP, can be applied to improve the flexibility and efficiency of chemical processes. In order to take full advantage of TES, optimization in design and control (such as MPC) is necessary.

The flexibility offered by TES is likely to grow more important, especially with the advent of the smart grid and the increase in intermittent renewable energy resources. Implementation of TES might allow chemical processes to increase the amount of on-site renewable energies. As smart grid technologies are deployed, chemical plants can use TES to improve their utility economics by enhancing their interactions with the grid as they buy and sell power (or simply curb power use) at optimal times.

Because TES can reduce required equipment sizes and increase system efficiencies, TES can be used to improve the economics of chemical processes. TES also reduces equipment cycling, which lengthens equipment life and decreases maintenance costs.

Based on the literature reviewed, the following future research directions are recommended:

- The development of new materials will continue to improve flexibility and efficiency of TES systems, thus giving controllers more opportunity to generate both energy and cost savings. For example, the development of a cost-effective PCM that changes temperature at ~4°C can reduce the TES size to close to that of ice TES while at the same time reducing the compressor lift of the chiller that must charge the TES (compared to ice storage).
- Energy systems are likely to become increasingly complicated and integrated, and controlling those systems will be possible only through advanced control. The integrated systems will leverage the benefits of each of the components of the systems, resulting in a more efficient and flexible systems. However, models might grow sufficiently complicated that the control cannot function optimally. Model reduction techniques and improved algorithms (especially mixed-integer algorithms) will need to be developed to address these issues.
- Increases in the amount of intermittent renewable energy sources will create a greater demand for storage. Integrating energy storage systems (e.g., TES, batteries, flywheels, etc.) might generate new opportunities to deal with these intermittencies. Research and development of new hybrid systems is likely to raise overall system efficiency and effectiveness

- As advanced control techniques such as MPC are developed, model mismatch might become a bottleneck for improvements. Model mismatch can be reduced by improving prediction capabilities of disturbance variables, by developing dynamic models of TES-related equipment than can be packaged into commercial or open source software, and by developing adaptive abilities into the controller so that it can adjust to changing process conditions.

Interaction between TES and intelligent systems such as the smart grid will become more beneficial and efficient as more companies develop products that can take advantage of intelligent storage. However, for that to be possible, interoperability and communication standards must be developed and implemented (e.g., [129]).

Chapter 3: Model Predictive Control of Novel Thermal Storage Configurations for Commercial Buildings[2]

INTRODUCTION

Thermal energy storage (TES) is a technology where thermal energy is stored as either sensible or latent energy in some medium. Thermal energy storage has the potential to make significant contributions to lowering peak electrical demand [130], converting an intermittent renewable resource into a constant supply resource [131], enhancing the flexibility of cogeneration or heating, ventilation, and air conditioning (HVAC) systems [132], and improving overall system efficiency [133]–[135]. For a more thorough discussion of TES systems see Chapter 2. This chapter focuses on the use of TES in building cooling systems. Since TES can be used to meet part of the peak cooling load, it can decrease the required size of chilling equipment. The TES can also improve the efficiency of chilling systems by shifting cooling loads from hot daytime hours to cooler nighttime hours where chiller condenser temperatures can be reduced. The extent of the efficiency increase depends on the design of the TES system and on the difference between day and night temperatures.

Many researchers have studied the use of advanced controls, especially MPC, on building cooling systems with TES ([133], [136]–[144]). However, most of them only considered short operation periods, such as one week or one month, to determine savings. For large buildings, cooling must be supplied year-round due to internal heat gains, so TES can provide benefits throughout the year. Examining TES performance throughout

[2] This chapter was included in W. J. Cole, T. F. Edgar, and A. Novoselac, "Use of model predictive control to enhance the flexibility of thermal energy storage cooling systems," in *Proceedings of the 2012 American Control Conference*, Montreal, Canada, 2012, pp. 2788–2793. Coauthors Edgar and Novoselac contributed general advising and editing.

the year will also lead to greater understanding as to what types of climates are most suited for TES cooling systems.

Previous work on control of TES systems primarily emphasizes operating cost savings rather than energy usage and savings. Thermal energy storage provides an opportunity to manage the electricity load profiles from heating and cooling systems. This work focuses on how use of year-round TES can bring energy and cost benefits to a large cooling system that serves multiple buildings with diverse cooling load profiles. This work presents a novel TES configuration to provide additional flexibility in reducing peak chiller electricity demand. Other variations of hybrid TES systems have been examined in [145]–[147].

SYSTEM DESCRIPTIONS

Chilled Water Systems

Three variations of a single system are analyzed in this study. The first (system 1) is a traditional chiller/cooling tower configuration (see Figure 3.1a). The second (system 2) is identical to the first except it has a chilled-water TES unit running in parallel with the chiller that supplies cold water to the buildings during peak hours (see Figure 3.1b). The TES is recharged by the chiller during off-peak hours. The third variation (system 3) differs from system 2 in that the relatively cold return water from the building can be sent to the chiller's condenser after it has been used to meet building cooling loads (see Figure 3.1c). A cooling tower is still used when the water is not recycled through the condenser. Although not shown in shown Figure 3.1, each chiller system has two identical chillers connected in parallel. In the case of system 3, only one of the two chillers has the condenser cooling recycle loop; the other is always cooled via the cooling tower.

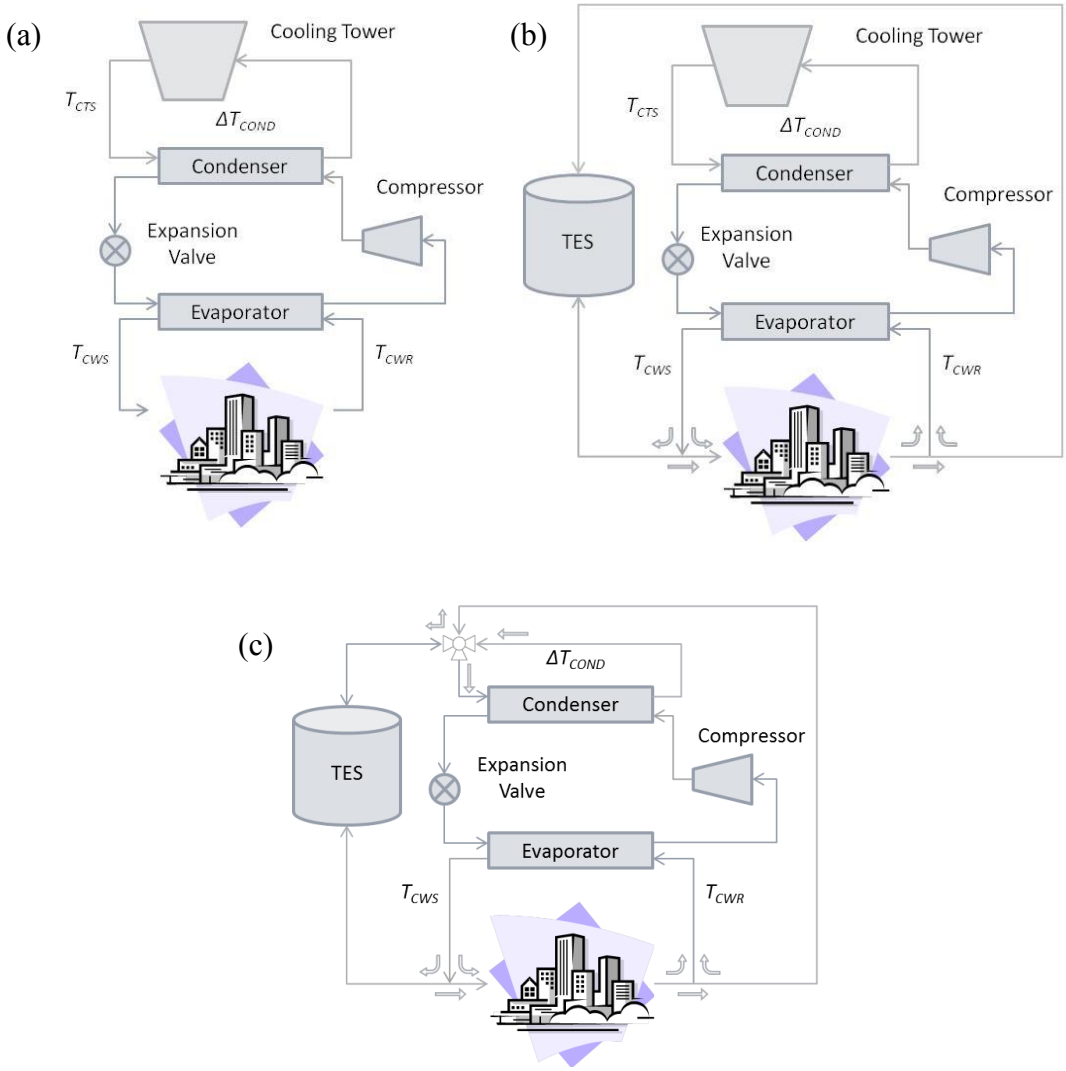

Figure 3.1: (a) System 1, chiller system with no TES, (b) System 2, chiller system with conventional TES system, (c) System 3, chiller system with TES and condenser cooling loop.

In all three cases the chillers, cooling tower, and campus chilled water loop are identical. The cooling system is sized to meet a maximum cooling demand of 6050 kW by using two identical 3025 kW centrifugal chillers. Two chillers are selected because during times of low or medium load, a single, large chiller would be operating far below

its design capacity. The temperatures of the chilled water supply (T_{CWS}) and chilled water return (T_{CWR}) are fixed at 4.4°C and 11.7°C, respectively.

Building Load Model

A section of the University of Texas at Austin campus is used to produce a realistic cooling demand for the three chiller system configurations. This section consists of five buildings: two mixed-use (classroom and office) buildings, an office administration building, a performing arts building, and a lab building. The five buildings have a total floor area of 65,500 m^2. Dynamic building cooing load profiles are calculated using DOE 2.2 building modeling software [148]. For each of the five buildings the software solves a system of ordinary differential equations (ODE) that describe the unsteady-state heat transfer in the building structure and in the building mechanical systems that include air handling units with variable air volume control. Model inputs include building and system properties, weather conditions, occupancy, ventilation rates, and internal loads. The solution of the ODEs defines the cooling load for each air handling unit at each time step. The hourly cooling demand for the chillers is the sum of cooling demand for the cooling coils in all the air handling units of the five buildings, assuming that building cooling loads are always met by the chillers. The weather data used for this analysis are the typical meteorological year (TMY2) data for Austin, Texas, USA.

Chiller System Models

For all three systems the chiller models developed in [149] are used to calculate the chiller power ($P_{CHILLER}$) at each time step:

$$CAPFT = a_1 + b_1 \cdot T_{CWS} + c_1 \cdot T_{CWS}^2 + d_1 \cdot T_{CTS} + e_1 \cdot T_{CTS}^2 + f_1 \cdot T_{CWS} \cdot T_{CTS} \quad (3.1)$$

$$EIRFT = a_2 + b_2 \cdot T_{CWS} + c_2 \cdot T_{CWS}^2 + d_2 \cdot T_{CTS} + e_2 \cdot T_{CTS}^2 + f_2 \cdot T_{CWS} \cdot T_{CTS} \quad (3.2)$$

$$PLR = Q_{EVAP} / (Q_{NOMINAL} \cdot CAPFT) \quad (3.3)$$

$$EIRFPLR = a_3 PLR + b_3 PLR^2 + c_3 PLR^3 + d_3 PLR^4 + e_3 PLR^5 + f_3 PLR^6 \quad (3.4)$$

$$P_{CHILLER} = P_{NOMINAL} \cdot CAPFT \cdot EIRFT \cdot EIRFPLR \quad (3.5)$$

where *CAPFT* is capacity as a function of temperature, *EIRFT* is energy input ratio as a function of temperature, *PLR* is part load ratio, *EIRFPLR* is energy input ratio as a function of part load ratio, Q_{EVAP} is the cooling load on the evaporator, $Q_{NOMINAL}$ is the nominal rating of the chiller (in this case 3027 kW), $P_{NOMINAL}$ is the nominal power usage of the chiller given a nominal coefficient of performance (COP) of 5.6, and a_i through f_i are constants for centrifugal chillers as given in Table 3.1. Temperatures for all equations must be in degrees Fahrenheit.

	a	***b***	***c***	***d***	***e***	***f***
CAPFT	-0.299	0.0300	$-8.00 \cdot 10^{-4}$	0.0174	$-3.3 \cdot 10^{-4}$	$6.31 \cdot 10^{-4}$
EIRFT	0.518	$-4.00 \cdot 10^{-3}$	$2.03 \cdot 10^{-5}$	$6.99 \cdot 10^{-3}$	$8.29 \cdot 10^{-5}$	$-1.60 \cdot 10^{-4}$
EIRFPLR	2.54	-7.75	15.5	-15.5	7.69	-1.50

Table 3.1: Constants used in (3.1), (3.2), and (3.4) for centrifugal chillers.

The cooling loads were calculated using the following equations:

$$Q_{EVAP} = Q_{LOAD} - Q_{TES} \quad (3.6)$$

$$Q_{COND} = 1.02\left(Q_{EVAP} + P_{CHILLER}\right) \tag{3.7}$$

where Q_{LOAD} is the combined building load given by the DOE 2 building simulation software, Q_{TES} is the cooling load met by the TES, and Q_{COND} is the load on the condenser. The 1.02 in (3.7) is included as suggested by Stanford [150, p. 116] to account for the heat added by the condenser water pumps.

The cooling tower supply temperature (T_{CTS}) is a function of the wet bulb temperature (T_w) and the temperature difference across the condenser (ΔT_{COND}):

$$\begin{aligned} T_{CTS} = {} & 9.14 + 0.771T_w + 0.00149T_w^{\,2} + \left(2.431 - 0.0196T_w - 3.51\cdot 10^{-5}T_w^{\,2}\right)\Delta T_{COND} \\ & + \left(-0.0209 - 3.91\cdot 10^{-5}T_w + 2.71\cdot 10^{-6}T_w^{\,2}\right)\left(\Delta T_{COND}\right)^2 \end{aligned} \tag{3.8}$$

To mimic realistic chiller behavior, the maximum ΔT_{COND} was limited to 8.3°C with a nominal value of 5.6°C. A variable speed pump is included on the cooling tower loop to keep T_{CTS} above 11.7°C.

The pumping through the cooling tower loop was determined using standard internal fluid flow equations. These pumping costs were included, though they amounted to less than 1% of total system costs. As a result of the small impact of pumping energy in this system, all other pumps were assumed to consume negligible amounts of energy and were not included. Pumping in the campus chilled water loop was not considered since those pumping costs are the same regardless of the system used.

The thermal storage is a chilled water tank with 19.7 MWh capacity when the temperature difference between the entering and exiting water is 7.2°C. In system 3 the potential TES capacity is 42.3 MWh since the maximum temperature difference is

15.6°C, but actual capacity depends on the actual temperature difference. The TES is assumed to have an energy efficiency of 98%, which is not unusual for a chilled-water TES system [151]. Chilled water is used instead of ice because ice requires a lower chiller evaporator temperature, thereby reducing chiller efficiency. Many investigations of optimal control of ice TES show that energy usage actually increases if ice TES is used (e.g., [138], [152]).

PROBLEM FORMULATION

The objective of the controller considered here is to minimize either electricity usage or operating costs. A time of use (TOU) rate structure from an actual utility in Austin, Texas, USA, was selected for this analysis. The rate structure has high on-peak demand charges, no off-peak demand charges, and relatively small differences between on- and off-peak electricity prices (see Table 2). Flat-rate prices are also included for comparison. Only electricity costs to run the chiller and cooling tower pumps are considered here. Other operating costs (e.g., make-up water for the cooling tower, maintenance costs) are assumed to be negligible.

A simplified storage-priority control is used for a base-line comparison. This control strategy discharges the TES at a constant rate over the peak period. For example, during a summer peak period, the TES discharges 2457 kWh of cooling energy every hour. If the load is less than this TES discharge rate, then the TES flow is reduced to match the load. The TES never discharges during off-peak hours.

	Winter	**Summer**

Time of Year	Nov 1-Apr 30	Mar 1-Oct 31
Peak Times	8am-10pm	1pm-9pm*
On-peak $/kW	$11.40	$12.54
Off-peak $/kW	$0.00	$0.00
Flat-rate $/kW	$11.11	$12.10
On-peak $/kWh	$0.04815	$0.05515
Off-peak $/kWh	$0.02815	$0.03665
Flat-rate $/kWh	$0.04605	$0.04605

*Excluding weekends, Memorial Day, Independence Day, and Labor Day

Table 3.2: The electricity rates used in the objective function of the model predictive controller. These rates are from a utility in Austin, Texas.

The controller is a model predictive controller. The controlled variables are the individual room temperature. The rooms have only two temperature set points per season: one for when the room is occupied and one for when it is not. The manipulated variables are the chilled water flow rate (which can be supplied from the chillers or to/from the TES) and, for system 3, the flow rate through the valve that recycles water to the chiller's condenser. The disturbance variables are weather and occupancy. In this investigation, only perfect predictions are considered (i.e., predicted variables are exactly equivalent to measured variables). Perfect predictions, while generally not possible in real-world settings, provide an upper-limit in savings potential.

Constraints are enforced to ensure that the system does not operate outside the acceptable operating limits of the equipment and to ensure that temperature set points are met. Because room temperatures are constrained to meet their set points, there is no opportunity to take advantage of the thermal mass of the building. In practice these

constraints could be relaxed to allow the room temperatures to fluctuate, so long as they stayed within some comfort region, but that is beyond the scope of this work.

Two objective functions are considered for the MPC: on which minimizes cost and one which minimizes energy consumption. The minimum cost objective function is

$$J = \min\left\{C_{energy} + C_{demand}\right\} \tag{3.9}$$

$$C_{energy} = \sum_{i=1}^{N} r_{elec,i} P_{elec,i} \Delta t \tag{3.10}$$

$$C_{demand} = \max_{1 \le i \le N} (r_{demand,i} P_{elec,i}) \tag{3.11}$$

where J is the overall operating cost, C_{energy} is the cost of the electrical energy used (cost for kWh usage), C_{demand} is the cost of the peak usage of electricity (cost for maximum kW draw), N is the total number of time steps in the one month billing period, $r_{elec,i}$ is the electricity rate (\$/kWh) at time i, $P_{elec,i}$ is the electrical draw (kW) at time i, Δt is the length of the time step, $r_{demand,i}$ is the demand charge (\$/kW) at time i. Service fees are not considered because those fees do not change from one billing period to the next. Computing C_{demand} presents a challenge because without the ability to predict weather, building load, and other disturbances over the entire one month billing period, it is impossible to minimize the demand costs directly. Rather, the current maximum value of P_{elec} is carried through each time step and updated whenever a new maximum in P_{elec} is reached. When the billing period concludes P_{elec} is reset to zero.

The objective function that minimizes energy consumption is

$$J = \min\left\{\sum_{i=1}^{N} P_{elec,i} \Delta t\right\}. \tag{3.12}$$

Considering total energy usage is of interest in order to investigate the potential of TES as an energy saving technology. Though not considered here, constraints or weights can be applied to the energy consumption, allowing the controller to optimize energy consumption to match a required load profile. This might have significant implications for thermal storage units connected to smart grids with high penetration of renewable energy technologies.

The problem is formulated in MATLAB and solved using sequential quadratic programming (SQP) and active-set algorithms. For the energy minimization case the problem is solved for the entire 24-hour horizon (i.e. N=24). However, for the cost minimization scenarios, the TES is always fully utilized during on-peak period, so rather than solving the problem over a 24-hour horizon, the problem is solved from the current time step to the beginning of the next day's on-peak or off-peak period. For example, if the current time step is during a peak hour, the remainder of the peak period and the subsequent off-peak period are solved. This strategy leads to prediction horizons that vary between 11 and 24 hours depending on the current time step. In the case of system 3, the optimal solution with the condenser cooling was compared to the optimal solution with no condenser cooling, and the better of those two solutions over an entire period was selected.

RESULTS

MPC-TES Performance

Annual operating costs and energy savings for the three systems are shown in Table 3.3. All configurations of systems 2 and 3 led to reduced annual operating costs over non-TES systems. The base case control scheme led to increased energy usage in

both systems 2 and 3, with very high energy increases in system 3. System 3 provided the lowest annual operating costs, but by only a marginal amount. The cost savings was achieved by shifting more peak energy to off-peak hours, even though total energy consumption was increased. This resulted in a reduction in peak energy usage costs and peak energy demand costs that was greater than the increase in off-peak energy usage costs. When (3.12) was applied to both systems 2 and 3 they produced the same result because the most energy efficient operation of system 3 is for it to act like system 2, never using the condenser cooling loop. System 3, then, adds flexibility for reducing peak energy usage, but cannot increase the flexibility of the system to achieve overall energy savings any more than system 2.

System and Controller	Objective Function	Operating Cost	Energy Usage (MWh)
Sys 1 Flat	-	$222,500	2489
Sys 1	-	$217,900	2489
Sys 2 base	-	$154,000	2495
Sys 3 base	-	$147,000	2737
Sys 2 MPC	Eq. 9, 11	$128,000	2428
Sys 3 MPC	Eq. 9, 11	$126,100	2654
Sys 2 MPC	Eq. 12	$156,400	2391
Sys 3 MPC	Eq. 12	$156,400	2391

Table 3.3: Comparison of annual operating costs and energy usage for the three systems under different control schemes. “Flat” indicates flat-rate structure. All others use the TOU rate structure.

Allowing the TES to discharge and recharge (rather than only recharge) during off-peak hours accounts for approximately $1600/year (1.3%) in cost savings and reduces energy usage by 45 MWh (1.8%). This savings is primarily accomplished by shifting loads during higher ambient temperatures to times with lower ambient temperatures with higher chiller efficiency.

Time of Year Savings

Energy savings of system 2 versus system 1 is shown in Figure 3.2. For an Austin, Texas, climate 75% of the year-round energy savings comes during the "winter" months (November-April), even though only 23% of the total year's cooling load occurs during this period. This happens in part because cooling loads are lower and variations in day and night wet bulb temperatures are greater. When there are lower cooling loads, the TES is able to prevent the chiller from operating at low part-load ratios where chiller operation is less efficient. Greater variations in wet bulb temperature mean that loads at higher temperatures can be shifted to times of lower temperatures where the chiller operates more efficiently. TES will therefore be most beneficial when applied to systems with high temperature variations and with frequent and low part-load ratios.

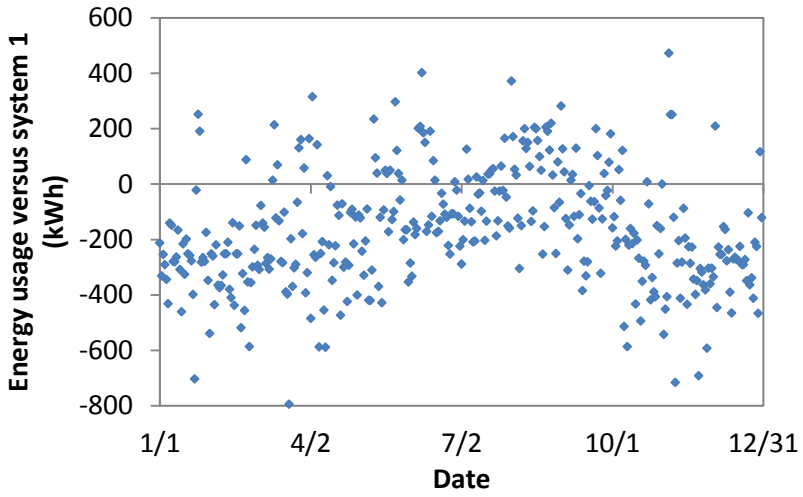

Figure 3.2: Daily energy usage of system 2 versus system 1. Negative values indicate that system 2 used less energy than system 1.

Cost savings is the reverse of energy savings. For both systems 2 and 3, 63% of the cost savings (versus system 1) occurred during the summer months, primarily due to the higher summer cooling loads that increased TES utilization. Clearly the objective (energy minimization, cost minimization, or some combination of the two) will affect the most appropriate period to be examined for an analysis.

Electrical Load Profiles

As electrical grids continue to improve and smart grid and renewable energy technologies become more commonplace, the ability to control a facility's electrical load profile will be of increasing importance. Figure 3.3 and Figure 3.4 show the load profile of system 2 when costs were minimized. Because of the rate structure, the objective function heavily penalized increases in electricity demand. Since P_{elec} is generally being established early in the month days earlier in the month have a flatter profile. Days late in the month might fluctuate but stay under the current month's maximum demand (when possible) to keep from incurring additional demand charges.

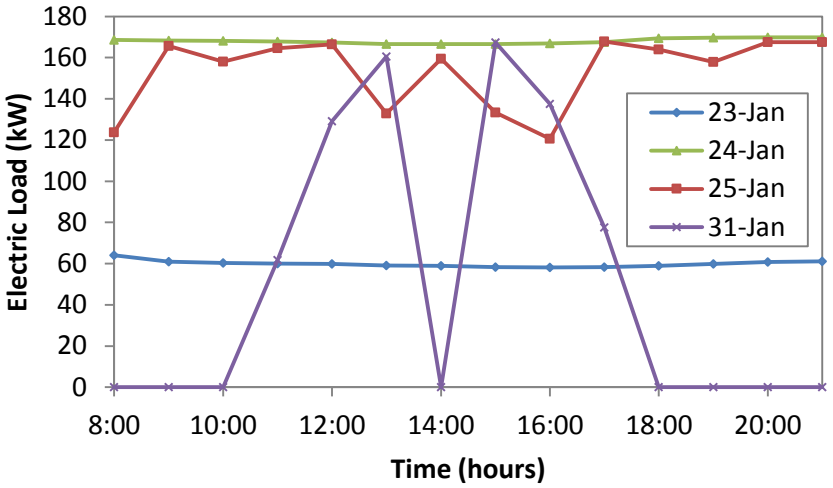

Figure 3.3: System 2 electrical load with MPC using (3.9)-(3.11) during the winter period.

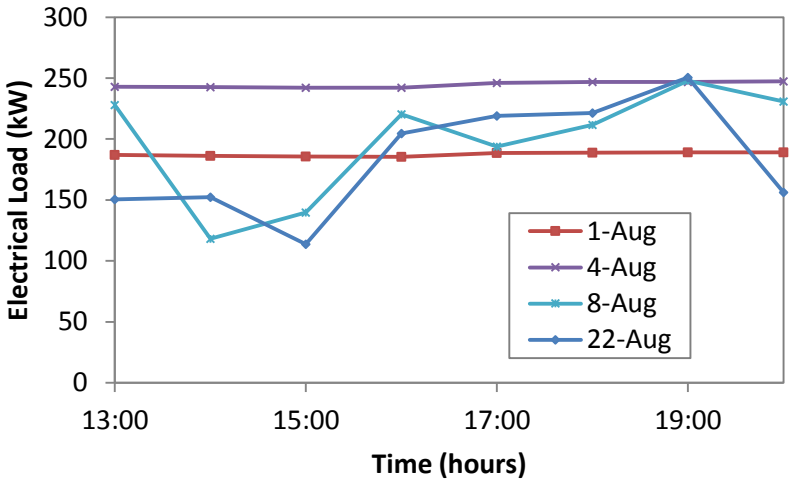

Figure 3.4: System 2 electrical load with MPC using (3.9)-(3.11) during the summer period.

Figure 3.5 shows system 3 for the same days as Figure 3.4, again using cost minimization. One obvious difference is that the electrical load profiles for system 3 are

flatter than for system 2, even on days later in the month. The reason for this is the constraint on the temperature increase across the condenser. If the chiller uses a lot of power, then it also rejects a lot of heat. If the TES flow is not sufficient to capture that heat without violating the temperature increase constraint, then the chiller load must be shifted to the second chiller that has no TES-condenser cooling, resulting in less efficient operation. The controller is encouraged to balance the load across the day, resulting in a flat electrical load profile.

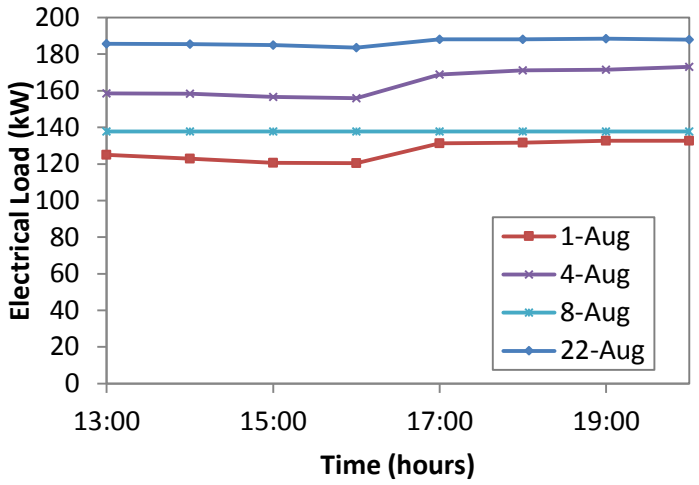

Figure 3.5: System 3 electrical load with MPC using (3.9)-(3.11) during the summer period.

When the MPC's objective function is altered to enforce demand charges on a daily basis, all electrical load profiles are flattened. This is because demand charges are so much higher than energy usage charges that priority will be given to lowering demand as much as possible. This slight change only increases annual operating costs by about $700 (less than 1%). This indicates that some significant modifications in energy usage profiles can come at very little cost.

CONCLUSIONS

The following can be concluded from this investigation:

- The TES is active during off-peak periods as loads are shifted to cooler times and low part load ratios are avoided.
- For an Austin, Texas, climate most of the energy savings (75%) occurs during the winter months, but most of the cost savings (63%) occurs during the summer months.
- Demand charges allow for a flexible electricity profile later in the month after the maximum demand has been well established.
- Rate structures with heavy demand charges hamper the ability of model predictive control systems to reduce their energy consumption.
- MPC is well suited to meet energy requirement needs while still maintaining most or all of the cost savings.

Future work includes enabling the controller to increase the chilled water temperature (e.g., from 4.4°C to 6.7°C) when buildings thermal loads are low. This gives the controller another degree of freedom to improve energy efficiency and electrical load profiles. Other work includes allowing the controller to control the electrical demand of the entire building instead of just the chiller system. That building can include intermittent energy sources (such as solar PV) or on-site cogeneration using fuel cells or microturbines. Lastly, new rate structures can be evaluated in order to identify those rate structures that will provide mutual benefit to the utility, the customer, and the environment.

Chapter 4: Integration of Turbine Inlet Cooling with Thermal Energy Storage for a Combined Heat and Power System[3]

INTRODUCTION

Cheap, clean energy has become a vital research area in recent years (e.g., [153]). However, many efforts focus on solar, wind, and other renewables, while overlooking the more efficient use of conventional power equipment. With the world so heavily reliant on fossil fuels for electrical generation [154] and with infrastructure for these systems already in place, electricity generation is an area ripe for improvements. Turbine inlet cooling (TIC) and thermal energy storage (TES) are technologies which complement conventional gas turbine power generation equipment. These technologies can potentially be used with marginally little capital investment to significantly enhance operation of gas turbine systems by increasing power production capacity and overall system efficiency. Although TIC and TES can be effectively used independently, this chapter focuses on opportunities to use these technologies together (TIC-TES systems).

This chapter is organized into three main sections: a background section, a section on TIC-TES systems, and an investigation section. The background section contains a brief description of the relevant technologies discussed in this chapter, the TIC-TES section reviews all pertinent literature on systems that couple TIC with TES, and the investigation section includes the description and results of an investigation into a TIC-TES system connected to a district cooling loop in Austin, TX.

[3] This chapter was included in W. J. Cole, J. D. Rhodes, K. M. Powell, and T. F. Edgar, "Turbine inlet cooling with thermal energy storage," *International Journal of Energy Research*, vol. 38, no. 2, pp. 151–161, 2014. Rhodes assisted in modeling the building energy loads using eQUEST. Powell assisted in building the optimization model for the TIC-TES system. Edgar contributed general advising and editing.

BACKGROUND

Turbine Inlet Air Cooling

TIC is a commercially proven technology that is used to increase power output and thermal efficiency of combustion turbines. Combustion turbine power output is rated at the ISO conditions of 15°C and 60% relative humidity. Among other factors, the power output of gas turbines depends on the mass flow rates of air passing through them. Because colder air is denser, higher mass flows can be achieved with cold air without increasing the volumetric flow. Higher mass flow rates permit higher power outputs as the air/fuel mixture is combusted and passes through the turbine. Furthermore, because it takes less mechanical work to compress a more dense fluid, the overall thermal efficiency increases. As can be seen in Figure 4.1, the power output of a combustion turbine typically decreases by 0.5-0.9% for every degree Celsius increase of the inlet air and the heat rate increases by about 0.2% per degree Celsius increase [155]–[158]. This means that as the ambient temperature increases, combustion turbines produce less power at lower efficiencies. This can be a serious problem for gas turbines that are used as peaking power plants because summertime peak hours often occur during the hottest times of the day. This also means that the maximum power production from gas turbines will vary from day to day, decreasing their flexibility and reliability to meet loads.

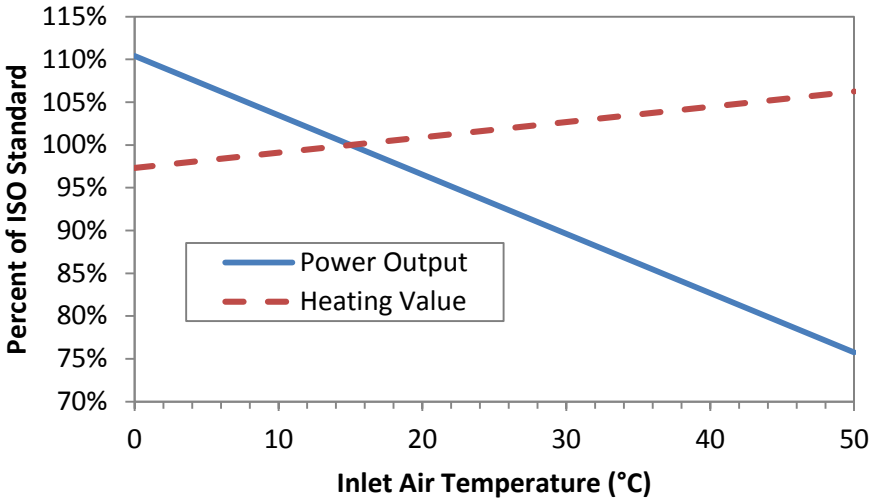

Figure 4.1. Gas turbine performance as a function of inlet air temperature. Correlations from [157] and [159].

The inlet air of a turbine can be cooled to recover this lost capacity and efficiency. There are many methods of TIC including evaporative cooling, fogging, over spraying (also called wet compression) and mechanical or absorption chilling [160]–[162].

Evaporative cooling can reduce inlet air temperatures by mixing the ambient air stream with water, thereby cooling the air stream as the water evaporates. An efficient evaporative cooling process will saturate the air stream with water vapor. Evaporative cooling methods include wetted media, where water flows over a solid material as the air passes through, and fogging, where very fine water droplets are sprayed into the air and evaporate. Over-spraying is an enhanced fogging method, ensuring that the air becomes oversaturated by spraying excess water. The additional water evaporates as the air is heated inside the compressor, absorbing more heat. Evaporative cooling, fogging, and over-spraying are simple and low-cost options, but they consume large amounts of water and are limited in capacity by ambient wet bulb temperature [163]. For example, if the wet-bulb temperature is 25°C, then that becomes the lower limit of the inlet air

temperature for evaporative-type TIC. Also, changes in ambient conditions can have small timescales and make it difficult for the plant operator to adjust. In regions with humid climates, evaporative cooling can only harvest a portion of the benefit of TIC because the wet bulb temperatures are higher. In regions where water supplies are scarce, evaporative cooling can also be limited by the availability of the water supply.

Mechanical or absorption chillers (see Figure 4.2) can cool the inlet air to as low as 4.4°C regardless of ambient conditions [164]–[166]. Below 4.4ºC, icing can occur which can cause serious damage to the turbine blades [164], [167]. These chillers, which rely on a refrigeration cycle, cool an intermediate fluid such as water or a refrigerant, which then removes heat from the turbine inlet air stream via heat exchangers. Chillers have advantages over evaporative cooling systems, as they can be used to achieve cooler air temperatures so that the TIC will have a greater impact on the gas turbine performance. However, chillers are more energy intensive than evaporative coolers and can have significantly higher capital costs. Therefore, chiller systems are more common in regions of water scarcity and high humidity.

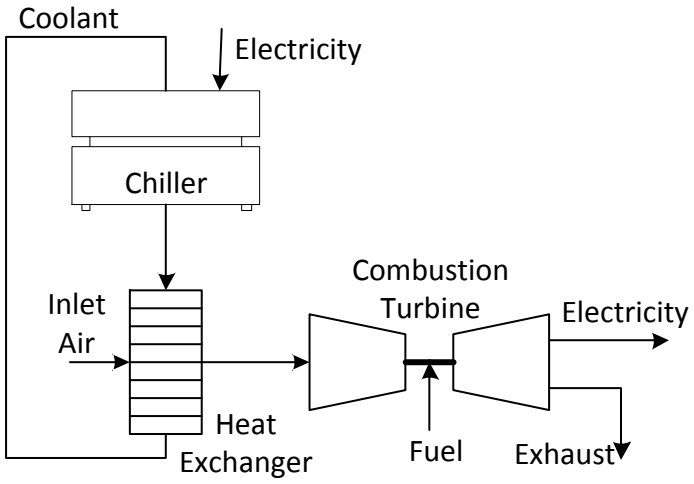

Figure 4.2: System that uses a mechanical chiller to perform TIC.

The humidity ratio (mass of water per mass of dry air) of ambient air plays an important role in TIC performance, although it has little effect on turbine performance [168]. As the humidity ratio increases, so does the heat capacity of air. Additionally, if a chiller for TIC is cooling the air past its dew point, then a portion of the water in the air is condensed. For humid climates chillers must work harder to cool the air to a given temperature. Amell and Cadavid [165] showed that for a 160 MW gas turbine the thermal load required to cool the inlet air to 4.4°C increased by 94% when the relative humidity of 30°C ambient air increased from 34% to 80%.

Also important in the TIC evaluation is the type of gas turbine used. Achievable power boosts by TIC are greater for aeroderivative turbines than for heavy duty turbines [161].

Thermal Energy Storage

TES for cooling has proven to be economical because of its ability to shift cooling loads to off-peak hours, thereby reducing on-peak electricity consumption (see Chapters 2 and 3). This is typically accomplished by storing "cold" thermal energy at night, when demands are low and cooling equipment is more efficient, and discharging the "cooling" energy during the peak times when cooling loads are very high, allowing mechanical chilling equipment to shut off. This lets the facility take advantage of pricing differences in time-of-use or real-time pricing schemes. Large-scale applications of TES could also have the potential to reduce total required electrical generation capacity, which is determined by total peak demand. Because TES for cooling has been applied most prominently to HVAC systems, it has been predominantly a demand-side energy storage technology. By coupling TES with TIC for gas turbine power generation, TES becomes a supply-side energy storage technology, giving the utility direct control over its use.

TURBINE INLET COOLING WITH THERMAL ENERGY STORAGE

Without TES, mechanical chillers must be running when the turbine is operating in order to cool inlet air, leading to high parasitic loads and reducing net turbine generation during peak hours. Turbine inlet cooling coupled with TES (TIC-TES systems, see Figure 4.3) allow mechanical chillers to be shut off during peak hours, thus reducing parasitic loads. In some cases, TES also allows the chillers or the gas turbines to be downsized and still meet the required thermal loads [169]–[171]. The chillers charge the TES during off-peak hours and the TES performs TIC during peak hours with minimal parasitic load. In order to be economical this operational strategy generally requires that electricity prices are higher during peak hours than off-peak hours [172]. Although absorption chillers can also be coupled with TES for TIC [173], nearly all TIC-TES systems use mechanical chillers as opposed to absorption chillers.

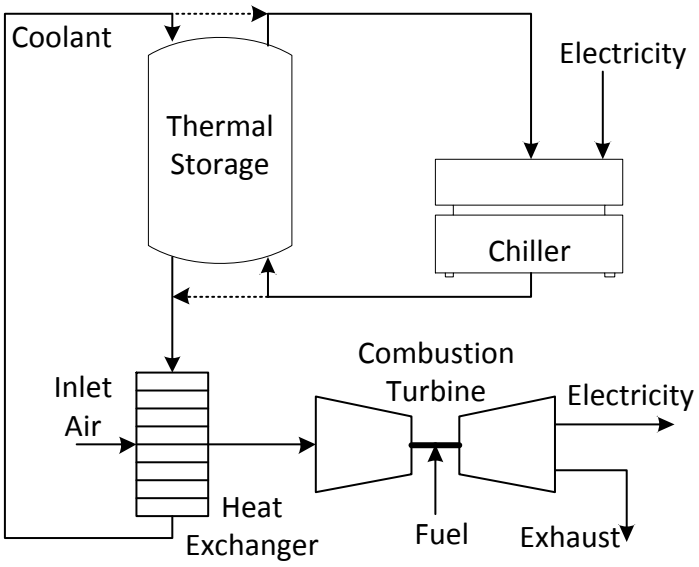

Figure 4.3: TIC-TES system using a mechanical chiller. The dotted lines show how the chiller can bypass the TES when necessary.

It appears that only water and ice have been employed as TES media for TIC. In ice TES systems the chiller has a lower coefficient of performance (COP) and higher capital cost, but the TES storage size is much smaller and the turbine inlet air can be cooled to lower temperatures, resulting in higher capacity and efficiency for the turbine. Chilled water TES will typically have a chiller that operates at a higher COP, but will have a much larger storage tank and will not be able to cool the turbine inlet air to temperatures as low as ice TES. Chilled water stored in aquifers (ATES) has also been examined, but high capital costs and difficulties in finding suitable aquifers have reduced its usability [174], [175].

The choice between water and ice TES for TIC was examined by Ameri et al. [157] to improve the power output of two 37.5 MW and two 16.6 MW turbines that lost up to 30% of their capacity during the hottest parts of the summer. They created five cooling scenarios ranging from the lowest summer cooling load to the highest summer cooling load and simulated each scenario using ice or chilled water TES. They chose a chilled water TES as the most economical option for TIC with a payback period of 3.66 years and a rate of return of 27.4%. The reason for the positive economic outlook was the ability to sell extra power during peak hours when electricity prices were highest while using cheap off-peak power to charge the TES at night. In all cases they examined, chilled water TES economically outperformed ice TES, primarily because chillers capable of making ice have a higher capital cost and lower efficiency. Modeling of TIC-TES systems by Cross et al. [176] also found chilled water TES to be more economical than ice TES.

Palestra et al. [177] demonstrated the importance of choosing the appropriate TIC-TES location along with size and type. They simulated four scenarios: a chilled water TES for Northern and Southern Italy, and ice TES for the same locations. In all

cases the TES was sized to meet 50% of the cooling demand on the hottest day. Following the simulation cases they performed a parametric analysis on the TES size. The simulation results indicated that ice storage had better economics, but the parametric study showed that chilled water TES ultimately had a lower payback period. Site location proved to be a very important variable due to climate differences—the net present value (NPV) of the Southern Italy site was nearly double that of Northern Italy. The importance of climate was also demonstrated by Boonnasa and Namprakai [178] who performed an economic analysis for TIC in Thailand where temperatures never dropped below the ISO condition of 15°C. They found that all observed cooling scenarios had payback periods of less than 1 year using absorption chilling, which proved to be more economic than including chilled water TES [173].

Popular choices for making investment decisions for TIC-TES systems include NPV, internal rate of return (IRR), and payback period [14]. The different metrics might point to different optima; considering them together allows one to make a more informed choice. For example, Palestra et al. [179] examined 6 TIC scenarios with various combinations of chilled water TES and turbine supercharging systems. They performed a parametric study by varying the inlet air temperature. The maximum NPV occurred with a turbine inlet temperature of ~12°C, but the minimum payback period occurred with ~16°C inlet air temperature.

Work by Chacartegui et al. [180] also demonstrated the importance of multiple economic metrics. They examined different TIC technologies, including evaporative media, two-stage fogging, mechanical chillers, gas chillers, steam chillers, absorption chillers, and ice thermal storage, for a CHP facility in Southern Spain. They found fogging to have the lowest payback (1.5 years), but its NPV was also very low due to its inability to cool below the wet bulb temperature. Mechanical chillers with TIC-TES had

higher NPVs compared to the non-TES systems. As an additional metric, they also showed the significance of installation time in choosing a TIC technology. Since the CHP facility examined was for a chemical plant, the cost of not operating the plant for one day was much greater than the cost difference between choosing one TIC technology over another.

A need remains for long-term validations of TIC-TES systems. Most reports only include projected results and only a few contain initial performance results. For example, Al Bassam and Al Said [181] reported the performance of a new six-turbine power plant with ice TES for TIC. They showed that the TIC-TES system increased the turbine electrical output by 22-26% for two days during commissioning, however no long-term performance was given.

Optimization of TIC-TES Systems

The addition of TES to TIC provides extra degrees of freedom in managing power generation and consumption. Optimization can be employed to best take advantage of this extra freedom. In optimization, an objective function (also called a performance index) that is to be minimized (or maximized) is defined. For example, objective functions for TIC-TES systems could be maximizing profit, electricity production, or efficiency. An optimization algorithm is employed that finds the optimal value of the objective function subject to any constraints imposed on the system. Common algorithms include interior point algorithms, sequential quadratic programming, and the simplex algorithm, though many others exist. For more information on optimization see [14].

Sanaye et al. [182] optimized a TIC system that incorporated mechanical chillers and ice TES. They employed two objective functions; the first included the capital and operational costs, and the second added an exergy destruction cost rate. No revenue terms

from the sale of electricity were included. The decision variables were compressor pressure ratio, air compressor isentropic efficiency, turbine isentropic efficiency, turbine inlet temperature, and refrigeration system evaporating pressure and condensing pressure. A genetic algorithm was used to solve the optimization problem. The use of the exergy destruction cost rate in the second objective function pushed the optimal design parameters towards more thermodynamically efficient values. The addition of TES to TIC increased the power output by 3.9-25.7%, the efficiency by 2.1-5.2%, and the payback from 4-7.7 years.

Arnulfi et al. [183] found the chiller and ice TES sizes of a TIC-TES system by maximizing NPV using a genetic algorithm. A 1°C increase in the maximum daily temperature range for a climate increased the optimal chiller size by 0.9% and the TES volume by 1.8%. They observed that economics of a TIC-TES system are much more sensitive to price variations than to variations in climate parameters. When the objective function was changed to minimize the payback period instead of NPV the optimization results led to smaller chiller and TES sizes and payback periods of 1-2 years. Optimal configurations led to a 3% increase in gas turbine efficiency.

Yokoyama and Ito [184] formed a mixed-integer linear programming (MILP) problem to minimize the unit sizing and cost of a cogeneration plant with ice TIC-TES. The objective function was the total annual cost of the plant which included equipment capital costs and the demand and energy charges from the utility, but ignored operation and maintenance costs. The optimization model included binary variables that differentiated between electricity purchased from the grid and electricity generated using the gas turbine. The optimization model was then linearized. The problem was solved using the branch and bound method combined with the Simplex method. They compared the results from the optimization to a cogeneration plant with ice TES that did not

perform TIC. The TIC system increased the optimal capacities of the gas turbine and ice storage, and decreased the optimal size of the conventional equipment. Costs over six representative days showed that the optimal solution with TIC reduced total costs by 1.1%.

Investigations of the optimization of TIC-TES systems are very limited, but they do provide an insight into why optimization is a beneficial tool for analyzing and improving TIC-TES systems. Optimization has only been performed on ice TIC-TES systems, and no optimization work has been done to compare ice TES and chilled water TES for TIC. There is significant potential for the development and application of optimization to TIC-TES systems.

There is also significant potential for the development of advanced controllers that can improve performance of TIC-TES systems. For example, in an application of TES to meeting a campus cooling load, Ma et al. [111] found that the TES for the chilled water loop was being overcharged, and implementation of a model predictive controller was able to help operators forecast future energy needs and reduce the amount of energy spent charging the TES. Controllers that can forecast electricity prices, weather, and electrical and thermal loads and then generate dynamic set points for the times and rates of TES recharge/discharge can increase the profitability of installed TIC-TES systems. For example, if tomorrow's weather predictions show that temperatures will be very high and that the peak demand will be very long, it might be optimal to only cool the inlet air to 18°C or 20°C (as opposed to 5-10°C) so that the TES has a longer discharge duration. Also, chiller efficiency is a function of ambient conditions. As the ambient temperature increases, chiller efficiency decreases. A predictive controller would be able to take into account changing chiller efficiencies as it determines when is the best time to consume electricity in order to recharge the TES.

Applying predictive controllers to TIC-TES systems would also increase the value of TIC-TES systems in the smart grid. By providing the turbine the ability to produce maximum power "on-demand" from the TES, the TIC-TES system becomes a "supply response" system, capable of quickly altering the amount of electricity supplied in order to meet changing loads. Gas turbines with TIC-TES in a distributed generation or micro-grid setting will have expanded flexibility in participating in the ancillary services market or in the smart grid.

Cost of TIC-TES Systems

The cost of TIC-TES systems vary based on chiller type, storage media, capacity requirements, and location. Specific costs of $141-454/kW of added power output have been reported (see Table 4.1). The cost of adding new combined cycle gas turbine capacity is on the order of $200-800 [185].

Reference	System Type	Size	Cost	Source
[181]	Ice Harvester	13000 m^3 / 19340 kWh	\$141-194/kW[i]	"the consultant"
[186]	Ice Harvester	131500 kWh	\$165/kW	Actual Cost
[176]	Chilled Water Ice Hybrid[ii]	Not specified Not specified Not specified	\$172-385/kW \$260-454/kW \$211-428/kW	Simulation
[174]	Not specified	Not specified	\$165/kW	[187]
[172]	Not specified	Not specified	\$150-250/kW	[155]
[155]	Not specified	Not specified	\$150-250/kW	[167]
[167]	Chilled Water Ice	- -	Formula[iii] Formula[iv]	Equipment vendors, published literature, and cost handbooks

[i] Reported costs were 530-731 Saudi Arabian Riyals/kW. A conversion rate of 0.267 was applied.
[ii] The hybrid system includes both water and ice TES.
[iii] $Cost = 572.4(Capacity)^{0.75}$ Where *Cost* is in dollars and *Capacity* is in ton-hrs.
[iv] $Cost = 163.6(Capacity)^{0.75}$ Where *Cost* is in dollars and *Capacity* is in ton-hrs.

Table 4.1: Summary of costs for TIC-TES systems as reported in literature.

Sanaye et al. [182] also included capital cost information. They listed all TIC-TES components separately (air compressor, combustion chamber, storage tank, refrigeration compressor, etc.) in equation form, so their cost information was not able to be included in the table above.

INVESTIGATION OF A TIC-TES SYSTEM IN A DISTRICT COOLING NETWORK

System Description

This analysis considers a unique configuration of a TIC-TES system. Instead of simply investigating the system shown in Figure 4.3, this investigation considers a TIC-TES system that is integrated in a district cooling loop in Austin, Texas (see Figure 4.4). The chillers in the loop are responsible for charging the TES, providing TIC, and cooling the buildings on the loop. When charged, the TES is able to supply cooling for TIC and/or for the buildings.

The system contains two identical centrifugal water-cooled chillers with a combined thermal capacity of 9230 kW. The centrifugal chiller models were the same as those presented in Chapter 3 which are based on the steady-state empirical model by Hydeman et al. [149]. The TES is a stratified chilled water tank with a capacity of 28000 kWh and can be discharged or recharged at up to 7000 kW. The gas turbine for this system is a Solar Mercury 50 turbine with a nominal capacity of 4.3 MW. The gas turbine model is a linear, empirical steady-state model that depends only on the inlet air temperature. The turbine is assumed to always operate at full-load (the actual turbine system from which the data were taken always operates at full-load). A heat recovery steam generator harvests much of the heat from the exhaust which is used to meet local steam requirements. Absorption cooling is not considered due to the lack of available steam.

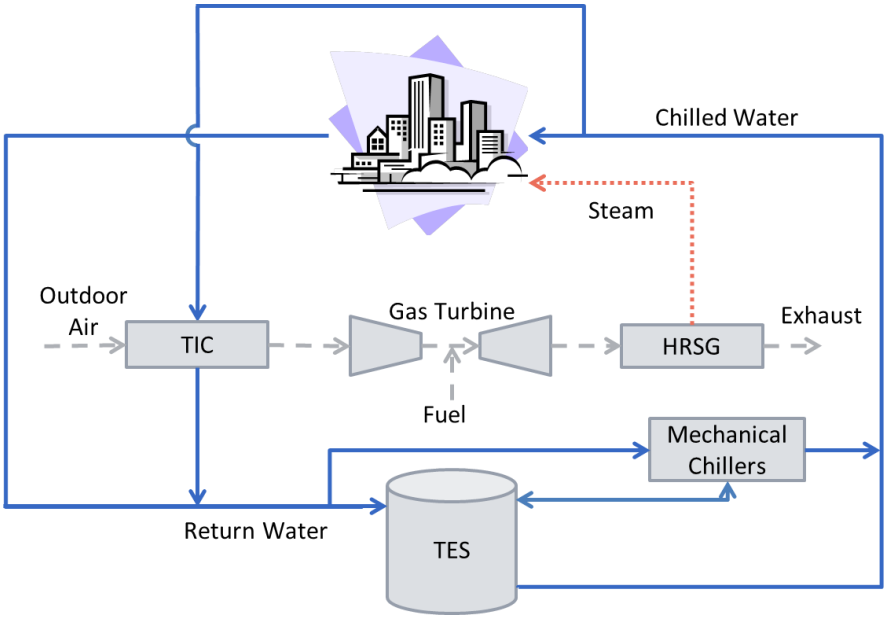

Figure 4.4: Schematic of TIC-TES system that is incorporated in a district cooling loop. The solid arrows represent water streams, the dashed arrows represent gas streams (e.g., air, natural gas), and the dotted line represents steam. The building icon represents all the buildings in the district cooling loop. HRSG stands for heat recovery steam generator.

To mimic realistic loads placed on the system, an actual district cooling loop in Austin, Texas, with a 4.3 MW Solar Mercury 50 gas turbine was simulated. Building cooling demand profiles were modeled using the eQUEST building energy simulation software [188]. Buildings of interest were those that draw cooling from the district-cooling loop associated with the TIC-TES system. These buildings are mostly associated with Dell Children's Hospital, including outpatient treatment facilities, physician's clinics, research facilities, administrative offices, and the hospital itself. In order to gather the size and geometry of the buildings, the buildings were first imported into Google SketchUp [189] using Google Building Maker [190]. Google SketchUp is a free computer aided drawing software package. Google Building Maker is a web-based

application that projects highly detailed aerial imagery as 3D objects in SketchUp. These objects can then be measured for size and then used as inputs into eQUEST.

eQUEST allows building geometry to be as simple or complex as desired. For example, one can set a percentage of a wall to be fenestration, or manually place windows and doors where needed. There are many default building types that can be used. When setting up a simulation, one can assign a certain building type that comes with standard constructions and operating schedules. These standards and schedules can be overwritten if needed. eQUEST simulates building energy usage by discretizing time into hours of the year and then writing and solving dynamic mass and energy balances. The simulation also responds to various stimuli such as temperature set point changes and building user schedules.

Once building geometry, type, and schedules are selected, a weather file is needed for simulation. Weather files are typically retrieved from the National Renewable Energy Lab (NREL) weather file database and consist of typical meteorological year (TMY) data. TMY data files consist of a "standard" year of meteorological data that represents the weather of a given location [191]. However, since replicating building cooling loads for 2011 was of greater concern (in order to match with 2011 electricity prices), the TMY file was edited to include actual 2011 weather data [192]. The measured data included 2011 Austin dry bulb temperature, relative humidity, wind speed, and wind direction. Actual solar irradiation data was not available, so TMY solar irradiation data were used in the simulations.

The electricity prices used for this analysis were the day-ahead settlement point prices (SPP) for the Austin load zone in the Electric Reliability Council of Texas (ERCOT) market for 2011. Thus the electricity prices corresponded with the weather

conditions used to generate the building cooling loads for the year 2011 for Austin, Texas. A natural gas price of $5/MMBTU was used.

Analysis Methods

An optimization problem was formulated to determine the optimal operation of the system shown in Figure 4.4. No design parameters were considered. The formulation is a receding horizon, multi-period optimization problem where predictions are used to determine the optimal operation *N* time steps into the future. While optimal inputs to the system during the entire time horizon are obtained in the solution, only the inputs for the first time horizon are actually implemented. The problem is re-solved at every time step to account for any deviations in measured variables versus model predictions. This technique is analogous to the popular moving horizon model predictive control framework [193]. The optimization problem was formulated as follows:

$$J = \max \sum_{i=1}^{N} \left(c_{elec,i} \left(P_{CHP,i} - P_{chiller,i} \right) - c_{fuel} m_{fuel,i} \right) \tag{4.1}$$

subject to

$$L_{chiller,i} = L_{building,i} + TIC_i - TES_i \tag{4.2}$$

$$P_{chiller,i} = P_{nominal} \cdot CAPFT_i \cdot EIRFT_i \cdot EIRFPLR_i \tag{4.3}$$

$$P_{CHP,i} = a + b\left(DBT_i - \frac{TIC_i}{m_{air,i} C_{p,air}} \right) \tag{4.4}$$

$$m_{fuel,i} = d + c\left(P_{CHP,i} \right) \tag{4.5}$$

$$l_1 \le TES_i \le u_1 \tag{4.6}$$

$$0 \le TIC_i \le u_2 \tag{4.7}$$

$$0 \le C_{TES,i} \le u_3 \tag{4.8}$$

where $c_{elec,i}$ is the price of electricity at time i, $P_{CHP,i}$ is the amount of additional electrical power produced by the CHP unit because of the TIC at time i, $P_{chiller,i}$ is the electrical power consumed by the chillers at time i, c_{fuel} is the price of the natural gas fuel, $m_{fuel,i}$ is the amount of extra fuel burned due to the TIC at time i, $L_{chiller,i}$ is the cooling load provided by the chillers at time i, $L_{buildings,i}$ is the cooling load required by the buildings at time i, TIC_i is the amount of cooling required for TIC at time i, TES_i is the amount of cooling provided by the TES (when it is negative it means that the TES is recharging, i.e., requiring rather than providing cooling), $P_{nominal}$ is the nominal power usage of the chiller given a nominal coefficient of performance (COP) of 5.6, DBT_i is the dry bulb temperature at time i, $m_{air,i}$ is the mass flow rate of air at time i, $C_{p,air}$ is the heat capacity of air, a, b, d, and e are fitting parameters estimated from the turbine operating data, l_1 is a lower bound, and u_1, u_2, and u_3 are upper bounds of their respective variables. Functions *CAPFT*, *EIRFT*, and *EIRFPLR* describe the nonlinear chiller model based on [149] and are shown in equations (4.9)-(4.12) (these are the same set of equations that were used for the chiller system in Chapter 3):

$$\begin{aligned} CAPFT_i = a_1 + b_1 \cdot T_{CWS,i} + c_1 \cdot T_{CWS,i}^2 + d_1 \cdot T_{CTS,i} \\ + e_1 \cdot T_{CTS,i}^2 + f_1 \cdot T_{CWS,i} \cdot T_{CTS,i} \end{aligned} \tag{4.9}$$

$$\begin{aligned} EIRFT_i = a_2 + b_2 \cdot T_{CWS,i} + c_2 \cdot T_{CWS,i}^2 + d_2 \cdot T_{CTS,i} \\ + e_2 \cdot T_{CTS,i}^2 + f_2 \cdot T_{CWS,i} \cdot T_{CTS,i} \end{aligned} \tag{4.10}$$

$$PLR_i = Q_{evap,i} / (Q_{nominal} \cdot CAPFT_i) \tag{4.11}$$

$$EIRFPLR_i = a_3 PLR_i + b_3 PLR_i^2 + c_3 PLR_i^3 + d_3 PLR_i^4 + e_3 PLR_i^5 + f_3 PLR_i^6 \quad (4.12)$$

where *CAPFT* is capacity as a function of temperature, *EIRFT* is energy input ratio as a function of temperature, *PLR* is part load ratio, *EIRFPLR* is energy input ratio as a function of part load ratio, T_{CWS} is the chilled water supply temperature, T_{CTS} is the cooling tower supply temperature (i.e., the temperature of the water that the cooling tower supplies to the chiller's condenser), Q_{evap} is the cooling load on the evaporator, $Q_{nominal}$ is the nominal rating of the chiller (in this case 4615 kW), and a_i through f_i are constants found by fitting the equations to actual chiller operating data. Note that T_{CTS} is a function of the wet bulb temperature and that all of these calculations are performed at each time step *i*.

The decision variables are TES_i and TIC_i. The number of decision variables, therefore, depends on the number of time steps, *N*, considered in the prediction horizon. Looking 24 hours into the future with time steps of one hour, for example, means that there are 48 decision variables.

The thermal storage tank is modeled as an ideally stratified tank with a 2% parasitic energy loss every time water is removed from or added to the tank. The loss term allows the model to behave externally as an actual stratified tank while maintaining the simplicity of an ideally stratified tank. The end results in efficiency are in line with the modeling comparison provided by [194].

An alternative objective function was also considered (subject to the same constraints), which minimized the amount of electricity consumed from the grid:

$$J = \min \sum_{i=1}^{N} \left(P_{CHP,i} - P_{chiller,i} \right) \quad (4.13)$$

The optimization problem was formulated in MATLAB and solved using the sequential quadratic programming (SQP) algorithm. The optimization was performed over the entire year of 2011 using the models described in the system description (i.e., the problem in (4.1)-(4.12) was solved 8760 times).

To provide a benchmark for measuring the effectiveness of this optimization-based control strategy, an on-off control strategy was also considered. In the on-off control strategy, the TES is discharged during a predefined peak period (1-9pm) and then recharged beginning at midnight.

RESULTS

Three typical summertime charge/discharge periods from using the maximum profit optimization strategy for the TES are shown in Figure 4.5. The tank is filled to maximum capacity during times when the electricity day-ahead settlement point price is lowest and discharged when the settlement point price is highest. Electricity prices (as opposed to weather or chiller loading) tend to dominate the TES charging and discharging.

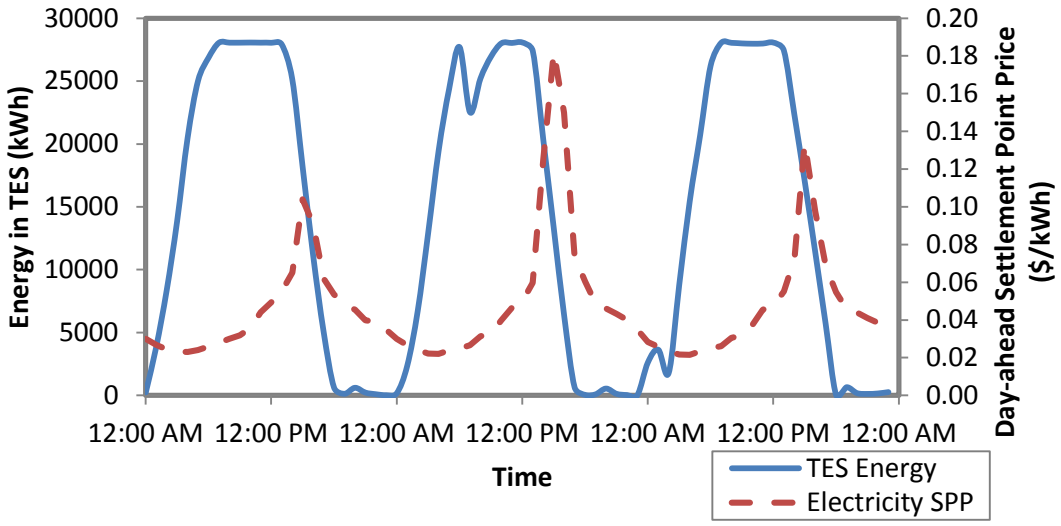

Figure 4.5: Energy remaining in storage during July 6-8. The maximum capacity of the TES is 28000 kWh.

The TES operation is quite different during the wintertime. The electricity prices during the winter are often "double-peaked"—there is a morning peak and an evening peak. This causes the TES system to be more active. Three typical wintertime periods are shown in Figure 4.6. During the cooler months, the storage tank is often not charged all the way because smaller amounts of cooling are needed.

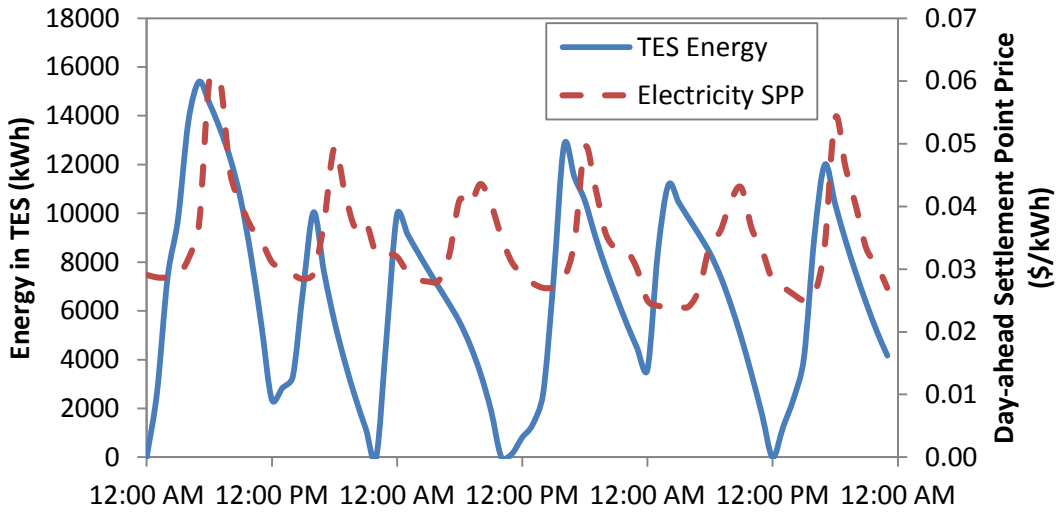

Figure 4.6: Energy remaining in storage during January 14-16. Note the "double-peak" in the electricity prices, and that the storage tank never reaches full capacity (28000 kWh) due to low cooling requirements.

The effect of the TIC-TES system on the gas turbine power output is shown in Figure 4.7. When there is no TIC, the power output follows the same pattern as the ambient dry bulb temperature, reaching a low in the mid-afternoon when electricity is most needed. For the Austin climate, the wet bulb temperature is nearly constant, so an evaporative TIC system would provide a near-constant power output, though it is still under the turbine rated capacity of 4.3 MW. With the TIC-TES system, inlet air cooling occurs when it is economical to do so. During several hours of the night, no TIC occurs because electricity prices are at their lowest. In the morning (~7:00 am) the TIC cools the air to near the wet bulb temperature in order to provide some power increase without the need to condense any water out of the air. As the electricity prices rise later in the morning, the TIC cools at full capacity, increasing turbine power output to well above the rated capacity of 4.3 MW. An important result of the TIC-TES system is that it decouples

the turbine power output from ambient conditions, giving the system more flexibility in responding to price signals from the grid.

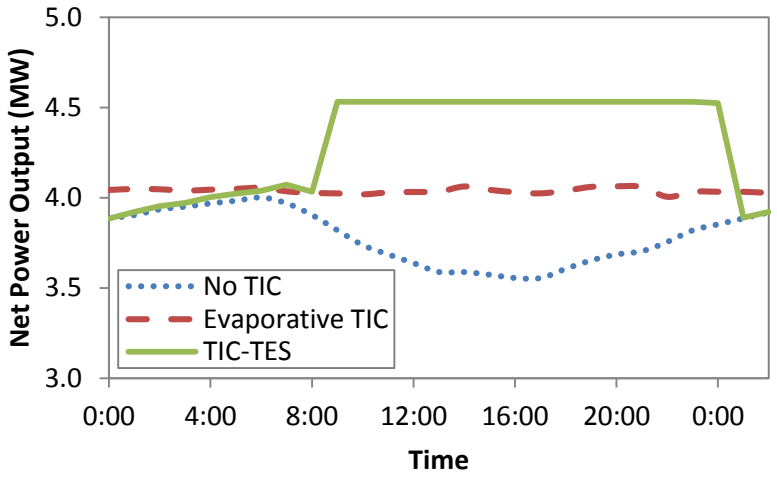

Figure 4.7: Gas turbine power output for July 25. The TES is used in conjunction with the TIC to raise the turbine capacity above the rated capacity during the daytime hours.

The savings obtained from employing optimization are shown in Table 4.2. A significant portion of the savings can be achieved from simply using the TES with the on-off control strategy. The optimization strategy further enhances savings. Using cost estimates of $20-33/kWh (which are in line with [42], [155]), this gives a 3-5 year simple payback period for the TIC-TES system, down from 4.4-7.3 if only the on-off strategy is used. The NPV under the optimal strategy (using a 6% discount rate and a 10-year life) ranges from $411,000-760,000, with a corresponding IRR of 15.1%-31.1%. The wide range in the payback period, NPV, and IRR is due to the uncertainty in the capital costs of the TIC-TES system. Using the on-off control strategy, the NPV ranges from $10,800-359,000 and the IRR ranges from 6.3%-18.8%.

	No TES	On-off Control Strategy	Optimal Strategy
Chiller Costs	$376,600	$252,400	$204,000
TIC Revenue	$141,800	$144,700	$154,000
Net Cost	$234,800	$107,700	$50,000
Change in Chiller Costs	-	33% Decrease	46% Decrease
Change in TIC Revenue	-	2.0% Increase	8.6% Increase
Change in Net Cost	-	54% Decrease	79% Decrease

Table 4.2: Comparison of chiller costs, TIC revenue, and net cost without TES, using the on-off control strategy, and using the optimal strategy. TIC revenue is the additional revenue gained from operating the TIC. All values are on an annual basis. The changes in costs are based on the "No TES" costs.

Value of TES

As discussed previously, one primary benefit of including TES for TIC is that the TES can perform the TIC in order to reduce the parasitic load that would otherwise be incurred by the chillers. Under the optimal control strategy the TIC increases the annual electrical energy production from the turbine by 4864 MWh. To perform this TIC without TES, the chillers consume 403 MWh of electric energy, meaning that the parasitic load from operating the chillers for TIC is 8.3%. However, because electricity rates are generally higher during warmer periods, this 8.3% parasitic load corresponds to a 20% decrease in TIC revenue (TIC revenue is the additional revenue gained from operating the TIC). The parasitic losses due to the chiller are over twice as great when considered in terms of costs rather than energy loss for this scenario. This also means that the addition of TES to a TIC system can increase profits by up to 20%. The reason the total savings for this entire system is much higher is that TES serves not just the TIC system, but also the buildings in the district cooling loop.

TES value can also be examined in terms of its ability to reduce electricity demand. Once charged, the TES can be used for providing TIC or for providing cooling to the buildings' air handling units for space cooling. By sending the TES chilled water to the buildings, the load that must be supplied by the chiller is reduced. For the year investigated here, the chillers operated with coefficients of performance (COP) of 3.9-8.8. This means that for every kW of cooling provided by the TES, the chiller's electricity demand was reduced by 0.11-0.26 kW. When the TES is used to provide TIC, the electrical output of the turbine is increased by 2-2.3 kW for every kW of cooling. In terms of power consumption (considering production as negative consumption), the value of cooling for TIC is an order of magnitude greater than the value of cooling for a building. In a system with a limited amount of cooling capacity that has both building cooling loads and TIC loads, the TIC cooling loads will always be given preference if the objective is to consume the least amount of power.

While the results of this study clearly show the benefits for operational cost savings of using TES with TIC, the capital investment required to install such a system is the main disadvantage. Therefore, when considering such an investment as an upgrade to a district cooling system with power generation, it is critical to consider the payback period and rate of return on such an investment. Typically, there is an economy-of-scale benefit associated with TES, which is the predominant reason that TES systems are most common in district cooling systems, where the maximum benefit/cost ratio can be achieved.

Effects of Prediction Horizon

In the scenario examined in this chapter, the chillers are large enough to meet the 2011 building loads, but not large enough to meet the building loads and the TIC loads.

This makes the TES especially valuable, since the TES allows the system to meet the combined cooling load without adding additional chiller capacity. In implementing a multi-period optimization scheme (i.e. N>1) to determine the best operating strategy for the TES and TIC, it is important that some level of forecasting is used. If no forecasting is used, the optimization strategy will never use the TES since it will never be optimal to charge the TES. This case reduces to the case where TES does not exist in the system. Using longer prediction horizons allows the controller to charge the tank in preparation for discharging during peak times when electricity is most expensive. In this investigation, the optimal prediction horizon was found to be 12 hours, though a time horizon of 10 hours comes within 1% of the optimal and would be sufficient for practical purposes. Net energy cost versus prediction horizon is shown in Figure 4.8.

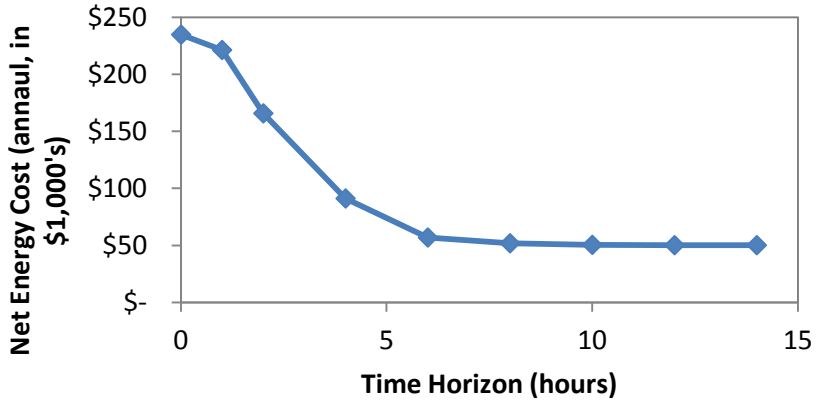

Figure 4.8: Annual chiller costs versus the time horizon (N) used in the optimization.

Effects of Objective Function

In the case where the objective function is changed to minimize the amount of energy consumed from the grid (Equation 13), the TIC always operates unless the outside air temperature is below the chilled water temperature. The chiller works in conjunction

with the TES to minimize energy usage. The chiller costs in the minimum energy scenario are $306,200, and the electricity production revenue from using the TIC is $143,900, yielding a net cost of $162,300. The annual net energy drawn from the grid is reduced from 2973 MWh to 837 MWh, a 72% reduction. This is accomplished entirely through the additional electricity production from running the TIC whenever possible. The chillers actually consume more electricity in this scenario because they are required to meet the additional load imposed by the more active TIC.

The system can be operated so that grid electricity is reduced by 72%; however, net annual costs increase by $112,300. A modified objective function could then be considered to allow the TIC to operate whenever the temperatures are above the chilled water temperature and then minimize the cost of the chiller operation as before. In this case, grid electricity consumption is 871 MWh, just 4.1% higher than the minimum energy case. This strategy increases net costs from $50,000 to $64,700. Thus, for a relatively small cost, a facility such as this could move significantly closer to net zero grid electricity consumption. The reason the cost is so small is that the cooling equipment efficiency generally follows the day-ahead settlement point price—when the electricity prices are lower, the equipment efficiency is generally higher, and when the electricity prices are higher, the equipment efficiency is generally lower.

CONCLUSIONS

Turbine inlet cooling (TIC) increases the power output and efficiency of gas turbines during periods of warmer ambient temperature. Evaporative-type cooling is cheap and often effective, but it is limited by the ambient wet bulb temperature and water availability. Chillers can provide much more cooling than evaporative methods, but are capital intensive and have high parasitic electrical loads. Adding thermal energy storage

(TES) shifts the chiller's cooling load to increase chiller efficiency and allows turbine inlet cooling to take place during peak hours without the chillers running. Because of the ability of TIC-TES systems to cool below the wet bulb temperature, they can have higher economic benefits than evaporative-type cooling which leads to higher NPV. However, because of the higher capital costs of the systems, the payback periods of TIC-TES systems are typically greater.

A year-long investigation was performed on a TIC-TES system connected to a district cooling loop. The system investigation was based on an actual district cooling system in Austin, Texas, and used real Austin weather and electricity pricing data for 2011. By applying multi-period optimization to determine system operation, cost savings of 79% were achieved. The benefits of the optimization were greater for the district cooling system than for the TIC system.

However, in terms of electrical power, the TIC system benefits far more from the TES cooling energy than the district cooling system. It was also found that the parasitic losses on TIC cooling are much greater when considered in financial rather than energetic terms in a time-of-use pricing scenario.

When the objective function was changed to minimize energy consumed from the grid, the TIC was able to provide significant grid energy reduction at relatively little cost. However, minimizing the energy of the district cooling system was costly and provided little energy savings. By minimizing energy consumption using the TIC while simultaneously minimizing cost using the district cooling system a reasonable compromise was achieved.

Chapter 5: Reduced-order Residential Home Modeling for Model Predictive Control[4]

INTRODUCTION

As of 2011, there were over 132 million housing units in the United States [195], 87% of which had air conditioning units [196]. In the southern United States, the percentage of homes with air conditioning approaches 100% [196]. These air conditioning units tend to exacerbate peak demand issues. For example, during the 2011 summer peak in the ERCOT (Electric Reliability Council of Texas) grid, over 50% of the total electrical load was from residential homes [197], whose loads were primarily driven by their air conditioning systems. Because of this, the residential sector has enormous potential to be a key player in the future of grid management.

Modeling tools have been developed to help understand the best way to manage building energy consumption, primarily heating, ventilation, and air conditioning (HVAC) energy consumption. Models provide insights into a building's design and operation that can lead to significant cost savings over the lifetime of the building. Some building certification programs (e.g., LEED) even require building simulation to be performed.

From the building operation side, model predictive control (MPC) has become increasingly popular for determining the optimal operation of building HVAC systems [198], so much so that new software that helps to evaluate MPC methods for building controls and help educate building control engineers about MPC tools have been recently developed [199]. Model predictive control uses a model of the system that is being

[4]This chapter was included in W. J. Cole, K. M. Powell, E. T. Hale, and T. F. Edgar, "Reduced-order residential home modeling for model predictive control," *Energy and Buildings*, vol. 74, pp. 69–77, 2014. Powell contributed the neural network modeling work, and Hale contributed expertise in using the OpenStudio analysis package. Edgar provided general advising and editing.

controlled to determine optimal controller actions. These control actions are generally implemented on a receding horizon basis, meaning that after an optimal control sequence is calculated, only the first control action is actually implemented. The problem is then updated with new data at the next time step and re-solved to determine the next control action.

Creating a suitable dynamic building model is one of the primary challenges of MPC [198], [200]. Accurate high-order dynamic models are readily available, but are generally not suitable for optimization and control algorithms. The higher-order models can be computationally expensive and often have model forms that are nonconvex, making it difficult for algorithms to converge to an optimal solution in time for the solution to be implemented. Therefore, model reduction is an important part of dynamic building modeling [201].

Creating a reduced-order model proceeds in two steps. First, an appropriate model structure is identified. Second, the values of the model parameters are estimated. Generating actual test data to perform model reduction can take months or years, and many of the inputs are not controllable (e.g., outdoor temperature). Building modeling software has been identified as a tool for creating input/output datasets for model reduction and parameter estimation [198], [200]. This allows inputs to be exactly specified and allows the system to be perturbed in ways that would be unacceptable to building occupants or harmful to equipment operating in an actual building. With a building simulation package, a wide range of operating conditions can be simulated to produce a data set that can be used to fit a simpler model, which is more amenable to optimization-based control. Furthermore, the synthetic data can be generated in a matter of minutes or hours, rather than the months or years required to generate a similar data set from an actual building.

Dynamic reduced-order building models come in a variety of forms. One common reduced-order model form is the resistor-capacitor (RC) model. In these models the buildings are modeled like an electric circuit with thermal resistances and capacitances. For example, Karmacharya *et al.* [202] created a lumped-node RC model of a residential home. They used the model to predict indoor air temperature and required HVAC energy for a heating environment. The model is implemented in MATLAB/Simulink and validated using BESTEST. In [203] Gouda *et al*. used nonlinear constrained optimization to reduce a model of a campus building to a lumped-parameter RC model. Optimization was used to determine the optimal parameters in the reduced-order model. They benchmarked their model against a 20^{th} order model and found that the reduced-order models suffered only minor accuracy losses yet had considerably better computational efficiency.

Another popular model structure for reduced-order modeling is the ARX (autoregressive with exogenous inputs) family of models. ARX models use previous inputs and outputs to predict future outputs. Malisani *et al.* [204] used a data-driven ARX model for building thermal modeling and discussed identification methods, including time-scaled methods. They benchmarked their reduced-order model against a 47^{th} order model and found good agreement.

Although it might not be a true reduced-order model by definition, making simplifying assumptions is one way of reducing model complexity and order. For example, Kelman and Borrelli [205] introduced several assumptions to develop a low-order model. The resulting model used for MPC is a bilinear model of a commercial HVAC system.

Once a reduced-order model is obtained, it can be used to determine the best inputs to the system. For example, a building can be precooled to avoid peak energy

costs. Using the HVAC system to precool a building has been examined extensively in the literature [140], [143], [205]–[207]. Precooling takes advantage of the building's thermal mass to store thermal energy before a peak time occurs. The cool thermal mass can then absorb heat during the peak period, which reduces or eliminates the load on the HVAC system. This use of thermal mass is also called passive thermal energy storage (see Chapter 2). One of the primary factors in determining the economic feasibility of passive thermal energy storage is the electricity rate structure [143], [208], [209]. However, for building occupants to take advantage of price differences, some sort of enabling technology (i.e., a device that automatically makes changes) is needed. Klos *et al.* [210] showed that those who have an enabling technology respond much more strongly to pricing signals than those without the enabling technology. Those with enabling technologies reduced peak loads by 21%, while those without the enabling technology reduced their load by 3%. The enabling technology considered in this chapter is model predictive control.

Simple HVAC models can also be used as a basis for developing whole home energy management systems (HEMS), such as in [211], [212]. These HEMS manage all the energy consumed in the home, from lighting to electronics. Because the HVAC system is the largest load in the home, modeling it accurately and simply is the first step to creating an effective HEMS.

This chapter describes an automated method for generating an input/output dataset and discusses how this dataset can be used to create a reduced-order home model. The reduced-order home model is unique in that its inputs and outputs are easy to implement in a HEMS-type system. The manipulated inputs to the model are the home thermostat set points and the outputs are the hourly air conditioning energy consumption (rather than room temperature). An appropriate model structure for this type of model is

identified. The reduced-order model is used in an MPC formulation to determine the optimal precooling strategy based on market electricity prices. Finally, the analysis of the cost savings and peak reduction is presented and discussed.

PROBLEM DESCRIPTION

The purpose of developing the reduced-order model is to have an accurate and computationally simple model that can be used by MPC to control a residential home's thermostat set point so that cost is minimized while staying within comfort bounds. Because MPC requires solving an optimization problem the model must be simple enough for the optimization algorithm to converge before the next time step and accurate enough to be applicable to the actual system. In this work, the desired model is one that takes in weather inputs (dry bulb temperature and relative humidity), thermostat set points, and time of day to predict air conditioning electricity consumption. For the MPC, the controlled variable is the air conditioning electricity consumption over the time horizon and the manipulated variable is the thermostat set point. The weather inputs are disturbance variables. The typical controlled variable for an HVAC system is temperature rather than electricity consumption, so the considerations here are somewhat different than those in other related work. More discussion on the consequences of choosing electricity consumption as the controlled variable is found in the model reduction section.

The building used in this analysis is a 197.7 m^2 residential home in Austin, Texas, shown in Figure 5.1. This building is part of the Mueller neighborhood, which is part of the Pecan Street Smart Grid Demonstration Project. Building geometry was taken from Google Building Maker [213] and implemented using BEopt [214], [215]. BEopt is a residential home modeling software packaged developed by the National Renewable Energy Laboratory (NREL). BEopt was used to generate an EnergyPlus simulation file.

Information for constructions, equipment efficiencies, schedules, duct leakage, etc. came from surveys and energy audits conducted by Pecan Street, Inc., for homes in the Mueller neighborhood [216], [217]. The home was assumed to be unoccupied from 8:00-17:00 with allowable thermostat set points given by Figure 5.2. Daily home energy use predicted by EnergyPlus (with 10 minute time steps) was compared to the metered energy use for homes in the neighborhood and found to be in good agreement. The point is not that this EnergyPlus model is an exact match of the home, but that it is a reasonable representation of a typical home in the area.

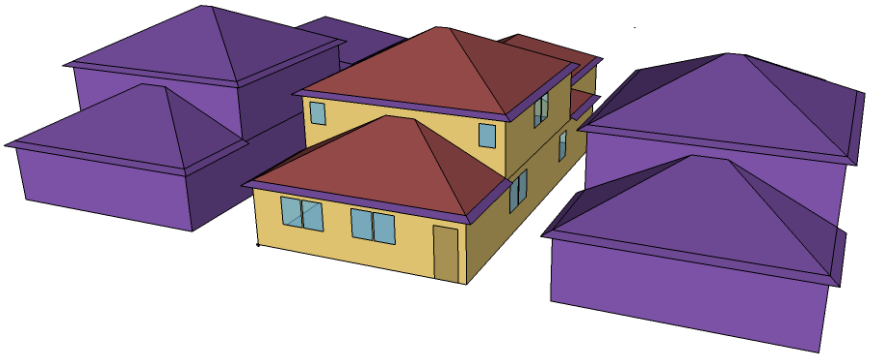

Figure 5.1: A SketchUp rendering of the residential home using the OpenStudio SketchUp Plugin. The purple houses on the left and right side of the modeled home represent neighboring homes that provide shading.

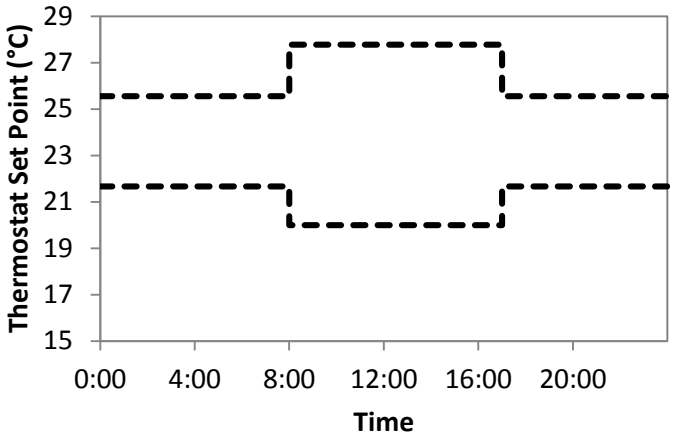

Figure 5.2: The upper and lower bounds for the thermostat set point. The bounds are wider from 8:00-17:00 because the home is unoccupied during that time.

The dynamics associated with the heat transfer in the system are described within the EnergyPlus simulation software, which combines ordinary differential equations (ODE) with algebraic expressions to determine heating and cooling loads as a function of time. EnergyPlus also includes models of the HVAC system that capture the nonlinear effects of system operation as a function of ambient conditions. For more information on EnergyPlus see [148].

OpenStudio was used to automatically generate modified EnergyPlus input data files (IDFs) and EnergyPlus weather files (EPW). OpenStudio is an open-source, cross-platform software development kit (SDK) and application suite that has the capability to use EnergyPlus as a simulation engine. OpenStudio includes an analysis framework and run manager that can automatically modify building energy models, simulate them in EnergyPlus, and collect the results in a single database. More details about the OpenStudio analysis framework and its capabilities are available in [218], [219].

EnergyPlus requires weather inputs for the dry bulb temperature, wet bulb temperature, and relative humidity, but due to psychrometric relationships, only two of

the three need to be specified. In this investigation, the dry bulb temperature and relative humidity are selected by a sampling algorithm, while the wet bulb temperature is calculated using the following relationship from [220]

$$\begin{aligned} WBT = DBT \tan^{-1}\left[0.151977\left(RH + 8.313659\right)^{1/2}\right] + \tan^{-1}\left(DBT + RH\right) \\ - \tan^{-1}\left(RH - 1.676331\right) + 0.00391838\left(RH\right)^{3/2} \tan^{-1}\left(0.023101RH\right) - 4.686035, \end{aligned} \tag{5.1}$$

where *WBT* is the wet bulb temperature (in °C), *DBT* is the dry bulb temperature (in °C), and *RH* is the relative humidity (entered as a percentage, e.g., a relative humidity of 43.5% is entered as 43.5).

EnergyPlus is an excellent building energy modeling tool; however, it has a relatively slow run-time due to its detailed energy calculations. For example, to simulate energy use for one day of the home shown in Figure 5.1 takes 20-25 seconds. This might be suitable for general simulation purposes, but not for optimal control implementation. Determining optimal set points for a 24-hour period using a gradient-based solver might require thousands or tens of thousands of model simulations. If EnergyPlus is the tool for those simulations, optimal set point calculations would take on the order of tens of hours, which is too long for practical application. Derivative-free solvers could be used to try to reduce the number of required simulations, but that might require settling for a suboptimal solution. Therefore, a reduced-order model that maintains the accuracy of the EnergyPlus model while reducing the computation time is very useful.

Once a reduced-order model is determined, it can be used in an open-loop economic model predictive controller that determines the optimal set points over the course of a day in order to minimize costs. The model predictive controller formulation used here is

$$J = \min\left(\sum_{i=k}^{k+N} r(i)\,y(i)\right) \tag{5.2}$$

subject to

$$y(k) = f\left(y, T, DBT, RH, k\right) \tag{5.3}$$

$$0 \le y(k) \le ub \qquad \forall k \in [k, k+1, \ldots, k+N] \tag{5.4}$$

$$lb \le T(k) \le ub \qquad \forall k \in [k, k+1, \ldots, k+N] \tag{5.5}$$

where J is the operating cost for the air conditioning system over the time period of k to $k + N$, k is the discrete time step (it can only take on nonnegative integer values), N is the length of the prediction horizon, r is the electricity rate ($/kWh) for the given time step, and y is the electrical energy (kWh) used by the air conditioning system at the given time step, T is the temperature set point (°C), and lb and ub are upper and lower bounds, respectively. Other common MPC formulations track a set point ([221]) or minimize energy use (see Chapter 3). Some consider combinations of two or more criteria (e.g., [222]). Minimizing energy consumption can also be considered here by setting r to the same value for all time steps. The reduced-order model is the function (f) given in (5.3).

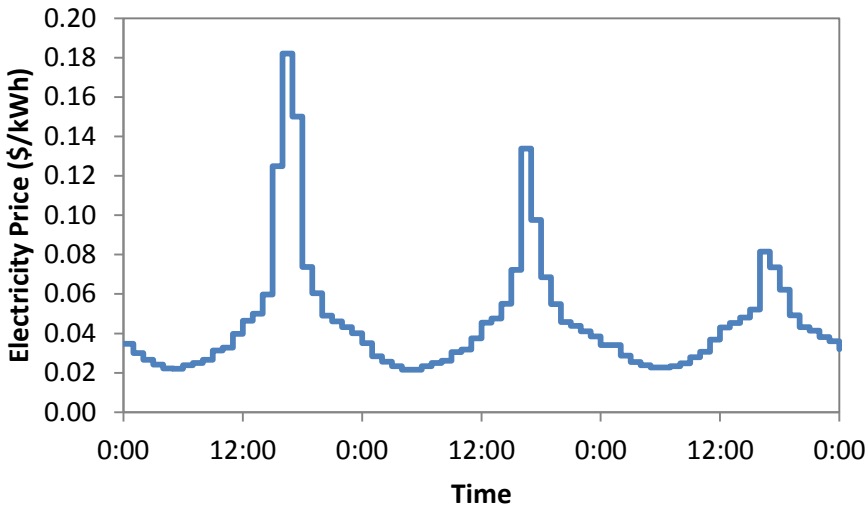

Figure 5.3: Day-ahead market settlement point prices for July 7-9, 2011, for the Austin load zone of the ERCOT market.

The electricity prices (r) used here are the day-ahead settling point prices from the Austin load zone in the 2011 ERCOT market. The prices represent actual electricity costs in a cooling-dominated climate with costs highest in the afternoon and lowest in the early morning hours (see Figure 5.3). Because the day-ahead settling point prices are published a day in advance (i.e. prices for July 7 are published on the afternoon of July 6), there is no need for a price prediction model.

MODEL REDUCTION

The general form of the reduced-order model considered here is a full quadratic model given by

$$y(k) = f(y, T, DBT, RH, k) \tag{5.6}$$

This general form can include any length of history (e.g., it can include the set point or dry bulb temperature from *n* hours ago) as well as interaction terms (e.g., $T \cdot DBT$). Each term in the model is associated with a coefficient that is determined from input/output data.

The general methodology in creating a reduced-order model was to generate an input/output dataset using the EnergyPlus model. This input/output data was then used to identify the model structure (i.e., which terms from the full quadratic model to keep) and estimate model parameters. The OpenStudio analysis framework was key to doing this with relative ease.

Each sample was a 24-hour EnergyPlus simulation, running from midnight to midnight. The only inputs perturbed were the thermostat set point at each hour, the dry bulb temperature at each hour, and the relative humidity at each hour, resulting in a total of 72 variables for each sample. All other model parameters were kept constant.

Determining how to perturb the model inputs was critical to identifying an appropriate model. For example, perturbing each input at every hour leads to identifying a model with very poor prediction capabilities. Things to consider when determining the best input sequence include:

- How frequently will inputs be perturbed?
- How large will input changes be when they are perturbed?
- Will parameters be perturbed simultaneously or independently?
- What is the allowable space for perturbations?

Preliminary input/output data gave several insights. Outdoor relative humidity was found to have little impact on air conditioning energy use, so it was eliminated from

further consideration. The settling time (the time it takes the system to return to steady-state after a perturbation) was determined to be approximately 22 hours, indicating that rapid changes in model inputs would hide some of the dynamic behavior of the system.

Zhu [223] recommends holding input values for ¼, ½, and ¾ of the 98% settling time when doing nonlinear system identification. He also recommends using at least as many levels as the order of the model considered. Because there is no noise, the input sequence can be relatively short, making a simple step test or a single cycle of PRBS (pseudorandom binary sequence) effective [224]. The lack of noise tends to lead to lower-order models [224].

Because the output of the system considered here is the air conditioning energy consumption, other complications arise in creating the input sequence. One of the inputs is the thermostat set point. If the house is at equilibrium, raising the thermostat set point will turn off the home's air conditioning unit, while lowering the set point will turn it on. These create very different responses, such that the overall response to the temperature set point is nonlinear. This is due to the fact that there is a closed-loop, on-off controller (the thermostat) in the system, but the system is treated as an open-loop system. Another associated challenge is that output data are averaged over the time step (one hour). The output (air conditioning energy consumption) is the average power draw by the air conditioner over the course of the hour. If the air conditioner uses 1 kW for one hour the output will be exactly the same as if it uses 2 kW for 30 minutes and 0 kW for the remaining 30 minutes.

The input dataset that was used consisted of 180 samples of step tests in T holding DBT constant and 120 samples of step tests in DBT holding T constant. Holding a variable constant meant that the variable did not change during that sample, but different samples had different (though constant) values of the variable. Because of the issue with

the air conditioning system turning off if T was raised, T was only allowed to have steps down. The magnitude, duration, and start time of the steps for both T and DBT were determined using the Latin hypercube sampling (LHS) algorithm [225], which is already included in the Dakota libraries used by OpenStudio. The magnitude of T was restricted to 20-27.78°C and the magnitude of DBT was restricted to 15-45°C. The range for T was taken from Figure 5.2 and the range of DBT was taken from historical summer weather data for Austin, Texas. Summer temperatures can be lower than 15°C, but in those cases it is assumed that the air conditioning electricity consumption will be zero. Of these 300 samples, 225 were used for parameter estimation while the remaining 75 were used as a validation set.

The general reduced-order model considered without RH is given by

$$\begin{aligned} y(k) = & \sum_{i=1}^{n_y} a_i y(k-i) + \sum_{i=0}^{n_{DBT}} b_i DBT(k-i) + \sum_{i=0}^{n_T} c_i T(k-i) \\ & + \sum_{i=0}^{n_{DBT,2}} d_i \left[DBT(k-i) \right]^2 + \sum_{i=0}^{n_{T,2}} e_i \left[T(k-i) \right]^2 + \sum_{i=0}^{n_{DBT,T}} f_i DBT(k-i) T(k-q) \\ & + \sum_{i=0}^{n_T} \sum_{j=i+1}^{n_T} g_{i,j} T(k-i) T(k-j) + \sum_{i=0}^{23} h_i hr_i \end{aligned} \tag{5.7}$$

$$hr_i = \begin{cases} 1 & \text{for } i = k \bmod 24 \\ 0 & \text{otherwise} \end{cases} \tag{5.8}$$

where n_x is the number of time steps considered for input x, a-h are model coefficients, and hr is the 0/1 variable given by (5.8). Equation (5.8) allows for a different constant term for each hour of the day, which accounts for other disturbances such as occupancy and solar irradiation. In the case that all disturbances were modeled, only a single h coefficient would be necessary.

In summary, the steps taken to generate a reduced-order model are

1. Build a residential home model in BEopt.
2. Convert the EnergyPlus model (IDF) developed in BEopt into an OpenStudio model (OSM).
3. Use scripts written in Ruby to automatically perturb model parameters (including weather data) within their specified ranges and generate unique OpenStudio models based on those perturbations. This means that generating 50 samples will lead to the creation of 50 different OpenStudio models with 50 different weather files.
4. Convert the OpenStudio models to EnergyPlus models.
5. Simulate the models using EnergyPlus.
6. Post-process the EnergyPlus output files to combine the results from all of the models into a single database.
7. Fit a reduced-order model to the simulation data using a statistical software package.

Steps 2-6 are run from a single automated script, for which the user specifies the sampling algorithm to be used, the allowable sampling ranges, the sampling distributions, and the number of samples desired. The majority of the work is handled by OpenStudio. An OpenStudio R library is currently under development that can also automate step 7. As a caveat to this automated process, because BEopt was used to develop the EnergyPlus model, some elements had to be manually changed before they could be imported into OpenStudio. For example, *Schedule:Week:Compact* objects had to be

converted to *Schedule:Week:Daily* objects. If the models are built in OpenStudio, or only include elements already supported by OpenStudio, then this step would not be present.

Due to the automation offered by OpenStudio, it is simple to alter parts of the model and generate new data for fitting a reduced-order model. For example, if the home's occupancy schedules changed, one would simply need to update the EnergyPlus model, and then the same OpenStudio script could be run to generate new output data. Thus the process is highly replicable.

RESULTS AND DISCUSSION

The general goal of the work presented here is to develop a reduced-order residential home model that can be effectively used in a model predictive controller in order to optimally manage home air conditioning energy use. This section presents the results from developing the reduced order model (see "Reduced-order Modeling Results") and then uses the developed model in a model predictive controller (see "Model Predictive Controller Results"). Results of using the MPC over the course of a summer are also presented in with the Model Predictive Controller Results section.

Reduced-order Modeling Results

In estimating the model parameters, the following model form was identified:

$$\begin{aligned} y(k) = ay(k-1) + \sum_{i=0}^{2}\left[b_i DBT(k-i) + c_i T(k-i)\right] + d\left[DBT(k)\right]^2 \\ + \sum_{i=0}^{2}\left[e_i\left[T(k-i)\right]^2\right] + fDBT(k)\cdot T(k) + \sum_{i=0}^{23} h_i hr_i \end{aligned} \tag{5.9}$$

where all $g_{i,j}$ from (5.7) are zero. The estimated parameters (*a*-*h*) in (5.9) had p-values (a measure of statistical significance) ranging from 0-0.0000169, and the model had an

adjusted R^2 of 0.990. However, the coefficients for e_i were very small. Forcing e_i to be identically zero lead to a simpler model that was linear in the inputs (T):

$$\begin{aligned} y(k) = ay(k-1) + \sum_{i=0}^{2}\left[b_i DBT(k-i) + c_i T(k-i)\right] + d\left[DBT(k)\right]^2 \\ + fDBT(k)\cdot T(k) + \sum_{i=0}^{23} h_i hr_i \end{aligned} \tag{5.10}$$

This model had an adjusted R^2 of 0.988 and the parameters *a-g* in (5.10) had p-values from 0-0.0120. Although the nonzero coefficients e_i were statistically significant, the simpler model lost very little predictive power. Also, because e_i from (5.9) contained both positive and negative numbers, the model in (5.9) was nonconvex. Setting e_i to zero in (5.10) leads to a linear, convex model in the manipulated variable. This has two advantages when applying this model in the MPC. First, because it is convex, the optimal solution found by the solver is guaranteed to be the global optimum, and second, the problem can be solved using a linear solver, which is extremely fast.

All results presented in the chapter use (5.10). The coefficients for (5.10) are given in the Appendix. The model is stable, with all poles and zeros inside the unit circle (see Appendix for these calculations). Also, the poles and zeros are real, indicating that there is no oscillation or inverse response. The steady-state gain for the model is a function of *DBT*, but it is always negative, meaning that an increase in the thermostat set point will always lower the steady-state energy consumption. For more information on analyzing discrete time dynamic models, see [226], [227].

Figure 5.4 shows the model given in (5.10) applied to the validation dataset. The R^2 for this fit was 0.986.

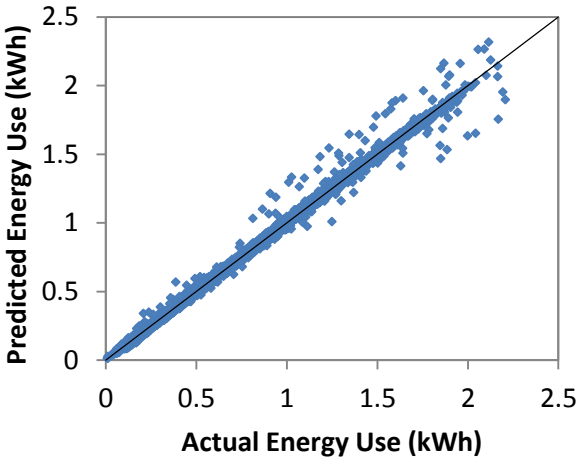

Figure 5.4: Parity plot of actual versus predicted energy use for the validation dataset using the model given in (5.10).

The reduced-order model takes ~10^{-4} seconds to calculate the energy usage for one day, while a day-long EnergyPlus run takes 20-25 seconds. This reduction in calculation time allows the optimization algorithms to determine the optimal set points in a fraction of a second.

One challenge of the reduced-order model provided here is that it was trained only on stepping the thermostat down (i.e., lowering the thermostat). Stepping the thermostat up resulted in the air conditioner turning off no matter the step size, causing errors in developing the input-output relationship. As a result of only stepping down, the model is less accurate when predicting energy consumption when the thermostat is raised. When the air conditioner is on, air is forced through the house, increasing heat transfer coefficients and mixing the air. When the air conditioner is off (which is what happens when the thermostat is raised), the air is mostly stagnant and heat transfer between the air and the house relies more on natural convection. Thus the dynamics of the house are slower when the air conditioner is off than when it is on. The inaccuracies

associated with the simplifying methodology will be seen in the model predictive control results.

In order to more fully evaluate this methodology, it is compared to a pre-packaged neural-network-based time series model, in this case, MATLAB's Neural Network Toolbox ®. This model uses the same input/output dataset as described in Section 4 to predict future energy usage. The neural-network model provides an excellent fit to the testing data, yielding an adjusted R^2 of 0.998. However, the model does not extrapolate well and produces very poor results when predicting energy use given inputs that are outside of the original step-test response data, meaning that optimal solutions generated from this model are unreliable. This remains the case even if the training data are expanded to include both up and down steps in the thermostat set point. Furthermore, the model introduces nonconvex nonlinearities with respect to the inputs. These nonlinearities are significant in that they require solving a nonconvex nonlinear programming (NLP) problem to determine the optimal set point profiles, which requires significant computational effort. It is therefore concluded that a neural network model would require a larger and more diverse set of training data in order to avoid extrapolation, which hampers the usefulness of creating a reduced-order model from a building simulator. It is also concluded that such a model is not well suited to a real-time control application as the corresponding NLP problem requires significant computation time (solving for a 24-hour optimal set point trajectory using a neural network model required hours of computation time).

Model Predictive Controller Results

The model predictive control problem in (5.2)-(5.5), using the reduced-order model presented above, was solved using the COIN-OR linear programming (CLP)

algorithm. The value of N in (5.2) was chosen to be 12 based on the objective function value using different values of N (see Figure 5.5). Extending the prediction horizon beyond 12 hours yielded improvements in the objective function of less than 0.1%.

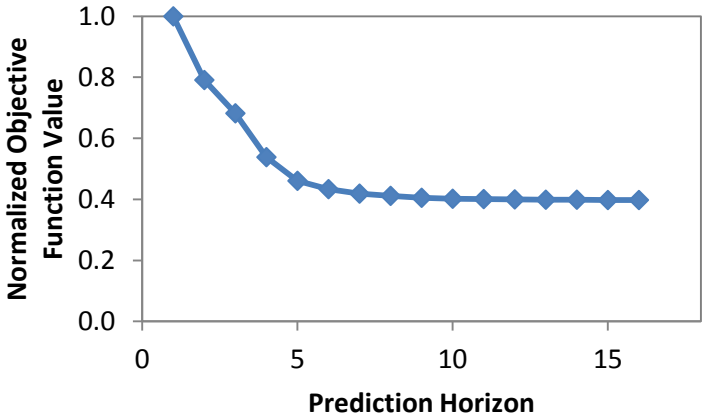

Figure 5.5: Normalized objective function value during July and August as a function of the prediction horizon (N).

A single-day solution to the model predictive control problem is shown in Figure 5.6. On this day, electricity prices are fairly typical for a summer day, ranging from about \$0.03/kWh in the early morning to \$0.13/kWh in the afternoon. The house is precooled in the morning and then the thermostat is raised throughout the afternoon so that energy use is lowest when electricity prices are highest. At the end of every hour, the room temperature is generally very close to the set point. The stair-step behavior from 11:00 to 15:00 is caused by the nonnegativity constraint given in (5.4), because raising the set point higher (e.g., all the way to the upper bound) would result in negative electricity consumption. If the model predictions were perfect, then the optimal set point solution shown in Figure 5.6 would be equivalent to raising the set point to the upper bound at

10:00 and leaving it there for the remainder of the day. This is because the air conditioning energy consumption is zero during the stair steps.

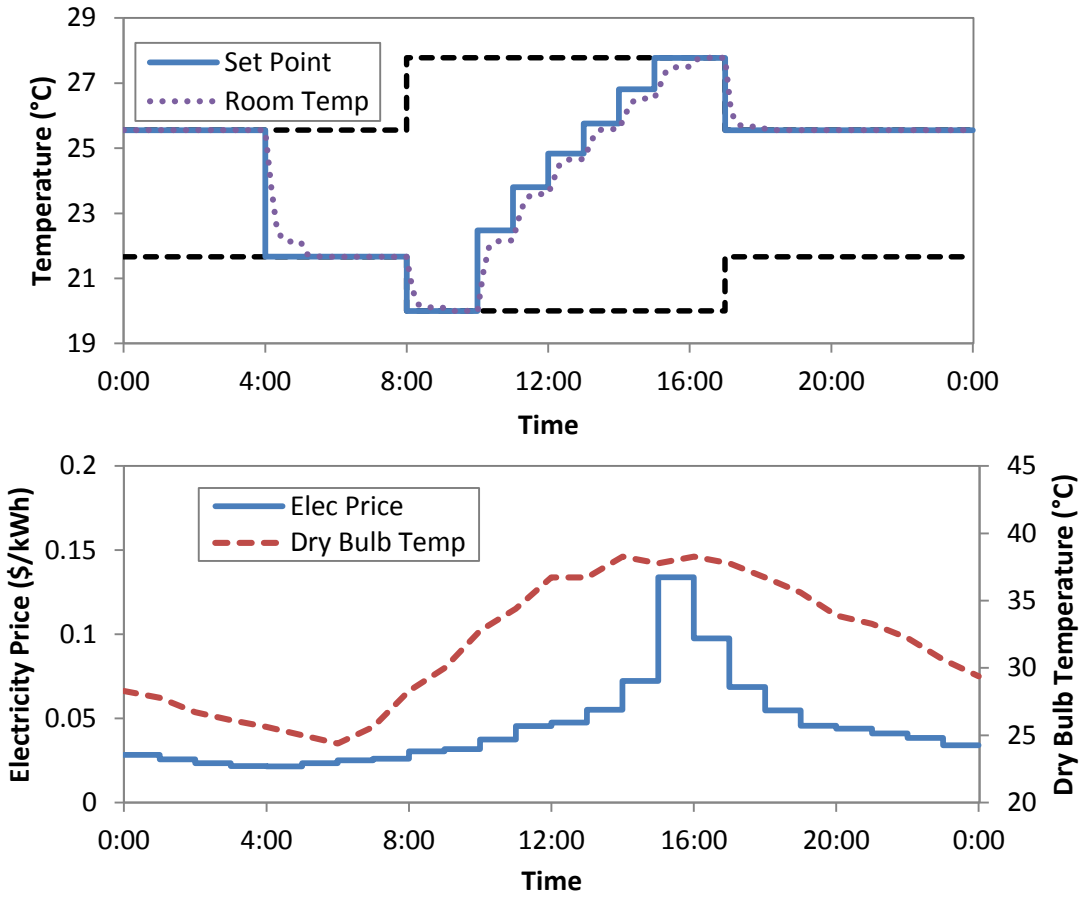

Figure 5.6: The upper plot shows the optimal temperature set point profile for July 8, with the upper and lower limits for the set point shown by the dashed lines and the room temperature shown by the dotted line. The lower plot shows the electricity prices and dry bulb temperature for the same day.

The actual and predicted energy use for July 8 is given in Figure 5.7. The R^2 between the actual and predicted data is 0.97. The inaccuracies in the reduced-order model primarily arise when the air conditioning system is turned off and kept that way for several hours by raising the thermostat from 11:00-15:00. The model was trained only

using step tests that *lowered* the thermostat, meaning the air conditioning system would come on. The model is therefore less accurate when the system is off, but the inaccuracies are relatively small.

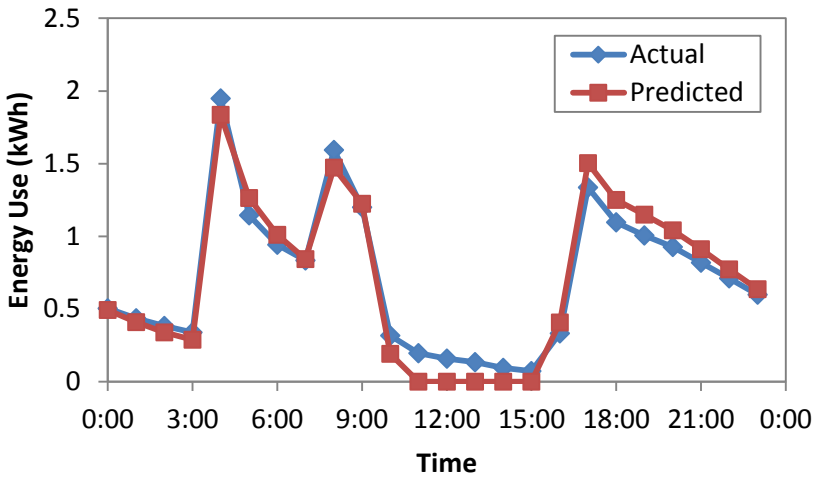

Figure 5.7: Actual and predicted energy use for July 8. Actual use is given by the EnergyPlus simulation, while predicted use is given by the reduced-order model (5.10).

Energy usage and costs for July 8 are given in Table 5.1. Using the optimal temperature set points from the model predictive controller, costs are decreased, but overall energy usage is increased. Peak energy usage is also dramatically decreased. An increase of 1.7 kWh in total energy use led to a peak energy reduction of 2.6 kWh.

	Base Case	**Optimal Case**	**Percent Change**
Total Usage (kWh)	15.4	17.1	11.0%
Total Cost	$0.80	$0.65	-18.8%
Peak Usage (kWh)	4.46	1.84	-58.7%
Peak Cost	$0.38	$0.14	-63.2%

Table 5.1: Total and peak energy consumption and costs for July 8. The percent change is the change from the base case to the optimal case.

The solution time for computing a single day's optimal solution is negligible (~0.01 s) because the formulation is linear with only 12 decision variables. Lengthening the time horizon increases the solution time, but the increase is small enough that it is not a concern.

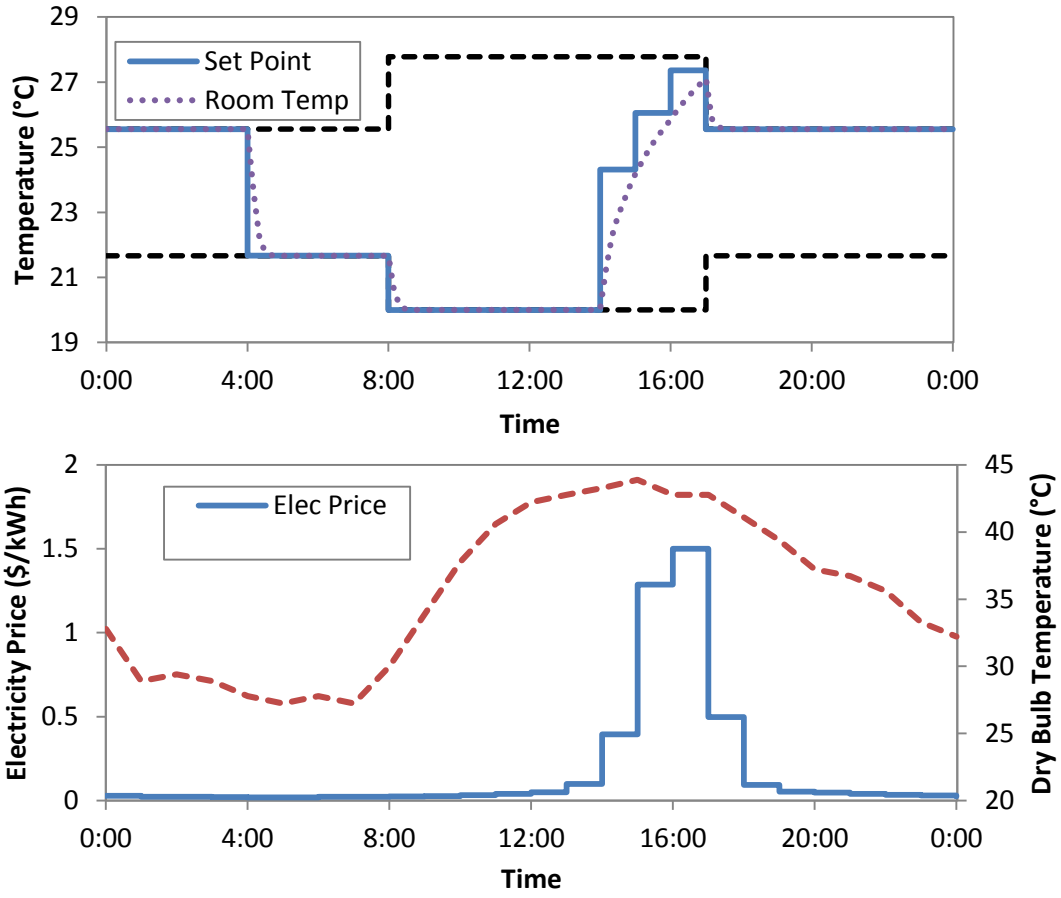

Figure 5.8: The upper plots shows the optimal temperature set point profile for August 28, with the upper and lower limits for the set point shown by the dashed lines and the room temperature shown by the dotted line. The lower plot shows the electricity prices and dry bulb temperature for the same day.

The optimal set point profile for a day (August 28) with more extreme temperatures and prices is shown in Figure 5.8. Precooling begins at the same time as on

July 8, but the temperature is kept at the lower bound until 14:00. The thermostat set point is raised during the extreme price period to keep energy use low. The thermostat never actually reaches the 27.78°C upper bound. Doing so would allow the cooling load at 13:00 to be lower, but would increase the cooling load at 17:00. Because prices are higher at 17:00 than 13:00, not reaching the upper bound is more economical.

The savings that come from implementing the optimal profile are significantly greater on August 28 (see Table 5.2). Because of the high peak prices (reaching $1.50/kWh), the solution performs as much precooling as possible in order to eliminate the need to do cooling during those expensive hours.

	Base Case	Optimal Case	Percent Change
Total Usage (kWh)	19.7	22.7	15.2%
Total Cost	$5.27	$1.65	-68.7%
Peak Usage (kWh)	5.7	1.37	-76.0%
Peak Cost	$4.63	$0.80	-82.7%

Table 5.2: Total and peak energy consumption and costs for August 28. The percent change is the change from the base case to the optimal case.

When compared to the EnergyPlus model results, the reduced-order model performs well for this hotter day (see Figure 5.9). The R^2 between the EnergyPlus model results and the reduced-order model results is 0.966. The good fit shows that the training data generated from step tests gives the model accuracy over a very wide range of circumstances.

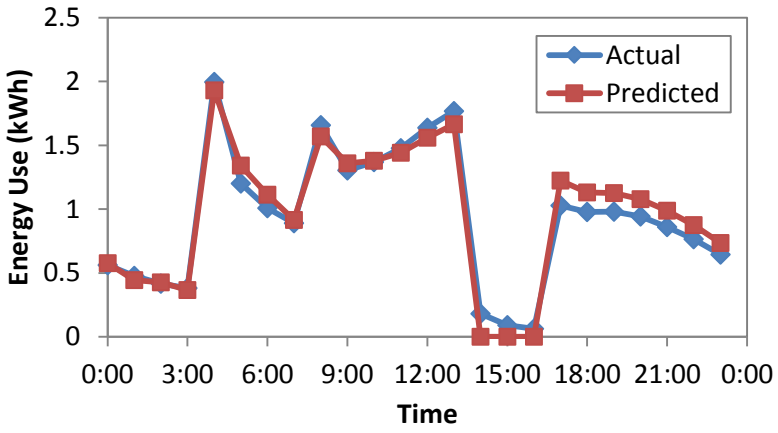

Figure 5.9: Actual and predicted energy use for August 28. Actual use is given by the EnergyPlus simulation, while predicted use is given by the reduced-order model (5.10).

Table 5.3 summarizes the energy usage and costs for the base case and optimal strategies for the months of July and August. The cost of the electricity to the customer and to the utility are considered separately, similar to [206]. Nearly one third of the energy in the base case scenario is consumed during peak hours, while under the optimal strategy less than 8% of the total energy is consumed during peak. It costs 132 kWh of extra energy to reduce the peak by 205 kWh.

It is obvious that under the base case scenario, the utility is losing money during peak hours. One solution considered here is to expose the customer to market prices so that the customer would pay the actual costs of the electricity, and then provide the customer with an enabling technology so they can take advantage of that information (i.e., through optimal precooling). In this way, the optimal strategy would lower the two-month energy bill from \$146.45 to \$58.48. Another approach would be to have the utility pay the customer for the right to control the customer's thermostat. The utility benefits from the optimal strategy by \$102.51 over the two months (see Table 5.3), while the customer's bill increases by \$14.54, so the utility should be willing to pay between

$14.54 and $102.51 in order to control the home's thermostat. For summer months and the home considered here, this translates to the utility being willing to pay $7-50/month for direct thermostat control.

	Base Case		Optimal Case		Savings	
	Total Energy	**Peak Energy**	**Total Energy**	**Peak Energy**	**Total Energy**	**Peak Energy**
Energy (kWh)	1007	291	1139	86.2	-132	205
Cost to Customer	$110.72	$32.06	$125.26	$9.48	-$14.54	$22.58
Cost to Utility	$146.45	$122.57	$58.48	$17.85	$87.97	$104.72
Profit to Utility	-$35.73	-$90.52	$66.78	-$8.37	$102.51	$82.15

Table 5.3: Summary of energy usage and costs. The base case is keeping the temperature set point at the upper bound for the entire day. The cost to the customer is using a fixed rate of $0.11/kWh. The cost to the utility is determined by the day-ahead settlement point prices. The utility's profit is the difference between the two. Note that "Total Energy" includes energy used during peak.

In all cases, reducing the peak via precooling the home leads to an increase in overall energy use. The amount of peak energy reduction is always greater than the amount of extra energy consumed. Figure 5.10 shows the amount of peak reduction achieved for a given amount of extra energy consumed. The relationship between peak energy reduction and extra energy consumption is strongly linear. The data points at the far left, where virtually no extra energy was consumed but significant peak reduction was achieved, occurred on days with cool mornings and hot afternoons. Because the air conditioner efficiency is a function of outdoor dry bulb temperature, the hot afternoon cooling was shifted to the morning when the system efficiency was significantly higher. Figure 5.10 also shows that the extra energy cost of reducing 1 kWh of peak energy is approximately 0.63 kWh (the slope of the data).

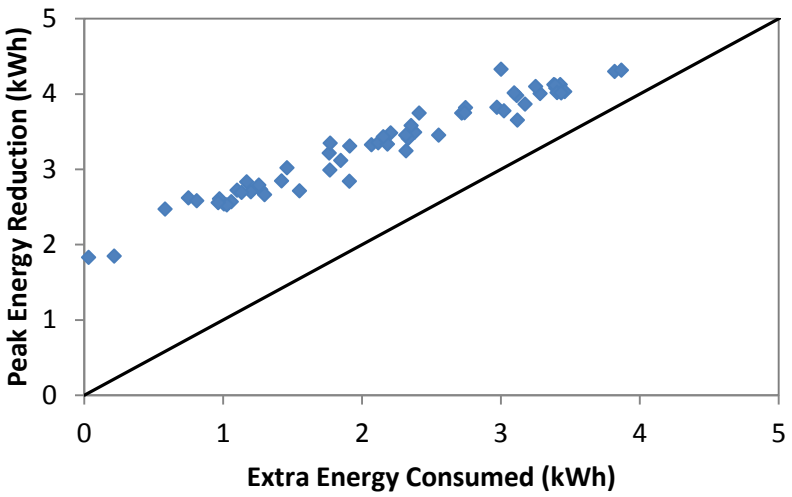

Figure 5.10: Extra energy consumed by the air conditioning system in order to reduce peak demand via precooling. Peak is defined as 3-7pm. The extra energy uses a baseline where the thermostat is kept at the upper limit for the entire day. Each data point represents a single day. The data have a slope of less than one and all lie above the parity line.

Figure 5.11 shows the amount of savings achieved in a day compared to the amount of extra energy (above the base case) it took to achieve that savings. It is clear that a significant amount of energy is expended to obtain very minor costs reductions. If consuming extra energy is a concern, including a small penalty in the objective function for that extra energy would ensure that extra energy is only consumed if significant cost savings are achieved. For example, if the precooling strategy was only implemented on days that would save more than $0.25 in electricity costs, then the cost to the utility is $62.70 (only $4.22 more than in Table 5.3), and total energy usage is reduced to 1104 kWh (35 kWh less than in Table 5.3).

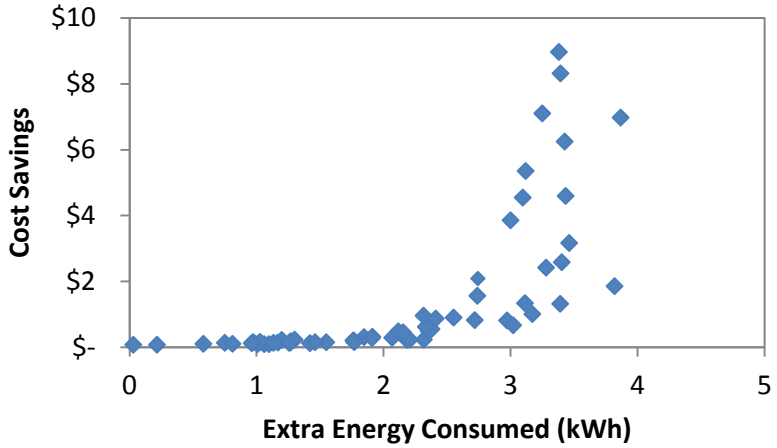

Figure 5.11: Extra energy consumed by the air conditioning system versus cost savings. Each data point represents a single day.

CONCLUSIONS

OpenStudio is an effective tool for developing an input/output dataset from an EnergyPlus model. The design of the input data, however, is very important. In this work relating to a residential home's air conditioning system, it was found that step tests in which only one variable was changed at a time over a 24-hour sample generated good output data.

The best-fit reduced-order model based on this input/output dataset was nonlinear in the control and disturbance variables. However, eliminating the nonlinear control variable terms resulted in a simple model that retained model accuracy. This simpler reduced-order model had an R^2 of 0.986 when applied to the validation dataset.

The reduced-order linear model was used in a model predictive controller to determine the optimal thermostat set points to minimize electricity costs in the face of electricity market prices. The open-loop MPC results predicted by the model matched the EnergyPlus simulations well. The MPC determined the precooling strategy that minimized costs, saving this home just over $100 for the two-month period of July and

August. This strategy reduced peak energy consumption for air conditioning by 70% over that 2-month period. This also demonstrated that reacting to market prices is an effective strategy for mitigating the peak demand issues.

Precooling the home always resulted in an overall increase in electricity consumption. On average for the summer, reducing peak energy consumption by 1 kWh resulted in 0.63 kWh of additional energy consumption.

The model and MPC framework are advantageous in that they use relatively straightforward inputs (weather, thermostat set point, and electricity price) and outputs (electricity consumption) that are easy to obtain. The resulting MPC would be simple to implement because it does not require a change to the home's thermostat—the controller simply needs to pass the optimal temperature set points to the existing thermostat. Because the objective of the controller is to minimize costs, using electricity consumption as an output, rather than using an output like room temperature, is advantageous.

Neural network models were also considered for creating reduced-order models. Although they provided excellent fits for the training and validation data, they performed poorly in the model predictive controller, even when the input data set was expanded to cover a wider range. When the neural network model was implemented in the MPC, the open loop optimization problem took orders of magnitude longer time to solve and produced inaccurate and unreasonable solutions due to extrapolation outside of the step-test-based training data. To make neural networks work for this application, a more extensive and comprehensive input/output dataset would be required.

Future work will use the methodology presented here to create simple linear models for an entire community of homes, all of which will be validated using the Pecan Street Smart Grid Demonstration Project data. These homes will have a variety of occupancy patterns, home constructions, orientations, appliances, etc. that will

differentiate them. With this larger system, community-level control can be studied to see the effects of implementing precooling strategies over a wider area.

Chapter 6: Community-scale Residential Air Conditioning Modeling and Control[5]

INTRODUCTION

Chapter 5 discussed how residential air conditioning systems are ubiquitous throughout the United States and are major contributors to the peak demand challenges in the electric grid. While the peak demand appears relatively coordinated in time, the discrete air conditioning systems that cause peak demand typically operate independently of each other. One hypothesis of this chapter is that implementation of intelligent control of these air conditioning systems can lead to better coordination of air conditioner operation, which would potential yield significant consumer cost savings and grid benefits [228], [229].

There are three general approaches taken in managing air conditioning electricity use. The first is to improve the efficiency of the home or the air conditioning unit through the implementation of energy efficiency measures [230]. These measures include actions such as adding insulation [231], sealing ducts and windows, or planting shade trees beside a home [232]. Subsequently, they reduce total air conditioning electricity consumption, which typically leads to a reduction in peak electricity consumption.

The second approach is often referred to as demand response. Demand response strategies generally curtail air conditioning usage for short periods of time. For example, a utility might broadcast signals to participating air conditioning unit thermostats to turn off the compressors for a brief period. After the curtailment period has ended, the air conditioning systems resume normal operation. This approach often induces an energy

[5] This chapter has been submitted as W. J. Cole, J. D. Rhodes, W. Gorman, M. E. Webber, and T. F. Edgar, "Community-scale residential air conditioning control for effective grid management," *Applied Energy*, under review 2014. Rhodes and Gorman built the EnergyPlus building models based in the smart grid data. Webber provided writing guidance in revising the manuscript, and Edgar provided general advising and editing.

rebound effect, where energy usage increases after the curtailment period as air conditioners work harder or longer to return the thermal zones to the desired temperatures [233]. This rebound effect has been demonstrated several times in the literature [234]–[236].

The third approach is a precooling strategy. Precooling involves cooling the building below the typical temperature to store "cooling energy" in the thermal mass of the building. This approach is also called passive thermal energy storage (see Chapter 2). Precooling generally consumes more energy than demand response approaches, but it is better at maintaining comfort within the home and does not suffer from the rebound effect [237].

Pricing signals can be used to help encourage the three approaches given above. However, there is concern that responding to pricing or other signals can lead to the creation of a new peak. For example, Bartusch *et al*. [238] implemented a demand-based electricity pricing program on several hundred residential households in Sweden. This pricing program led to the creation of a new off-peak "peak" due to the shifting of loads from peak times to off-peak times. In addition to the potential creation of a new peak, it is also difficult to quantify the effects of the pricing signals [239], [240]. For example, by encouraging people to alter their behavior through price signals, it is difficult to say how they would have behaved had those price signals not been used, especially because other non-behavioral factors (e.g., weather) impact total energy use.

In this chapter, a 900-home community was simulated (see the methodology section for details on how this simulation was assembled) where home air conditioning thermostat set points are controlled using either a centralized or decentralized model predictive controller. These controllers have the flexibility to minimize operating costs or the peak demand of the community. Related studies have been conducted for centralized

thermostat controllers. Callaway [241] considered the manipulation of 60,000 air conditioner thermostat set points to follow the dynamic output of a wind farm at a resolution of one minute. The air conditioning models were based on resistance-capacitance (RC) models. Callaway and others (e.g., [228], [242]–[246]) have considered the dynamics associated with controlling a large number of thermostatically controlled loads or electric vehicles to achieve short-term grid benefits. Because they consider shorter-term periods, weather is held constant for the simulations. This chapter focuses less on short-term dynamics (such as those required to follow the minute-by-minute output of a wind farm) and more on the ability to shift load and/or flatten the peak, the work presented here includes the effects of weather. Using actual weather data is a key factor in evaluating the energy performance of buildings [247]. While those studies offered different insights, they did not have access to the primary data that could be used for verification and for building the models. Furthermore, they did not directly compare centralized versus decentralized configurations.

This chapter's main contribution is to address those issues. First, a novel data set comprised of energy audits, homeowner surveys, and direct meter measurements from a statistically significant sample of actual homes were synthesized for the modeling and simulation of a larger community of homes. Consequently, this work offers the prospect of a verified model that can be used to estimate the potential for peak reductions. Second, the simulation considers the effects of allowing all homes to automatically respond to market electricity prices. The analysis compares decentralized versus centralized control strategies and provides a method for replicating the centralized control results through a penalty-based decentralized control strategy.

METHODOLOGY

In this investigation air conditioning thermostat set point control methods were applied to a notional community of 900 individual homes. The process for developing the 900 homes models and applying the control is shown in Figure 6.1. These homes are derived from a pool of 60 physical homes that are part of a smart grid demonstration project based in Austin, Texas, USA. The average year of construction for the 60 physical homes is 1965 with a standard deviation (σ) of 18 years. One-third of the homes are two-story, and the rest are single-story. The homes have an average conditioned area of 165 m^2 (σ = 83 m^2). Roughly half of the homes have older single paned windows, and the average R-value of insulation is 22. The average air conditioning system is 10.6 kW (3 tons) with a coefficient of performance (COP) of 2.9 and 12% duct leakage [248].

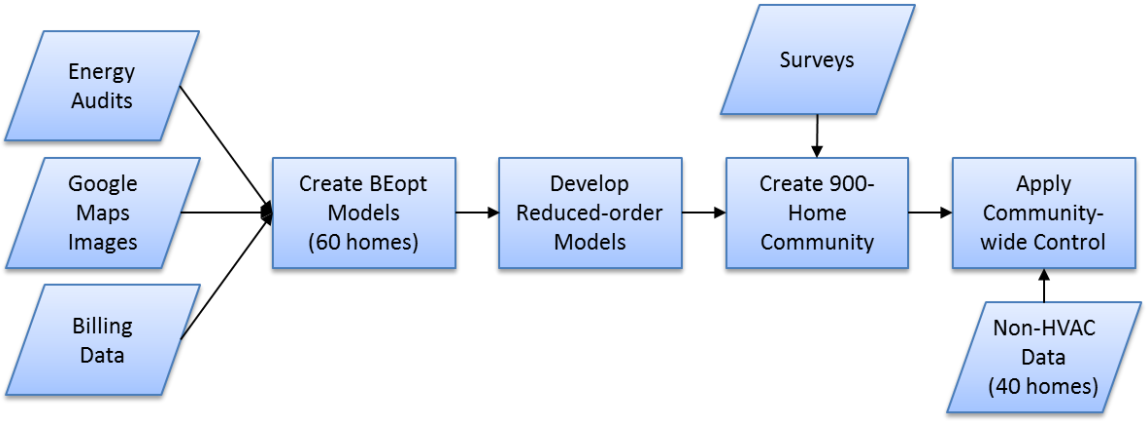

Figure 6.1: This flowchart illustrates the data sets and sequence of steps for creating and controlling the air conditioning units in a notional 900-home community.

Models of the 60 physical homes were initially constructed using BEopt, a GUI residential front-end for EnergyPlus, developed by the National Renewable Energy Laboratory (NREL) [214]. The BEopt models were created from energy audits and images from Google Maps; however, not all model inputs were recorded in the audits, so

the model defaults were used in this case. To verify the accuracy of the models, the simulated total yearly electricity use from the models was compared to actual annual billed electricity use, which was provided by the local electric utility for 2011 for 48 of the 60 homes (billing data from 12 of the homes was unavailable or unreliable). Individual homes had an average absolute error of 23.5% versus the billing data (for yearly energy consumption), with a minimum of 0.02% and maximum of 71.2%. A histogram of the error between the model output and the annual billing data is shown in Figure 6.2. While the errors for individual homes were non-trivial, the aggregated energy use of the homes only had a 1.2% error when compared to the aggregated billing data over the year, which is acceptably accurate for this project's research objective.

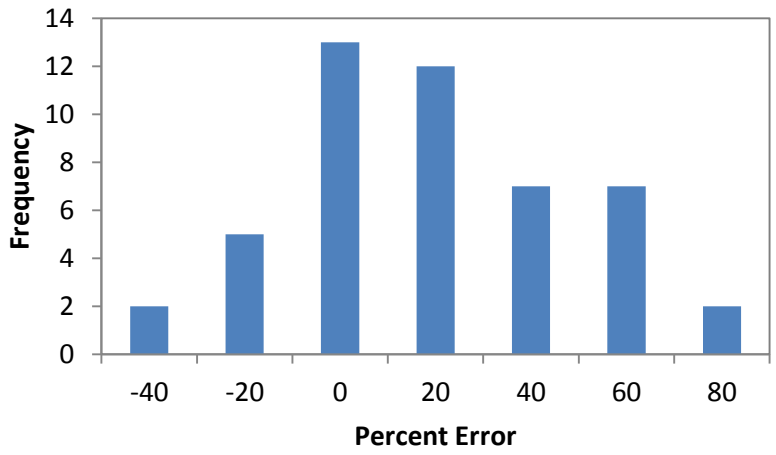

Figure 6.2: This histogram of the error between the annual energy consumption predicted by the BEopt model and the annual billing data provided by the utility shows that the most common errors were +/- 20% or less for individual homes, and the largest error was just over 70%. The error for the aggregated consumption of all homes was 1.2%.

The EnergyPlus models obtained using BEopt were too computationally slow to be effectively used in an optimization-based control scheme, reduced-order dynamic

models of the homes were created. To develop a reduced-order model from an EnergyPlus home model, a custom MATLAB script was written to process input/output data from the EnergyPlus model. A reduced-order ARX model was then identified and parameters fitted using this input/output dataset. Details on this method for developing a reduced-order ARX model are described in Chapter 5. This method results in an ARX model that predicts a home's hourly air conditioning electricity consumption as a function of the outdoor dry bulb temperature, the home's thermostat set point, and the hour of the day. This model is expressed as follows:

$$y_{i,j} = ay_{i,j-1} + \sum_{k=0}^{2}\left[b_k DBT_{j-k} + c_k T_{i,j-k}\right] + d\left[DBT_j\right]^2 + fDBT_j \cdot T_{i,j} + h_j \tag{6.1}$$

where $y_{i,j}$ is the air conditioning electricity consumption for home i at time j, DBT_j is the outdoor dry bulb temperature at time j, $T_{i,j}$ is the thermostat set point for home i at time j, and parameters a-h are home-specific model coefficients. The parameter h_j is indexed by time j because there is a different value of h for every hour of the day (e.g., the value of h at 1:00 is different than at 2:00). This h parameter helps in accounting for unmodeled disturbances such as solar irradiation. For all homes, the value of c_0 is negative, indicating that raising the thermostat will result in a decrease in air conditioning energy consumption.

A notional community of 900 homes was created for the analysis using two steps. First, each of the 60 home models was replicated 15 times to create the 900-home community. Second, the 900 homes were individualized by integrating different occupancy profiles (which will be explained later). Thus, the 900 virtual homes are

comprised from variations of 60 physical homes for which comprehensive data were available.

The reduced-order models are used in an economic model predictive control framework to determine the optimal thermostat set points that minimize electricity costs over the prediction horizon (M). Model predictive control solves a limited-horizon optimal control problem that minimizes some objective function subject to a set of constraints. For the economic model predictive control case the formulation is

$$J = \min\left(\sum_{i=1}^{N} \sum_{j=t}^{t+M} r_j y_{i,j} \right) \tag{6.2}$$

subject to

$$y_{i,j} = f\left(y_{i,j-1}, T_{i,j-2:j}, DBT_{j-2:j}, j\right) \qquad \forall i, j \tag{6.3}$$

$$0 \le y_{i,j} \le maxLoad_i \qquad \forall i, j \tag{6.4}$$

$$lb_{i,j} \le T_{i,j} \le ub_{i,j} \qquad \forall i, j \tag{6.5}$$

where J is the objective function value, i is the index for the homes, j is the index for the time, r_j is the electricity rate at time j, N is the total number of homes, t is the initial time, f is the linear reduced-order model given by (5.10), $maxLoad_i$ is the maximum electricity consumption of the air conditioning unit of home i for one time step, and $lb_{i,j}$ and $ub_{i,j}$ are the lower and upper bounds, respectively, of the thermostat set point for home i at time j. It does not matter whether decentralized or centralized control is used for this minimum cost scenario because the homes are thermally and financially independent of one another. For the scenarios considered here, the thermostat set point (T) is the manipulated

variable and the air conditioning electricity consumption (y) is the controlled variable, with the outdoor dry bulb temperature (DBT) and the electricity rates (r) acting as disturbance variables. Weather predictions for the dry bulb temperature are assumed to be perfect in this chapter. However, for building heating and cooling systems a predictive controller using a simple weather model can get within 1-2% of an optimal, perfect-prediction solution [112], so this assumption is not likely to introduce much error. The electricity rates used here (r_j) are the day-ahead settlement point prices from the ERCOT system which are published a day in advance and therefore do not require a prediction model. All wholesale market prices and weather used in this analysis are actual data for Austin, Texas, from 2011. This formulation assumes that there are no behavioral changes due to the electricity prices—changes occur purely through the manipulation of the thermostat set point within the specified bounds. It is also assumed that occupants cannot override the set points chosen by the controller.

Solving (6.2)-(6.5) leads to optimal set points ($T_{i,j}$) for $j = t$ to $j = t + M$ for each home i. Only the first solution is implemented, then the time is increased by one time step and the problem is re-solved. This method is known as receding horizon control.

In Chapter 5, it was determined that the optimal value of M was 11 (with one hour time steps), and thus that value is used here. That means that index j will always run from $j = t$ to $j = t + 11$. There are 900 homes (N), so index i will always run from 1 to 900.

The upper and lower bounds for the thermostat set point were determined by the occupancy of each home. Homes had a desired thermostat set point temperature, which was also the upper bound for the set point while the house was occupied. The lower bound was taken to be 2.22°C (4°F) lower than the desired thermostat set point. When unoccupied, the upper and lower bound were set to 27.78°C (82°F) and 20°C (68°F), respectively. Desired thermostat set points were randomly assigned to houses according

the distribution in Figure 6.3. The data in Figure 6.3 are from homeowner surveys of 162 residents in the Pecan Street Smart Grid Demonstration Project (see [248] for more details). Based on clustering analysis and survey data of residential home energy profiles from the smart grid demonstration project [249], it was determined that approximately 50% of homes were occupied during the entire day while 50% of homes were unoccupied during typical workday hours (~8:00-17:00), thus when homes were randomly assigned occupancy profiles, they had a 50% probability of being occupied all day. Lastly, for the homes that were unoccupied for a portion of the day, random departure and arrival times were assigned based, again, on the data from the smart grid demonstration project. Departure and arrival times were randomly selected based on a uniform distribution from 6:00-10:00 and 16:00-19:00, respectively. An example of the upper and lower thermostat set point bounds for a home that was unoccupied for a portion of the day is shown in Figure 6.4. A home that is occupied for part of the day is defined as part-time occupied and a home that is occupied for the entire day is said to be full-time occupied.

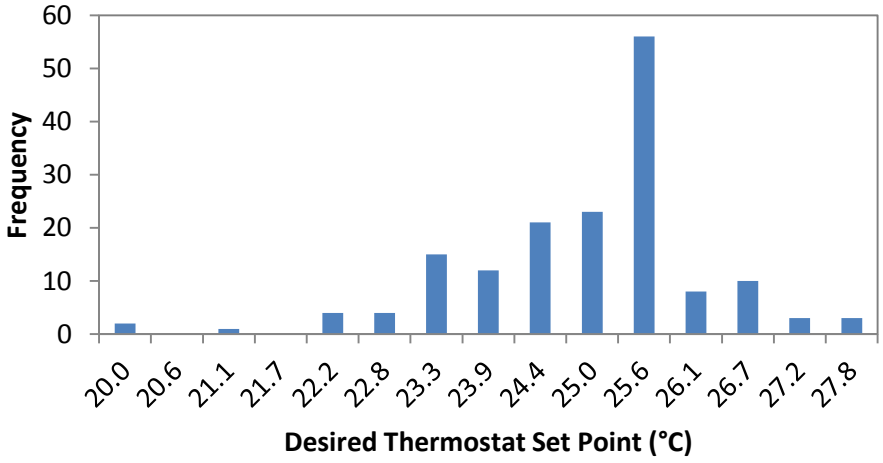

Figure 6.3: A distribution of desired thermostat set point temperatures based on 162 homeowner surveys shows 25.6°C (78°F) to be the most common set point.

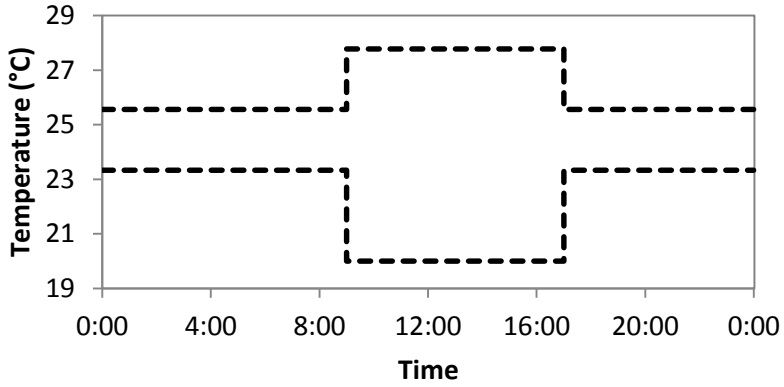

Figure 6.4: Upper and lower bounds for a part-time occupied home. The home is unoccupied from 9:00-17:00 and has a desired thermostat set point temperature of 25.6°C (78°F). These bounds constitute *lb* and *ub* in (6.5). If this home was occupied for the entire day (i.e., full-time occupied), then the upper and lower bounds would have remained constant at 25.6°C and 23.3°C, respectively, for the whole day.

Because a small number of homes have either undersized air conditioning units or thermally inefficient building envelopes coupled with low thermostat set points, the upper bound of the thermostat set point given by the constraint in (6.5) could not always be met during exceptionally hot afternoons, i.e., the air conditioner could not keep the temperature inside the house at or below the upper bound on the hottest days. To mitigate this issue the upper bound in (6.5) was enforced as a soft constraint with a high penalty weighting for violation.

Minimizing the peak electricity demand of the entire community through centralized control is done by changing the objective function of the model predictive controller to

$$J = \min\left(\max \sum_{i=1}^{N} \left(y_{i,j} + E_{i,j} \right) \right) \tag{6.6}$$

where $E_{i,j}$ is the non-HVAC (heating, ventilation, and air conditioning) energy usage for home i at time j, so that the sum of $y_{i,j}$ and $E_{i,j}$ is the total energy usage for home i at time j. In order to reformulate this problem as a linear program (LP), a new variable, z is added such that

$$J = \min z \tag{6.7}$$

subject to

$$z \geq \sum_{i=1}^{N} \left(y_{i,j} + E_{i,j} \right) \qquad \forall j \tag{6.8}$$

Equations (6.3)-(6.5)

where z is the maximum energy use of the community of homes over the time horizon of $j = t$ to $j = t + M$.

For decentralized control the peak electricity consumption of each individual house is minimized and the problem becomes

$$J = \min \sum_{i=1}^{N} z_i \tag{6.9}$$

subject to

$$z_i \geq y_{i,j} + E_{i,j} \qquad \forall i, j \tag{6.10}$$

Equations (6.3)-(6.5)

where z_i is the maximum energy use of home i from $j = t$ to $j = t + M$.

The 60 physical homes used to create the BEopt models described earlier had annual, whole-home billing data available, but had no information regarding the amount

of energy used for strictly non-HVAC loads. The non-HVAC energy ($E_{i,j}$) was instead taken directly from measurements of a separate set of 40 homes. These 40 homes are part of the Pecan Street Smart Grid Demonstration Project. The demographics of the 40 homes are roughly the same as the demographics of the 60 homes [248]; thus, it is assumed that behaviors affecting the non-HVAC loads would be similar. In addition, the average conditioned space of the 40 homes was 176 m^2, which is only 7% different than the average conditioned space of the 60-home dataset. Each of these 40 homes had been metered with a sub-circuit monitoring system that reported whole-home average power draw and HVAC average power draw on a one-minute interval. The HVAC energy was subtracted from the whole-home energy consumption to obtain the non-HVAC energy use. For each home and day, the one-minute data were averaged into hourly energy use data. Figure 6.5 shows the one-hour HVAC and non-HVAC loads for a single home for a July day.

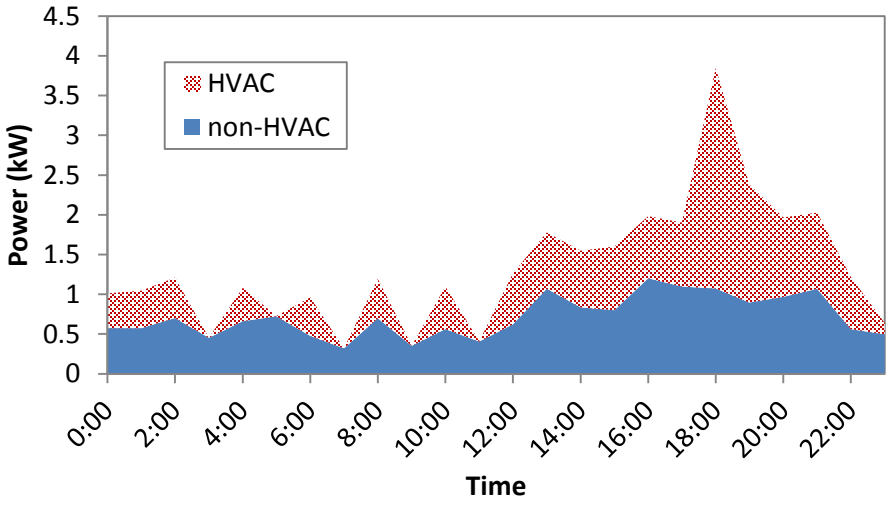

Figure 6.5: Measured HVAC and non-HVAC loads for a single home for a day in July. The total electricity usage and HVAC electricity usage are metered separately, so the non-HVAC load is determined by subtracting the HVAC usage from the total usage.

A one-day, single-home non-HVAC profile was created by averaging the non-HVAC profiles of the 40 homes over three months of summer. This average profile, shown in Figure 6.6, was used for all 900 homes in this investigation (i.e., for a given j, the $E_{i,j}$ for all homes is the same). Real homes have unique non-HVAC profiles, but because only community-level effects are considered, using an average profile instead of a unique profile will lead to the same net result for the economic and centralized control cases. For the economic case, this is because $E_{i,j}$ does not appear in the formulation. For the centralized case, $E_{i,j}$ is summed over all i, so summing the average yields the same as summing the unique profiles. In the decentralized case, the objective function will be slightly improved by using an average $E_{i,j}$ because an average $E_{i,j}$ value inherently contains some information about non-HVAC loads in other homes in the community.

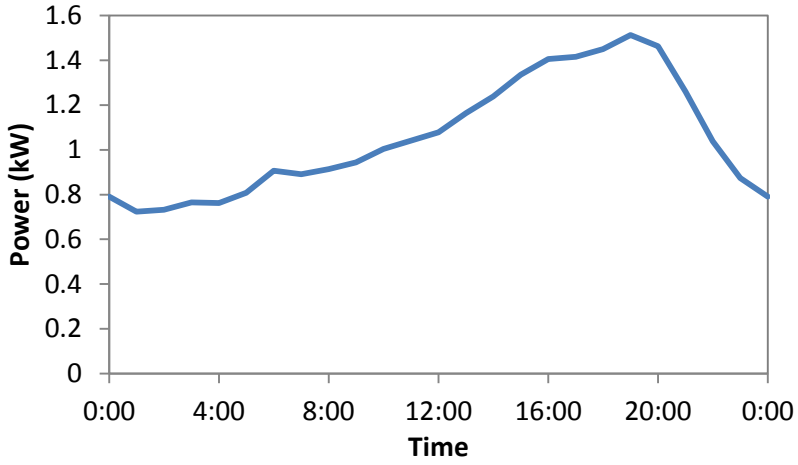

Figure 6.6: Average non-HVAC profile ($E_{i,j}$) that was applied to all 900 homes.

In addition to the decentralized and centralized control strategies presented above, an additional penalty-based decentralized control strategy is considered that attempts to mimic the control actions given by the centralized controller in (6.7) and (6.8). This

decentralized control strategy uses an objective function like the one in (6.2), but instead of using wholesale market electricity prices for r_j, this strategy attempts to flatten the system peak energy demand using randomly assigned custom penalty terms. These penalty terms vary both across times and homes, so for this scenario the problem formulation becomes

$$J = \min\left(\sum_{i=1}^{N} \sum_{j=t}^{t+M} \rho_{i,j} y_{i,j} \right) \tag{6.11}$$

subject to

Equations (6.3)-(6.5)

where $\rho_{i,j}$ is the penalty term for home i at time j. The overall goal of this strategy is to determine if an economic-like model predictive control strategy can achieve the same benefits as the centralized, minimum peak control strategy. In this way, no information needs to be shared between homes, reducing privacy risks and communications infrastructure requirements.

All scenarios are compared to a base case scenario. In the base case scenario each home's thermostat set point is kept at the desired thermostat set point for the entire day. This means that in the base case scenario the thermostat set point is at the home's desired set point while the home is occupied, and that the set point is raised to 27.78°C (82°F) when the home is unoccupied.

In summary, there are five scenarios considered in this chapter for the 900-home community:

1. Base case, $T_{i,j} = ub_{i,j} \ \forall \ i, j$
2. Minimum cost using wholesale day-ahead market prices, (6.2)-(6.5)

3. Minimum peak using centralized control, (6.7), (6.8), (6.3)-(6.5)
4. Minimum peak using decentralized control, (6.9), (6.10), (6.3)-(6.5)
5. Minimum peak using decentralized control and custom penalty terms, (6.11), (6.3)-(6.5)

RESULTS AND DISCUSSION

The results of the five different scenarios are presented here. The first section ("Minimum Cost Results") considers the minimum cost scenario using wholesale market electricity prices and compares the results to the base case. The results are presented using August 28 as a representative day because that day had the highest peak of all summer days in 2011 for the base case. Summertime results are also presented, where summertime is defined as the 92 days of June, July, and August.

The second section ("Minimum Peak Results") considers the scenarios 3-5 that are intended to minimize the peak for the community. Because the purpose of these controllers is to minimize the peak, only results from August 28 are presented. This second section is relevant to locations where peak demand is of primary concern, such as in constructing a microgrid where generation equipment has to be sized to meet the loads of the community without grid support.

Minimum Cost Results

Minimizing costs according to (6.2)-(6.5) for August 28 for the 900 homes is shown in Figure 6.7. Significant precooling in the community causes an increase of air

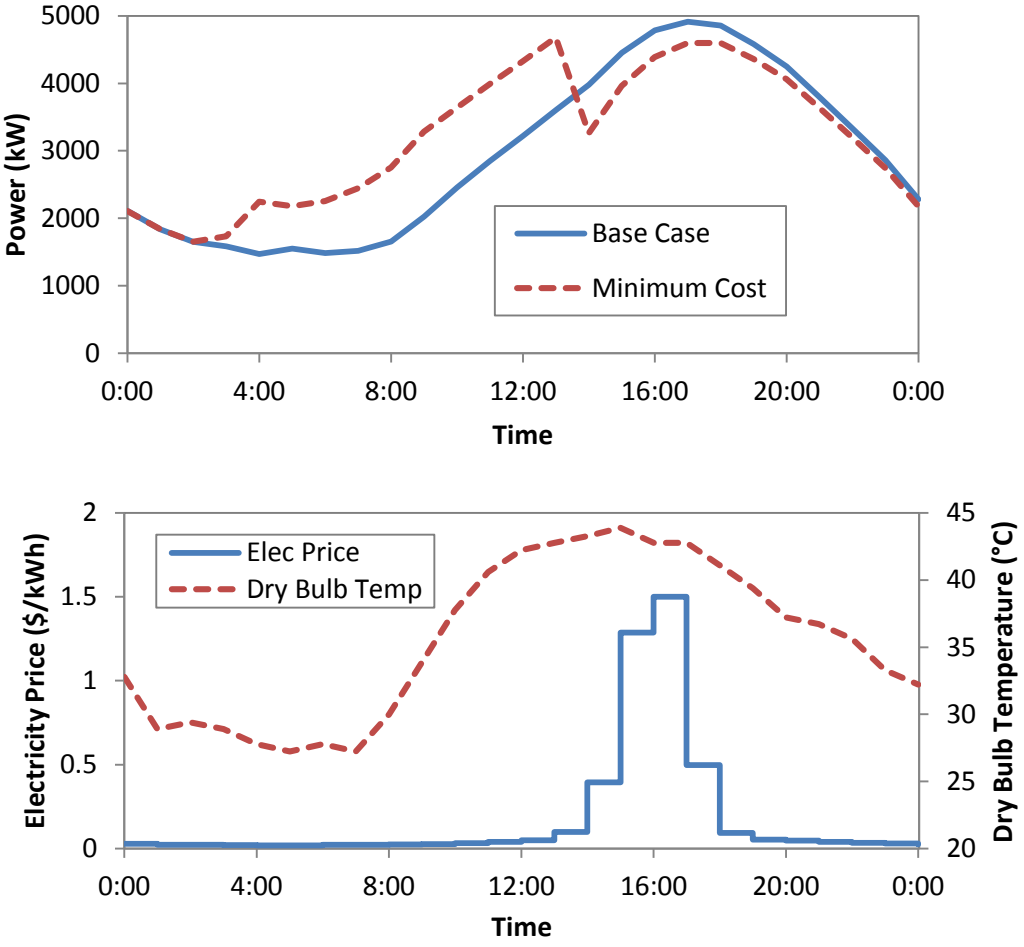

Figure 6.7: The upper plot shows the air conditioning power consumption for the 900-home community under the minimum cost scenario for August 28, 2011. A new peak is created earlier in the day, but it is lower than the original peak in the base case. The lower plot shows the actual ERCOT day-ahead settlement point prices (r_j) and the ambient dry bulb temperature (DBT_j) for the same day.

conditioning energy consumption during the morning hours with a sharp decrease in energy use in the afternoon when prices are high. This precooling effect results in an overall reduction in electricity cost from $19,300 to $17,900 for the community, or 7.0% versus the base case. Peak energy demand is reduced from 4912 kW to 4678 kW, or 4.8%. However, total energy use for the day increases from 70,800 kWh to 77,900 kWh,

or 10.1%. Although prices are unusually high for this day (the average hourly price is $0.18/kWh with a peak of $1.50/kWh), it will be shown later that the 7% cost savings is not atypical for the 2011 summer.

Because of the precooling, there is no traditional rebound effect. In fact, from Figure 6.7 it can be seen that the minimum cost scenario consumes less energy in the evening than does the base case. As long as there is only a single afternoon price peak, there is no concern about the air conditioning units all turning on at the same time when the high price period ends. There are two reasons that there is no concern. The first reason is that when the peak afternoon price occurs, the controller ensures that the set point is at the upper bound in order to minimize costs because the upper bound will yield the lowest energy consumption. Assuming there is no price spike later in the evening, the controller will never move the set point from the upper bound because doing so would cause an increase in the objective function. The second reason is that all the homes are thermally dissimilar and have stored different amount of "cooling" energy in the thermal mass of the home by the time the peak afternoon price occurs. Some homes have very little thermal energy stored either due to lack of thermal mass or due to limited precooling, while other have significant amounts of thermal energy stored. This variation in stored thermal energy coupled with the variety of thermal envelopes means that the homes will warm up at different rates and air conditioning systems will be turned on or up gradually over time.

Using the economic model predictive controller appears to always lower the community's peak demand. For the 92 summer days considered (June-August), there were no days when the morning peak generated by the precooling exceeded the afternoon peak from the base case. The maximum peak for the neighborhood occurred on August 28 (shown in Figure 6.7), and in this case the peak was reduced by 4.8% using the

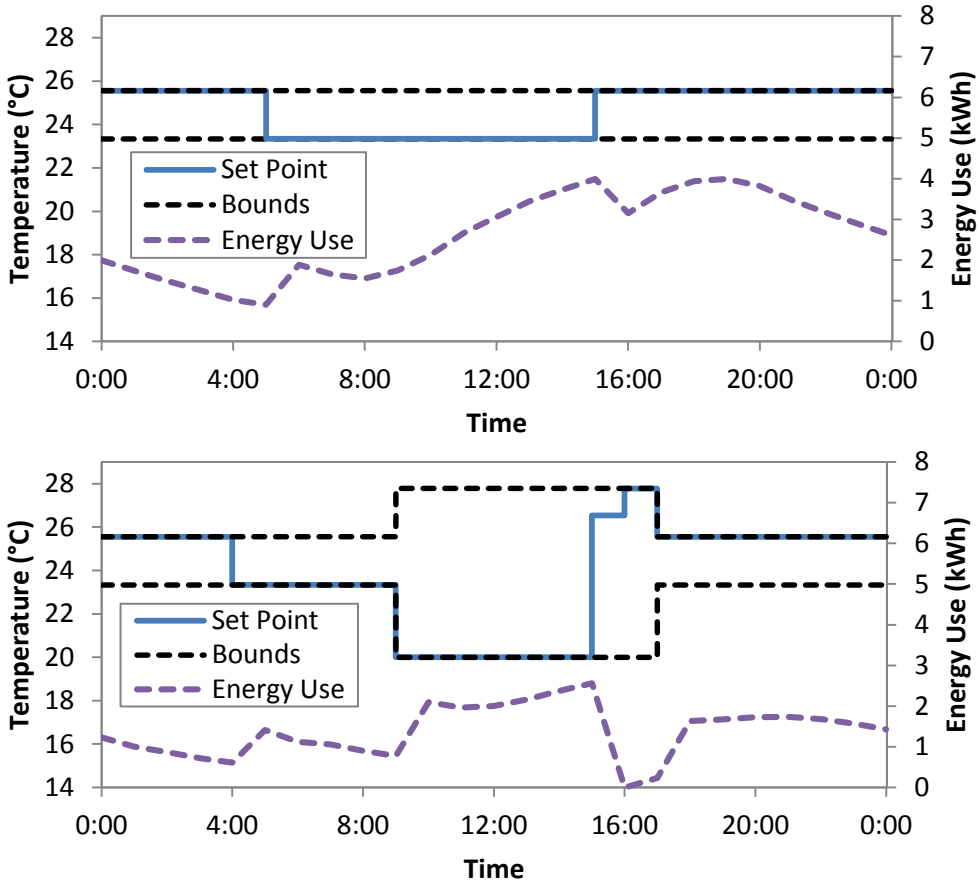

Figure 6.8: Comparison of a home that is occupied all day (upper plot) and a home that is unoccupied from 9:00-17:00 (lower plot) for August 28. The home that is unoccupied during the daytime hours has much more flexibility in precooling the home in anticipation of the high afternoon prices (see Figure 6.7).

minimum cost strategy when compared to the base case. On average, the minimum cost strategy yielded a 2.7% reduction in the daily peak versus the base case. This peak reduction demonstrates that a higher peak is not likely to be created in an automated, community-wide response to wholesale market prices in a minimum cost scenario. There is not likely to be a new peak because of the inflexibility of those homes that are always occupied. Homes that are unoccupied for a portion of the day can perform much more precooling because the comfort limits are largely removed while no one is at home.

Occupied homes can only perform marginal precooling without violating set point bounds (see Figure 6.8).

Table 6.1 summarizes the results from the minimum cost control strategy over the course of the summer. For summer 2011, the minimum cost controller achieves a 5.7% cost savings and a 4.8% reduction in total peak, but increases overall energy usage by 3.9%. Because the costs in Table 6.1 are based on the wholesale market prices, the values represent potential savings to the utility and not necessarily to the customer. On average, this operating scheme would save the utility about $13 per home per month, so a utility would likely not be willing to pay more than this amount in order to implement this minimum cost control scheme for the homes in this investigation.

	Base Case	Min Cost Scenario	Savings
Total Cost	$ 607,300	$ 572,500	5.7%
Air Conditioning Cost	$ 405,000	$ 370,100	8.6%
Non-HVAC Cost	$ 202,300	$ 202,300	-
Total Energy (kWh)	5,492,000	5,705,000	-3.9%
Air Conditioning Energy (kWh)	3,357,000	3,570,000	-6.4%
Non-HVAC Energy (kWh)	2,135,000	2,135,000	-
Total Peak Demand (kW)	4912	4678	4.8%
Air Conditioning Peak (kW)	3638	3630	0.2%
Non-HVAC Peak (kW)	1361	1361	-

Table 6.1: Summertime (June-August) costs, energy consumption, and peak demand for the 900-home community for the minimum cost scenario using the objective function given by (5.2). Total values are subdivided to those from the air conditioning systems and those from the non-HVAC systems.

As a side note, if the minimum cost scenario is solved using constant electricity prices (i.e., a flat rate) instead of wholesale market prices, then the optimal solution matches the base case. This means that the base case (keeping the thermostat set point at

the upper bound for the entire day) is the best strategy for reducing costs in a flat rate environment or for minimizing energy consumption.

Homes that are unoccupied for a portion of the day reap the majority of the savings from precooling. This savings is due to the additional flexibility given in precooling the homes. Figure 6.8 shows the effect of the additional precooling. In the home that is always occupied (Figure 6.8 upper plot) the power draw dips from 4 kW to 3.2 kW when the thermostat set point is raised. In the home that is unoccupied during the daytime (Figure 6.8 lower plot) the power draw drops from 2.6 kW to 0 kW. The additional flexibility in precooling allows a significantly greater decrease in energy use during the expensive afternoon hours. Figure 6.9 provides a summary of the savings achieved by each of the homes over the course of the 3-month summer. Savings versus the base case range from 0-46%, with the part-time occupied houses reaping substantially higher savings in most cases. The high variation in savings between homes is caused by the differences in occupancy schedules, desired thermostat set point, home construction, home orientation, home size, number and location of windows, and air conditioning equipment efficiency. This high variation in savings between homes also indicates that there are certain home attributes or occupant behaviors that are conducive to passive thermal storage. Identifying those attributes and behaviors will be the subject of future research.

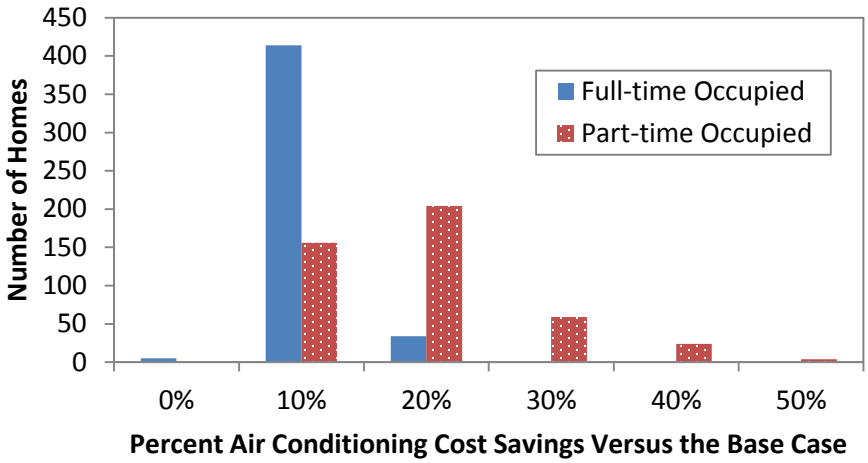

Figure 6.9: Histogram of air conditioning cost savings for the 3-month summer using the minimum cost objective function across the 900 homes. Homes that are occupied during only part of the day experience much greater cost-savings than those that are always occupied.

Minimum Peak Results

In this section, the objective of the different control scenarios is to minimize the total peak of the system by applying centralized or decentralized thermostat set point control. In the centralized case, the controller knows what every house is doing and is therefore able to minimize the system peak to the maximum extent possible. This capability leads to a system demand curve that is level throughout the afternoon (see Figure 6.10). For August 28, the day of the summer with the highest system peak, the centralized control strategy in (6.7), (6.8), and (6.3)-(6.5) reduces the peak demand by 430 kW, or 8.8% from the base case. However, this shift comes at the cost of an extra 9430 kWh of energy use, which is an increase of 13.3% over the base case.

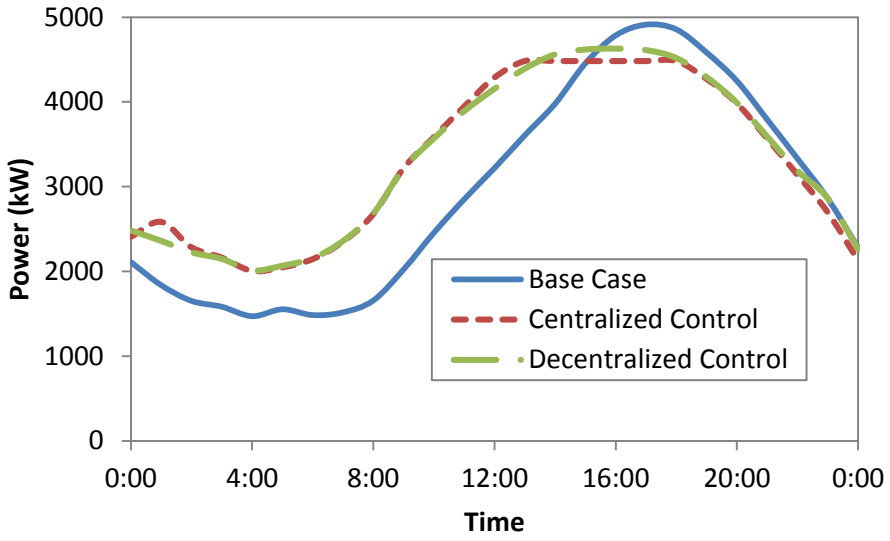

Figure 6.10: Power consumption of the 900-homes community for August 28. The centralized control strategy flattens the system peak. The decentralized strategy reduces the system peak, but not to the same extent as the centralized strategy.

Using the decentralized control strategy in (6.9), (6.10), and (6.3)-(6.5), each house only knows what it is doing and only attempts to minimize its own peak. This approach leads to a lower peak than in the base case, but a higher peak than the centralized controller (see Figure 6.10). For August 28, decentralized control leads to a 5.7% reduction in the system peak versus the base case. Because the centralized controller is managing all the homes simultaneously, it can coordinate thermostat set points to perfectly flatten the peak. Decentralized control does not have that capability. However, decentralized control has the advantage that information does not need to be shared with a centralized controller, which reduces the amount of required communication equipment and lessens concerns surrounding data privacy.

The tradeoff between peak demand and energy consumption is shown in Figure 6.11. This figure was created using the objective functions (6.2)—with r_j set to a constant

value for all *j*—and (6.9) simultaneously and modifying the relative weight given to each objective function. The points in the figure follow a quadratic curve that has a slope varying from -2.9 to -40.6. This slope indicates the relative value of energy consumption to peak reduction, meaning that it takes from 2.9-40.6 kWh of additional energy consumption to reduce the peak demand by 1 kW. The first few kW of peak reduction cost less energy (2.9 kWh), while the final few kW of peak reduction cost more energy (40.6 kWh). Current pricing structures in Austin, TX, value power at ~12.00/kW and energy at ~0.11/kWh, giving a ratio of 109 kW/kWh. This real-world price ratio is much higher than the 2.9-40.6 kW/kWh tradeoff identified here, meaning that for single-day events, the cost-based controller will preferentially reduce the demand at the expense of consuming extra energy.

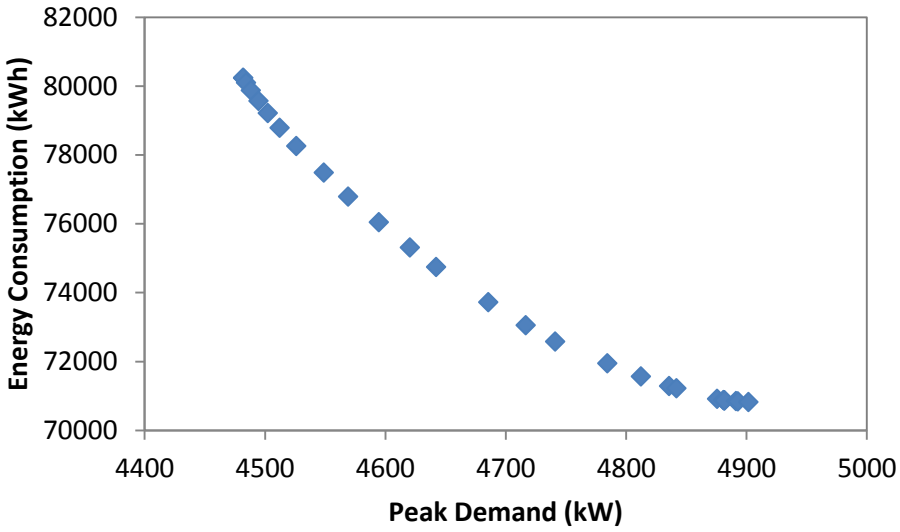

Figure 6.11: This figure shows the tradeoff between peak demand and energy consumption for the community of homes. The points follow a quadratic curve, implying that it is increasingly costly (in terms of energy consumption) to reduce peak demand. The right-most point is the base case and the left-most point is the centralized, minimum peak case.

Figure 6.12 shows the relative tradeoff between the peak demand reduction and energy consumption. The percent reduction in peak demand is greater than the percent increase in energy use up to 5.3%. Beyond 5.3% the percent increase in energy use is greater than the percent reduction in peak demand.

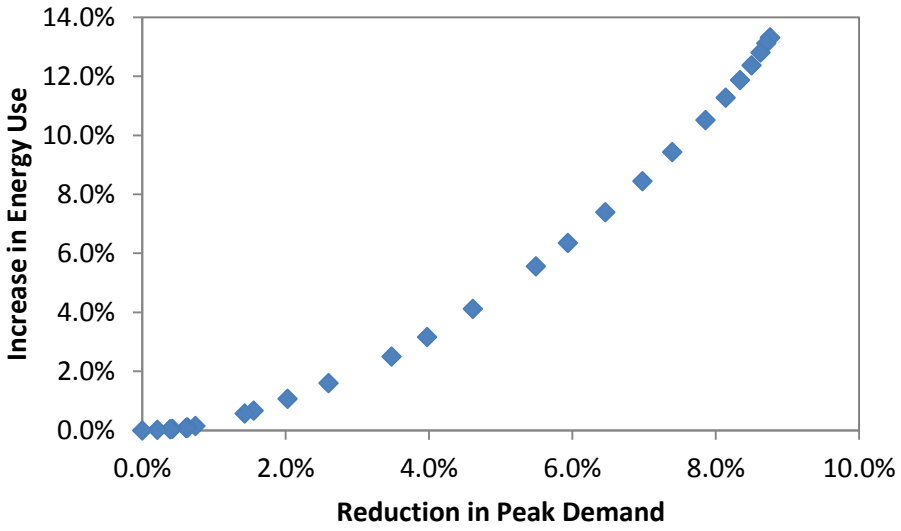

Figure 6.12: Relative reduction in peak demand versus the increase in energy required to achieve that peak demand reduction. The percent reduction in peak demand is greater than the percent increase in energy use up to 5.3%. The left-most point (0,0) is the base case, and the right-most point is the centralized, minimum peak case.

To obtain the benefits of both centralized and decentralized control, a decentralized control strategy was implemented that used the economic-like penalty function given in (6.11). The penalty term, $\rho_{i,j}$ varies from home to home, though it retains the same general structure. A sample penalty term is shown in Figure 6.13. Penalty terms were generated by setting an off-peak penalty that was $1/100^{th}$ of the peak penalty. Each home was randomly assigned a three-hour peak penalty period beginning between 14:00 and 19:00 according to the probability distribution shown in Figure 6.14.

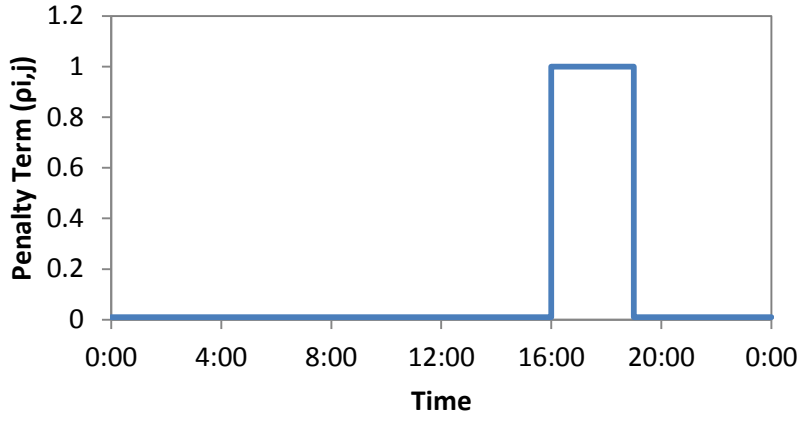

Figure 6.13: Sample penalty term for the economic-like decentralized control strategy. The exact starting time of the peak period is randomly determined based on the distribution in Figure 6.14. The off-peak penalty is 0.01.

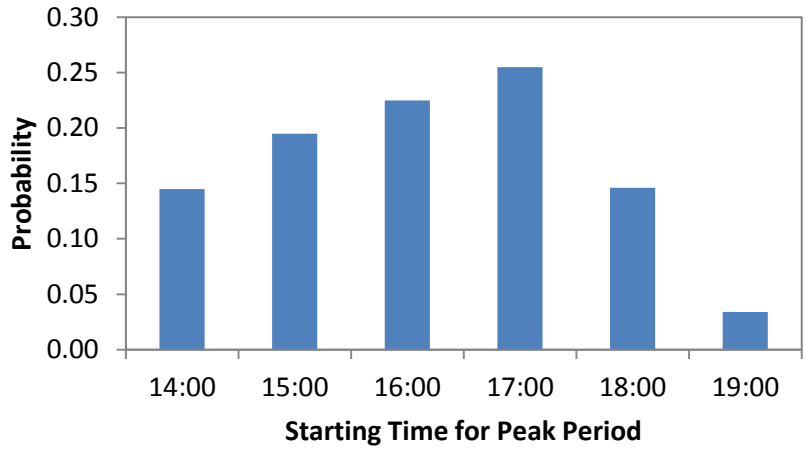

Figure 6.14: Probability distribution for the start time of the peaking periods for designing price structures.

By applying these penalty terms and allowing each home to minimize its own penalty function, the decentralized solution approaches the centralized solution (see Figure 6.15). The peak under this price-based decentralized control strategy is within

1.1% of the peak of the centralized control strategy, but requires no sharing of information between homes.

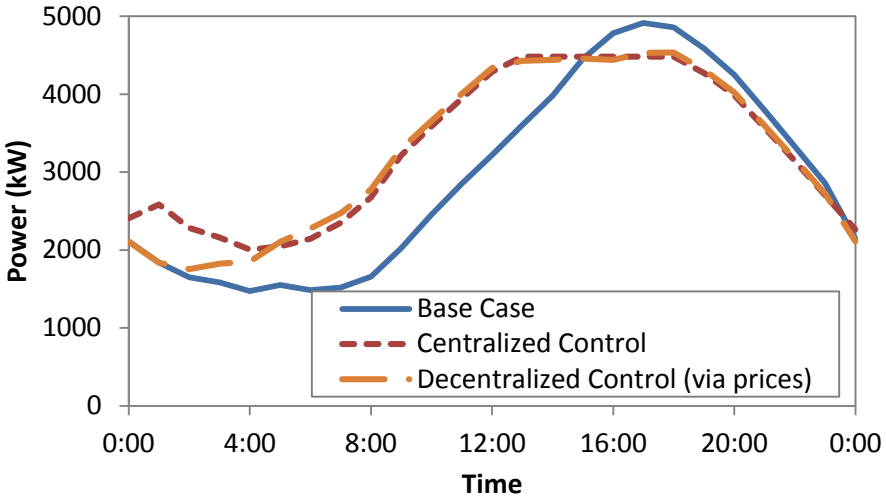

Figure 6.15: Power consumption of the 900-homes community for August 28. By tuning the penalty distribution for the decentralized controller, the decentralized solution approaches the centralized solution.

Table 6.2 summarizes the peak reduction results of the five different scenarios. Centralized control is the most the most effective at reducing peak demand.

Scenario	Peak Demand (kW)	Peak Reduction
1. Base Case	4912	-
2. Minimum Cost	4678	4.8%
3. Centralized	4482	8.8%
4. Decentralized	4631	5.7%
5. Decentralized (with Penalty Function)	4535	7.7%

Table 6.2: Peak demand and peak demand reduction versus the base case for the five scenarios for August 28.

The minimum cost scenario and the minimum peak scenarios presented here assume that thermostat set points can be set at any desired value, when in reality most thermostats in the United States have a resolution of 0.5 or 1°F (0.27 or 0.56°C). However, Perfumo *et al.* [246] presented a method for addressing that shortcoming through applying a distribution of discrete set points that have the same mean as the high-resolution desired set points. In the case that these control strategies were to be implemented, a similar approach could be applied here.

CONCLUSIONS

By considering a notional community of 900 homes built with attributes taken from 60 actual homes in Austin, Texas, the baseline operational conditions and large-scale effects of four thermostat control schemes were investigated. Based on the simulated community, if all homes responded in a cost-optimal way to market electricity prices by adjusting air conditioning thermostat set points, their consumption would be shifted. While this shift is significant, it would not likely create a new peak that is higher than the original peak. In fact, the summertime peak for this simulated community was reduced by 4.8% in the minimum cost scenario.

Potential savings from one home to another varies greatly across the 900 homes, although more savings are achieved in homes that are unoccupied during daytime hours. The additional flexibility offered to the controller during those unoccupied periods enables substantial precooling activity and, on average, an order of magnitude more of cost savings than homes that are occupied during the entire day.

In the case of minimizing the peak electricity demand for the community, the centralized controller achieves the maximum reduction in peak possible (8.8%). The decentralized control strategy in which each house minimizes its own peak results in a

peak reduction that is just over half that of the centralized controller. However, by implementing a penalty-based decentralized control strategy with tuned penalty terms, the decentralized control solution can approach the centralized control solution to within 1.1%.

In the future the simulations can be expanded to include a larger variety of home types that are representative of those across the ERCOT grid service area. This expansion would allow consideration of the effects of thermostat control strategies on the overall grid peak. Additionally, home characteristics that make homes better candidates for automated thermostat control can be identified. Identification of these characteristics can help utilities make more informed decisions when implementing peak management programs.

Chapter 7: Community-scale Air Conditioning Control for High Penetration of Rooftop Photovoltaics[6]

INTRODUCTION

The installed capacity of solar photovoltaic (PV) systems in the United States has increased in recent years due to declining costs. Reported installed prices of U.S. residential and commercial PV systems declined 5%–14% per year, from 1998–2012 [250]. The decreasing cost of PV panels makes their installation especially appealing in warmer climates, where PV generation aligns with high demand periods and can be utilized to lower peak electricity demand from the grid [251]. Residential energy consumption is highly dependent on outside air temperatures and in hot weather, contributes significantly to peak demand through increased use of the air-conditioning (A/C) [197]. Using PV systems to provide energy to the A/C systems during peak times can be a powerful tool to reduce peak demand from the grid.

However, like A/C use, PV power output is affected by fluctuating weather conditions. Even on clear, sunny days, PV generation changes substantially throughout the day. Often peak loads in the home or on the electric grid extend into the evening where solar production is very low. Household electricity demand might be relatively low when PV generation is highest. So while rooftop PV by itself can reduce peak demand, it is limited by the amount of sunlight available during the peak demand period.

One way to shift more of the energy generated by rooftop PV to peak times is through the use of energy storage. While battery storage would likely be cost prohibitive

[6] This chapter was included in W. J. Cole, K. X. Perez, J. D. Rhodes, M. E. Webber, M. Baldea, and T. F. Edgar, "Community-scale air conditioning control for high penetrations of rooftop photovoltaics," in *Proceedings of the 2014 American Control Conference*, Portland, OR, USA, 2014. Perez and Rhodes contributed the non-HVAC energy use and measured PV data. Webber, Baldea, and Edgar provided general advising and editing.

for a residential setting, thermal energy storage (TES) is an inherent characteristic of any home via the homes' walls, foundation, etc. acting as the thermal medium. As discussed in Chapters 2 and 5, TES uses the thermal mass in the home to store "cooling" energy by pre-cooling the home during periods of lower energy demand. The cooling energy in the thermal mass maintains thermal comfort later when outdoor air temperatures increase. By taking advantage of passive TES, the non-peak PV energy can be used to operate the A/C during lower use times, thereby reducing A/C energy consumption during peak hours. Passive TES has already been proven successful for commercial buildings in reducing peak cooling demand largely because the size of thermal mass has made the strategy economically feasible [209], [252]–[255]. In commercial building applications, control methods for passive TES are often implemented using a model predictive control framework to maximize storage benefit [143], [256]. The application of passive thermal storage in residential homes has been limited. Due to the size and variety of home types, the benefit of passive TES from a single home can be negligible. However, in the aggregate, the passive TES offered by residential homes is likely to be substantial. While aggregated passive TES has been modeled (e.g. [241]), and the effects of solar PV are relatively straightforward, to my knowledge the integration of the two at scale (e.g., hundreds of homes) has not been modeled to estimate their peak reduction potential. It is hypothesized that the use of intelligent control can effectively manage energy generated from rooftop PV in conjunction with passive TES to lower peak energy demand. Because the integrated effects on peak demand from the combined systems are non-obvious (just adding the two together does not sufficiently approximate the real-world conditions) testing this hypothesis requires an adequate model. Developing and demonstrating the model of a community of homes was the subject of Chapter 6. The work in this chapter applies the community model in Chapter 6 to investigate the coordinated control of

residential passive TES (through the manipulation of A/C thermostat set points) when the homes also include rooftop PV. Centralized and decentralized model predictive control methods are used to minimize the peak demand in response to changes in weather, PV generation, residential internal loads, and occupancy.

METHODOLOGY

In this investigation, A/C thermostat set point control strategies are applied to the simulated community of 900 individual homes that was described in Chapter 6. Specifically, this chapter considers the benefits of thermostat set point control for peak demand reduction when the 900-home community has rooftop PV installed on 0%, 50%, or 100% of the homes. Only the centralized and decentralized peak demand reduction formulations—((6.7), (6.8), (6.3)-(6.5) and (6.9), (6.10), (6.3)-(6.5)), respectively—from Chapter 6 are considered in this investigation.

The formulation for the model predictive controller remains unchanged from Chapter 6, except that PV generation data ($P_{i,j}$) are now included in the objective function for minimizing peak demand:

$$J = \min\left(\max \sum_{i=1}^{N} \left(y_{i,j} + E_{i,j} - P_{i,j} \right) \right) \tag{7.1}$$

The PV generation data came from 226 rooftop PV arrays (one array per house) metered by the Pecan Street, Inc., from June 1-August 31, 2013. Of those homes, 125 had south-facing arrays with an average capacity of 3.57 kW. The remaining 101 arrays were west-facing with an average capacity of 3.24 kW. The measured PV generation data were averaged into hourly values, thus for a given hour j, $P_{i,j}$ is the average power generation of the 226 arrays during hour j. Note that unlike non-HVAC data ($E_{i,j}$), $P_{i,j}$ is different for

each day (e.g., values for $P_{i,j}$ for August 1 are the average measured values from August 1).

Weather data were taken from a weather station located at the University of Texas at Austin in Austin, Texas. Weather data were collected from June 1-August 31, 2013 and thus matched the PV generation data.

The non-A/C energy ($E_{i,j}$) was taken directly from measurements of a set of 180 homes from June 1-August 31, 2013. These 180 homes are part of the Pecan Street Smart Grid Demonstration Project.

A total of nine scenarios are considered: no control (base case), decentralized control, and centralized control each with 0%, 50%, and 100% of homes having rooftop PV installed. The results of the various control strategies and PV adoption levels are first presented for a single summer day (June 28) and then presented for the entire summer (June-August). June 28 was chosen because it had the highest peak electricity demand of any summer day in the base case. All results presented are simulation results.

RESULTS

Figure 7.1 shows the results of using no control (the base case), decentralized control, and centralized control for the 900-home community for June 28, 2013, when none of the homes have rooftop PV. In the base case, the peak occurs at 17:00 at 4955 kW. The peak is reduced by 365 kW (7.4%) and 488 kW (9.8%) using decentralized and centralized control, respectively. Because the centralized controller has knowledge of all the homes in the system it can coordinate the precooling of the various A/C units to achieve the maximum peak reduction. This peak reduction comes at the cost of increased overall energy consumption; the decentralized and centralized control strategies increase energy consumption by 10.3% and 9.9%, respectively.

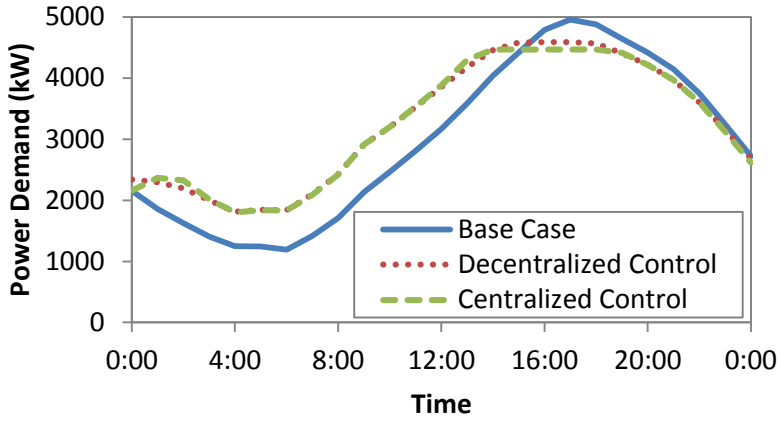

Figure 7.1: Simulated power demand for the 900-home community on June 28, 2013, with no rooftop PV adoption.

The community profile changes dramatically when all homes are assumed to have rooftop PV (see Figure 7.2). In the base case the peak is shifted to 20:00 and reduced to 4386 kW, and during the middle of the day PV production nearly causes the community power demand to be negative (i.e., electricity is sent to the grid rather than consumed from the grid). The decentralized and centralized control methods are almost identical, reducing the peak by 345 kW (7.9%) and 374 kW (8.5%), respectively. In the absence of PV generation, the individual homes peak at different times. When all homes have rooftop PV installed, they all reach a peak at nearly the same time (when the sun goes down). In other words, the PV tends to temporally align the peaks of all the homes, which means that minimizing the peak of a single home contributes directly to minimizing the peak of the community. Thus, the control actions taken by the decentralized controller will be very similar to those taken by the centralized controller.

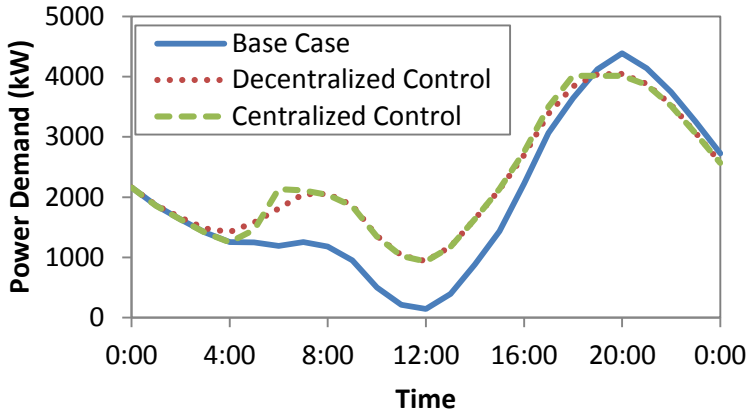

Figure 7.2: Simulated power demand for the 900-home community on June 28, 2013, with 100% rooftop PV adoption.

Figure 7.3 and Table 7.1 summarize the peak demand reductions for the entire summer (June-August) in the nine different scenarios. More than half of the peak reduction benefit from the PV is captured when only 50% of homes have PV installed. This can be seen in both the base case scenario and in the decentralized and centralized control scenarios (see Table 7.1). The reason that 50% PV adoption achieves most of the peak reduction benefit is two-fold. The first is that once the peak has been shifted to late evening when the PV generation is near zero, adding more PV capacity will not lead to more generation (and therefore more peak reduction). The second is that nearly all homes are occupied during evening hours so the thermal comfort bounds are tighter, restricting the capability of the decentralized and centralized controllers to shift load.

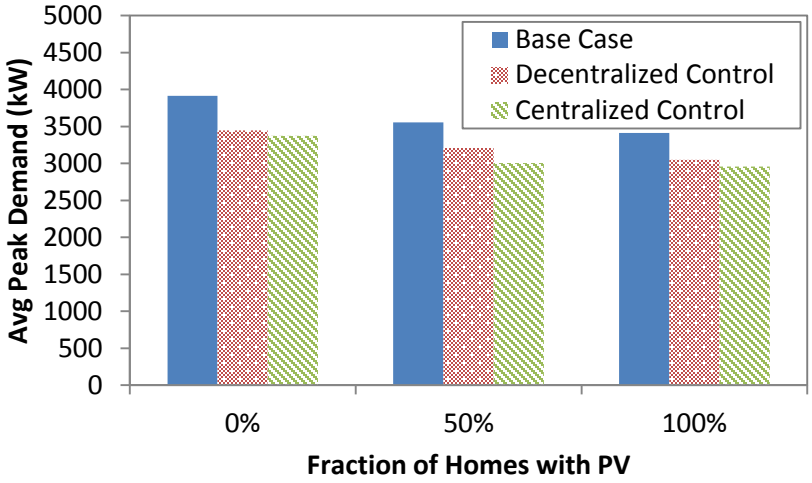

Figure 7.3: Average simulated daily peak demand of the 900-home community for the summer (June-August).

	Fraction of Homes with PV		
	0%	**50%**	**100%**
Base Case	-	9.2%	12.8%
Decentralized Control	12.0%	18.0%	22.1%
Centralized Control	13.8%	23.3%	24.4%

Table 7.1: Percent reduction in average daily peak demand of the 900-home community for the summer (June-August). All percentages are with respect to the base case with 0% of the homes having PV. The 0%, base case peak is 3913 kW.

As noted for June 28, the controllers implemented a precooling strategy that leads to an increase in energy use. The average daily increase in energy use for the summer is summarized in Table 7.2. Additional energy use because of precooling is higher as the level of PV adoption increases. This high energy use happens because PV generation shifts the peak to later in the day, which also causes the precooling to be shifted to later in the day. The afternoon precooling means that the A/C is operating at a high load when it

is least efficient to do so (because ambient temperatures are highest, making it more difficult to reject heat to the outside air). Additionally, thermal gains to the house will be higher due to a higher indoor-to-outdoor temperature gradient.

Both the increased energy use and the marginally lower improvements in peak reduction as PV adoption increases indicate that the peak reduction of precooling strategies is somewhat reduced as PV generation increases.

	Fraction of Homes with PV		
	0%	**50%**	**100%**
Base Case	-	-	-
Decentralized Control	5950	6500	7090
Centralized Control	5690	7080	7300

Table 7.2: Average daily increase in consumption (in kWh) versus the base case of the 900-home community for the summer (June-August). For example, centralized control strategy with 100% of the homes having PV consumed, on average, 7300 kWh more electricity per day than the base case with 100% of the homes having PV.

In terms of percent reduction in peak demand, there was essentially no difference between cloudy days and sunny days. Obviously PV generation decreases considerably during cloudy days, but daytime clouds also reduce solar heat gains in the homes and tend to lower ambient dry bulb temperatures. The lower cooling loads on the buildings made it easier to shift a larger portion of the cooling load away from peak hours, so high performance was still achieved.

CONCLUSIONS

The following can be concluded from this investigation:

- High penetration of rooftop PV leads to a reduction in peak power drawn from the grid and shifts the peak to later in the afternoon.
- Decentralized control performs almost identically to centralized control when all homes have rooftop PV.
- The benefit of implementing decentralized or centralized control is slightly decreased as the fraction of homes with PV increases. However, in all cases implementing decentralized or centralized control led to a decrease in the community's peak demand by more than 10%.
- The centralized and decentralized precooling strategies increased overall energy consumption by 5600-7300 kWh (10-20%).

Future work includes evaluating the significance of assuming that PV loads can be perfectly predicted. This work can also be expanded to include other types of electricity sources and sinks, such as micro-CHP units and electric vehicles.

Chapter 8: Optimal Electricity Rate Structures for Peak Demand Reduction using Economic Model Predictive Control[7]

INTRODUCTION

Economic model predictive control (EMPC) has found considerable popularity in managing building energy systems. This has in large part occurred as electricity rate structures have moved away from constant electricity prices to variable electricity prices, so the ability of including these variable rates in an objective function is valuable. Buildings inherently contain thermal mass which can be used to store thermal energy, and because a significant component of a building's electricity consumption is related to the heating, ventilation, and air conditioning (HVAC) system, the building's thermal mass can be used as thermal energy storage to shift loads in time. This thermal energy storage allows the building to consume electricity for the energy intensive HVAC system during times when electricity prices are lower, and draw from the thermal storage when prices are higher. However, managing this kind of thermal storage system requires advanced control, and, as discussed in Chapter 2, model predictive control has been found to be a useful tool for managing such a system. By using model predictive control, the variable electricity prices can be placed directly into the objective function [257], and the building's energy system can be modeled using dynamic models. Thus, the EMPC manages the HVAC system, thermal mass, and occupant comfort requirements in a way that minimizes the electricity costs of the system, especially when electricity prices change throughout the day. Other energy systems such electric vehicle charging networks [258], chilling networks [259], and IGCC power plants [260] have also found success

[7] This chapter has been submitted as W. J. Cole, D. P. Morton, and T. F. Edgar, "Optimal electricity rate structures for peak demand reduction using economic model predictive control," *Journal of Process Control*, under review 2014. Morton contributed expertise and guidance in building the modified dual formulation, and Edgar provided general advising and editing.

using EMPC in the face of variable electricity prices, but this chapter will focus on EMPC for residential building HVAC systems.

There are most commonly two general types of variable electricity rate structures: time-of-use (TOU) electricity prices and real-time or spot electricity prices, though variations of these rate structures exits. Time-of-use rate structures are known in advance and typically have several levels of electricity prices based on the time of day, day of the week, and season of the year. For example, the TOU rate for residential homes in Austin, Texas, USA, is shown in Figure 8.1. Real-time electricity rates are typically set through market mechanisms, where bids for buying and selling electricity are used to set the electricity price. These prices are generally not known in advance and can potentially vary quite dramatically. Figure 8.2 shows the real-time market prices for August 21, 2011, in the Austin Load Zone of the Electricity Reliability Council of Texas (ERCOT) grid.

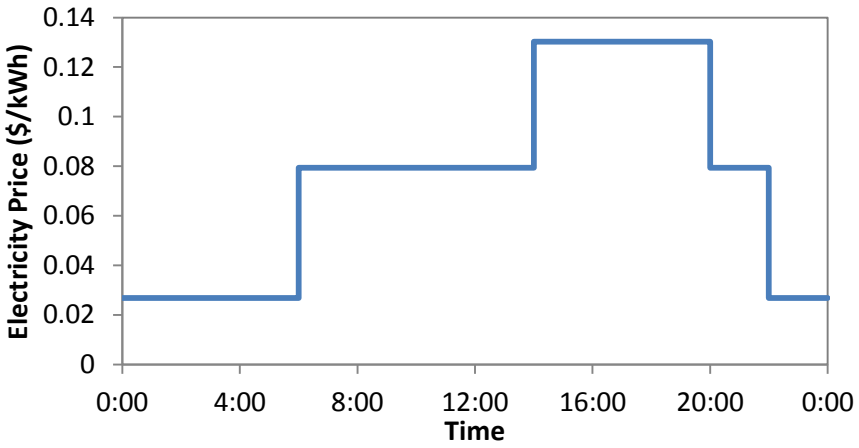

Figure 8.1: Time-of-use prices in Austin, Texas, for a weekday in the summer [261]. The highest prices ("on-peak" prices) occur from 14:00-20:00.

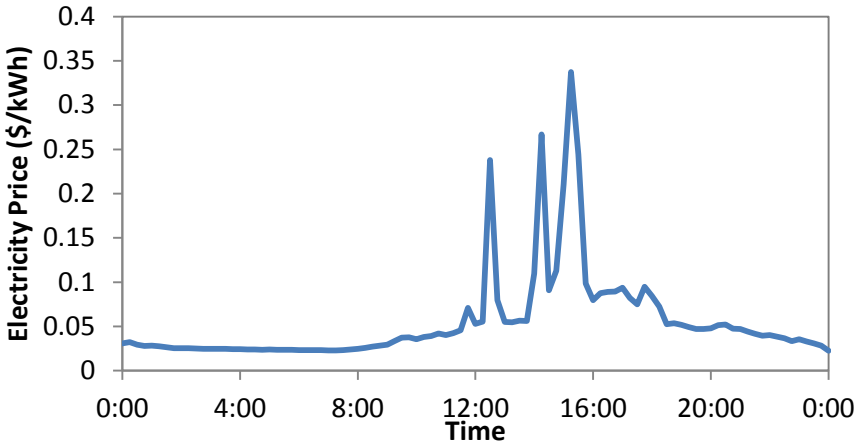

Figure 8.2: Real-time settlement point prices for the Austin Load Zone in the ERCOT market on August 21, 2011. These prices were set every 15 minutes by a bidding process. Electricity demand was especially high this day, which is one of the reasons for the higher-than-normal price spikes during the middle of the day.

One variation of TOU prices that is important to the results in this chapter is critical peak pricing (CPP). Critical peak pricing is typically a higher-priced, shorter duration TOU rate structure that is only implemented on a few days during a season. Customers are generally notified a day in advanced of a critical peak day, and then the high prices are realized. An example CPP rate structure is shown in Figure 8.3. A review of time-varying pricing trials by Newsham and Bowker [262] suggests that CPP is the most effective pricing strategy for peak reduction, yielding peak reductions of 30% when enabling technology is available. They also suggest that a simple TOU rate will result in a 5% peak reduction.

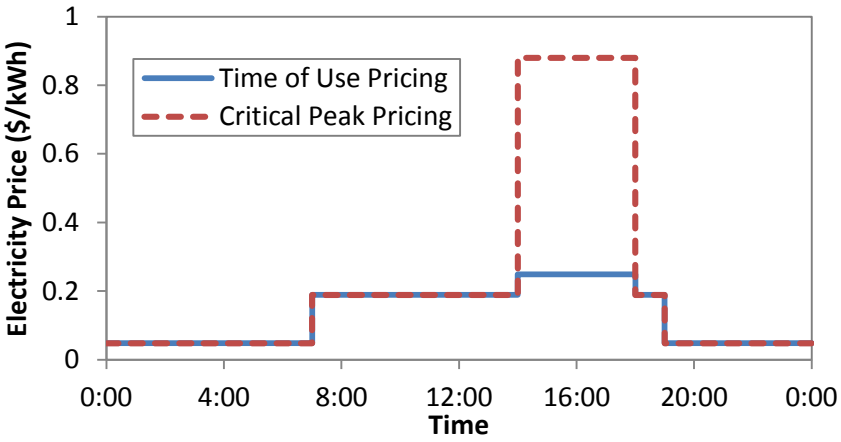

Figure 8.3: Critical peak pricing (CPP) rate structure from a utility in Milwaukee, Wisconsin [263]. The CPP pricing event can be called by the utility up to 25 times per year. Customers are notified by 19:00 on the evening before a CPP event occurs.

Commercial building energy systems have received more attention in the literature for EMPC than residential buildings, primarily due to the larger scale of commercial buildings. Ma *et al*. [264] developed a simulation environment for EMPC of a commercial building using TOU electricity prices. They were able to implement the strategy for an actual office building [256], demonstrating its ability to reduce peak energy consumption.

Henze *et al*. [136], [265] evaluated EMPC for active and passive thermal storage systems. They found EMPC to be an effective means for managing both passive and active systems. Similar investigations of EMPC for commercial buildings have been performed by a variety of other researchers [138], [139], [144], [266].

Oldewurtel *et al*. [141] used an EMPC formulation in conjunction with forecasts for electricity spot prices to lower peak demand. They concluded that the electricity prices must be properly tuned in order to optimally decrease peak demand, but do not investigate methods to do so.

Economic MPC for residential buildings has been performed, but in fewer instances. Touretzky and Baldea [123] compared EMPC to set point tracking MPC using nonlinear reduced-order models for residential homes, finding that EMPC can maintain the required thermal comfort while simultaneously reducing costs. Halvgaard *et al*. [267] used EMPC to manage a ground source based heat pump for providing heating to a residential home. They found that in the face of variable electricity prices, the EMPC system can reduce electricity costs by 25-35%.

Electricity use in the residential sector is especially important in regions with high penetration of air conditioning because of the influence of the residential sector on peak demand [197]. Increasing peak demand creates challenges for utilities because peaking plants are generally unattractive due to the fact that they might operate for only tens or hundreds of hours per year. This underutilization often results in peaking plants that are the least capital intensive, and therefore often the most inefficient. The residential sector creates a ripe area for shaping demand to lower its peak, rather than increasing supply in order to meet that peak.

In this chapter, a method is presented that uses a primal-dual formulation to determine the optimal pricing structure for reducing the peak demand in a simulated community of homes. Coupling the primal and dual formulations of the system makes it possible for the prices to become decision variables for achieving the desired peak reduction results. The next section gives an overview of the community of homes that comprises the dynamic system considered here. The following section presents the methodology for using the dual formulation to obtain the optimal prices. The results are then presented and discussed.

The use of a dual formulation to find optimal prices for an electricity system is not new. Bohn *et al*. [268] used the dual variables of a minimum cost optimization

problem to find optimal electricity prices 30 years ago. The difference in this work is that the minimum peak problem is not an economic formulation, so the dual variables do not represent electricity prices. Rather in this case, the minimum peak problem is solved, and its solution is used in conjunction with the dual formulation of the minimum cost problem to determine optimal prices. While only a peak demand reduction case is considered here, the methodology presented can readily be applied to a wide variety of situations, including emissions reduction, renewable energy generation capacity, standby capacity, etc.

SYSTEM DESCRIPTION

The system considered in this chapter is a simulated community of 900 homes. These homes are the same community of homes that were presented in Chapter 6. Details of how the model of the 900 homes was created can be found there.

Each home is assumed to have a thermostat that responds to control inputs given by a decentralized or centralized controller. The controller's only action is to assign thermostat set points to the thermostat. It is assumed that the user cannot override the thermostat set point given by the controller, though in actual implementation this feature would be necessary. It is also assumed that there are no behavioral changes associated with the thermostat set points or price signals for the thermostats. While behavioral changes are important and can impact peak demand reduction, they are beyond the scope of this work.

METHODOLOGY

The decision variables for this system (i.e., the community of 900 homes) include the air conditioning electricity consumption (y), the thermostat set point (T), and the

amount that the upper bound of the thermostat set point is violated (δ). The vector x includes these decision variables:

$$x = \begin{bmatrix} y & T & \delta \end{bmatrix}^T \tag{8.1}$$

The total number of decision variables is therefore $3PN$ where P is the prediction horizon times and N is the number of homes.

The desired outcome of the EMPC formulation here is to minimize the peak demand of the community using a centralized control method. The objective is to minimize the maximum electricity demand of the community of homes:

$$\min_x \left(\max \sum_{i=1}^{N} \left(y_{i,j} + E_{i,j} \right) \right) \tag{8.2}$$

where $E_{i,j}$ is the non-HVAC (heating, ventilation, and air conditioning) energy usage for home i at time j, so that the sum of $y_{i,j}$ and $E_{i,j}$ is the total energy usage for home i at time j. As in Chapter 6, a new variable, z is added so that this problem can be reformulated as a linear program

$$\min_{x,z} z \tag{8.3}$$

subject to

$$z \geq \sum_{i=1}^{N} \left(y_{i,j} + E_{i,j} \right) \qquad \forall j = 1...P \tag{8.4}$$

$$A_{eq} x = b_{eq} \tag{8.5}$$

$$A_{ineq} x \le b_{ineq} \tag{8.6}$$

$$lb \le x \le ub \tag{8.7}$$

where constraint (8.5) represents the equality constraints, constraint (8.6) represents the inequality constraints (for the violation of the upper bound of the thermostat set point), and constraint (8.7) represents upper and lower bounds for the decision variables. Solving model (8.3)-(8.7) for a prediction horizon of 24 (i.e., j = 1,…,24) yields a solution $\hat{x}$, which contains the thermostat set points that satisfy the comfort requirements and minimize the peak demand of the community of homes. Now it is desirable to find a cost vector, c, for which those same thermostat set points ($\hat{x}$) will be chosen, which is done using ideas from inverse optimization [269]. It begins with the minimum cost formulation for the system, assuming for the moment that the cost vector, c, is known:

$$\min_{x} cx \tag{8.8}$$

subject to

$$A_{eq} x = b_{eq} \tag{8.9}$$

$$A_{ineq} x \le b_{ineq} \tag{8.10}$$

$$x \le ub \tag{8.11}$$

$$x \ge lb \tag{8.12}$$

Note that $\hat{x}$ is a feasible solution of model (8.8)-(8.12), and that while model (8.3)-(8.7) must be implemented in a centralized fashion, model (8.8)-(8.12) can be implemented as a decentralized controller because the control actions of one home do not

affect the control actions of any other home. Advantages of decentralized control include less communication equipment and reduced privacy concerns as there is less sharing of personal information. Now consider the dual of (8.8)-(8.12):

$$\max_{\pi_{eq},\pi_{ineq},\lambda,\gamma} \pi_{eq} b_{eq} + \pi_{ineq} b_{ineq} + \lambda ub + \gamma lb \tag{8.13}$$

subject to

$$\pi_{eq} A_{eq} + \pi_{ineq} A_{ineq} + \lambda + \gamma = c \tag{8.14}$$

$$\pi_{ineq} \leq 0 \tag{8.15}$$

$$\lambda \leq 0 \tag{8.16}$$

$$\gamma \geq 0 \tag{8.17}$$

where π_{eq}, π_{ineq}, λ, and γ are the dual row vectors associated with the constraints given by (8.9)-(8.12), respectively. Strong duality indicates that at the optimum the primal and dual objective functions will hold the same value, that is

$$cx^* = \pi_{eq}{}^* b_{eq} + \pi_{ineq}{}^* b_{ineq} + \lambda^* ub + \gamma^* lb \tag{8.18}$$

where the "*" indicates the optimal values. Also, at the optimum the constraints (8.9)-(8.12) and (8.14)-(8.17) must be satisfied. By using $\hat{x}$, constraints (8.9)-(8.12) are satisfied because $\hat{x}$ is a feasible solution to model (8.3)-(8.7). Therefore, a cost vector, *c,* that is consistent with the given solution, $\hat{x}$*,* can be obtained by solving the following optimization problem:

$$\min_{c,\pi_{eq},\pi_{ineq},\lambda,\gamma} \left| c - c_{\min} \right|_1 \tag{8.19}$$

subject to

$$c\hat{x} = \pi_{eq} b_{eq} + \pi_{ineq} b_{ineq} + \lambda ub + \gamma lb \tag{8.20}$$

$$\pi_{eq} A_{eq} + \pi_{ineq} A_{ineq} + \lambda + \gamma = c \tag{8.21}$$

$$\pi_{ineq} \leq 0 \tag{8.22}$$

$$\lambda \leq 0 \tag{8.23}$$

$$\gamma \geq 0 \tag{8.24}$$

$$c \geq c_{min} \tag{8.25}$$

where c_{min} are the lower bounds for c, and where $\left| \cdot \right|_1$ yields the one-norm of its argument. Because c represents electricity prices, c_{min} should be greater than zero. The optimal vector c to model (8.19)-(8.25) is denoted as c^*. Note that not all the values of c are decision variables; only those values of c that pertain to the variables y are decision variables, the others (associated with T and ρ) are fixed. In some instances it is desirable to allow the prices to vary only during certain peak afternoon hours (e.g., from 15:00-17:00). For these cases, an upper bound was added to the off-peak hours restricting c for those hours to be less than or equal to c_{min}.

When solving model (8.19)-(8.25), equation (8.20) had to be enforced as a soft constraint because for this system the problem becomes infeasible. This occurs because, as indicated above, the components of c that do not correspond to variables y are fixed. In implementation, a large penalty was assigned for violating the equation (8.20).

The optimization problems (8.3)-(8.7), (8.8)-(8.12), and (8.19)-(8.25) were formulated and solved in MATLAB using the CLP algorithm in the OPTI Toolbox [270].

Solutions are implemented using a receding horizon where only the first solution is implemented for a given time step.

Results are considered using weather and occupancy information for Austin, Texas, for August 28, 2011. Based on simulations, August 28, 2011, yielded the highest peak demand for the community due to record heat during the summer of 2011. Thus, in minimizing peak demand for the community of homes, only the most extreme day will be considered because that is the day when reduction in peak demand will be most needed. Results for each scenario will be compared to a base case in which the thermostat is kept at the upper bound for the entire day (i.e., $T = ub$ for $j = 1,\ldots,24$). Weather predictions for the dry bulb temperature are assumed to be perfect in this analysis.

RESULTS AND DISCUSSION

Solving model (8.3)-(8.7) to minimize peak demand with $P = 24$ yields a solution ($\hat{x}$) with a perfectly flat demand during the afternoon peak period (see Figure 8.4). Because this model is implemented in a centralized fashion, the controller knows the status of each home and can therefore manage the homes in a way that creates the flat afternoon demand profile. This control strategy gives the largest possible peak demand reduction (10.0%) versus the base case, but increases energy consumption by 11.4%. The controller is able to reduce the peak demand by precooling the homes, thereby storing cooling energy in the thermal mass of the home. During the afternoon thermostat set points are raised (lowering electricity consumption) but the homes remain comfortable due to the stored cooling energy.

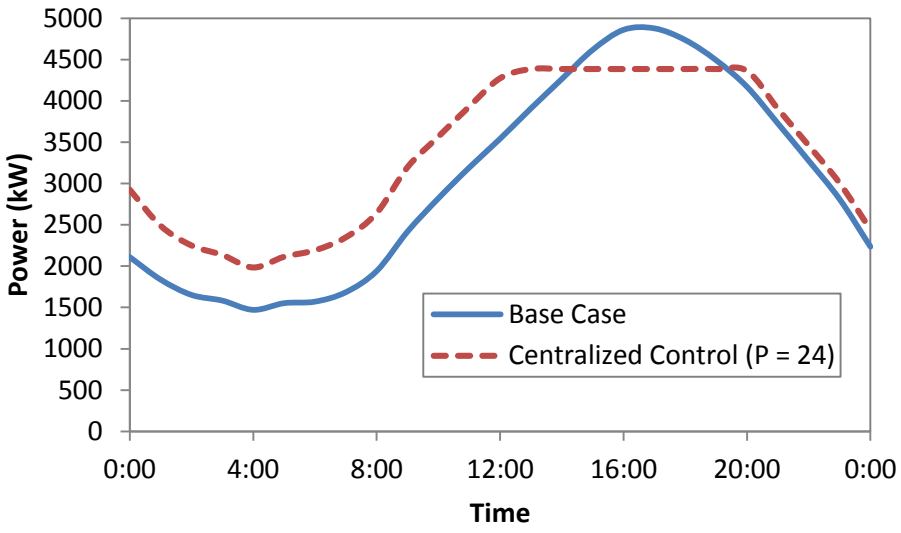

Figure 8.4: Power consumption for the simulated 900-home community for August 28, 2011. The centralized control strategy (model (8.3)-(8.7) with $P = 24$) reduces peak power demand by 10.0% compared to the base case and increases energy consumption by 11.4%.

With $\hat{x}$ now known, model (8.19)-(8.25) is solved to determine the optimal electricity prices for the 900 homes. These hourly prices, c^*, are shown in Figure 8.5 with c_{min} set to \$0.01/kWh. While these prices are specific to this particular set of homes, there are some interesting observations from looking at the prices. First, all 900 price profiles exhibit a one-hour peak period, that is, the prices are relatively low (<\$0.07/kWh) for every hour except for one hour. And for that one peak hour, prices are very high, with peak prices ranging from \$0.05-0.61/kWh and an average peak price of \$0.31/kWh. These prices have the form of critical peak pricing rate structures. Second, the peak prices occur over a six-hour period, indicating that to minimize the community's peak demand, peak demand responses need to occur over six hours. The distribution of the peak prices across the six hours is shown in Figure 8.6. According to this distribution, approximately half of the homes should be responding to the peak event at 16:00 and 17:00 hours, about

35% of the homes should be responding at 14:00 and 15:00, and the fewest number of homes (~20%) should be responding at 18:00 and 19:00. In homes that are unoccupied for a portion of the day, occupants tend to return home at 16:00 and 17:00, so it is not surprising that there are more homes with peak prices during those times than during other times.

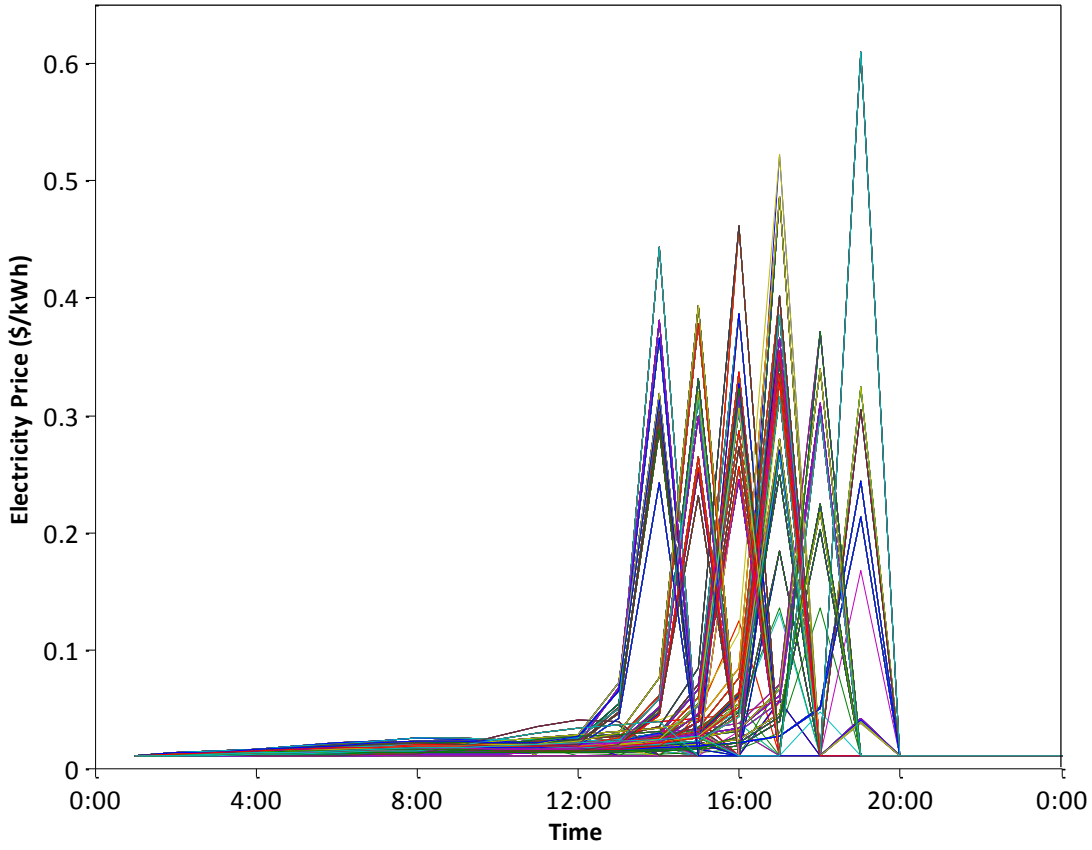

Figure 8.5: Optimal prices (c^*) for the 900 homes. The peak periods are only one hour in duration and occur between 14:00 and 19:00. The variation in the peak price ranges from \$0.05-0.61/kWh with an average of \$0.31/kWh.

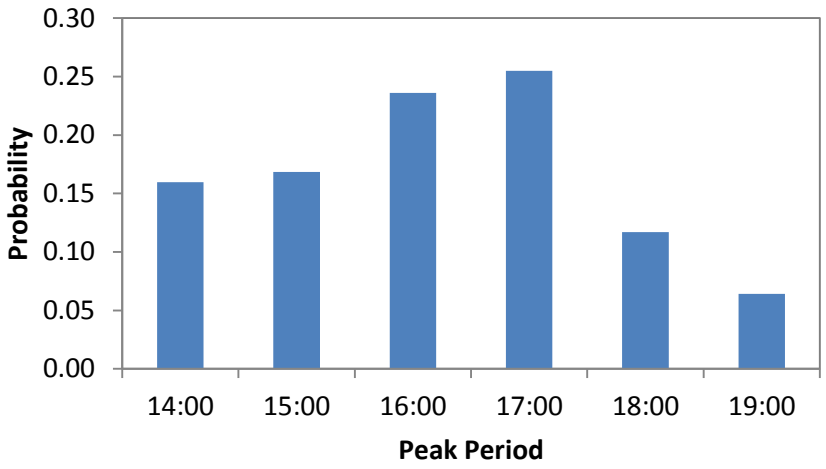

Figure 8.6: Distribution of the starting times of the six peak periods. Each home is assigned a one-hour peak period with a starting time from this distribution.

The prices in Figure 8.5 scale linearly with the choice of c_{min}. In this case, c_{min} is set to \$0.01/kWh. Increasing c_{min} to \$0.05/kWh would increase all the prices (c^*) by a factor of five. In essence, the results in Figure 8.5 show the ratio of on-peak to off-peak prices necessary for a home to implement precooling and reduce the peak demand of the community.

Figure 8.7 shows the results from using the optimal prices (c^*) from Figure 8.5 in the minimum cost model (8.8)-(8.12) with $P = 24$. The results are not identical to solving model (8.3)-(8.7) because the strong duality condition (equation (8.18)) cannot be met at equality, so there is a gap of 0.05% between the solutions achieved by the two models. Figure 8.8 shows the power consumption for the community using the optimal prices (c^*) in the minimum cost model (8.8)-(8.12), but with $P = 12$. In this case, the peak is slightly increased, but the early morning energy consumption is noticeably lower. With $P = 12$, most of the homes have not been exposed to their peak prices, which occur around 16:00, until 4:00.

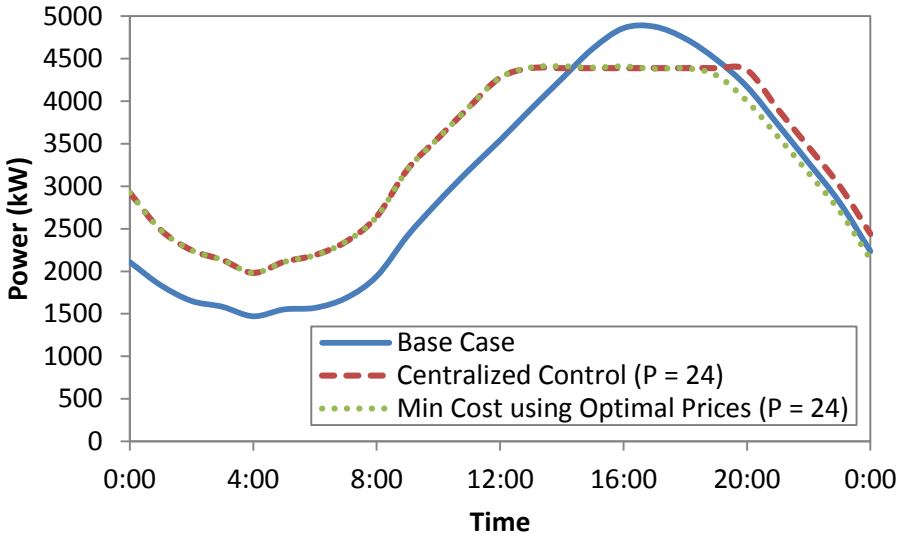

Figure 8.7: Power consumption for the simulated 900-home community using minimum cost formulation (model (8.8)-(8.12) with $P = 24$) with the costs (c^*) determined from model (8.19)-(8.25).

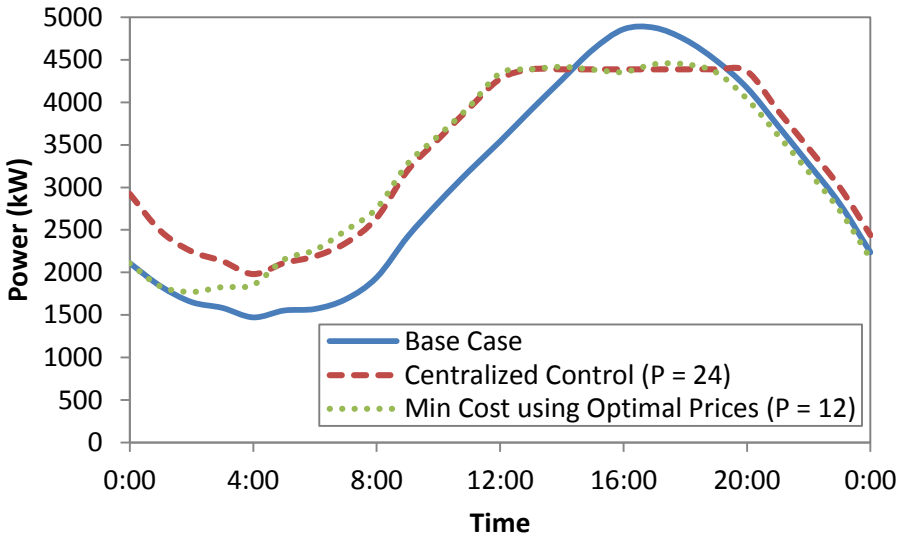

Figure 8.8: Power consumption for the simulated 900-home community using minimum cost formulation (model (8.8)-(8.12) with $P = 12$) with the costs (c^*) determined from model (8.19)-(8.25) when $P = 24$. Note that when $P = 12$, the peak demand is reduced by 8.8% but the energy is increased by only 7.5%.

Table 8.1 summarizes the peak demand and energy consumption results of the four scenarios considered in this chapter. The summary shows that reducing the prediction horizon from 24 to 12 results in a 0.9% loss in peak demand reduction, while lowering the amount of energy consumption by 2.1%. The time constants for the homes are on the order of 8 hours, so a 12-hour prediction horizon is able to achieve the peak reduction benefit without as much peak cooling. If energy were penalized, then the P = 24 and P = 12 solutions would be very similar.

Model	Peak Demand (kW)	Change vs Base Case	Energy Consumption (kWh)	Change vs Base Case
Base Case	4877	-	73113	-
Min Peak (4)-(8), P = 24	4387	-10.0%	81485	11.4%
Min Cost (9)-(13), P = 24	4409	-9.6%	80142	9.6%
Min Cost (9)-(13), P = 12	4447	-8.8%	78578	7.5%

Table 8.1: Summary of peak demand and energy consumption using the indicated model. Percent changes are relative to the base case.

Although the optimal price configuration for minimizing peak demand shows six peak periods (see Figure 8.5) it might be desirable to implement a pricing scheme with fewer peak periods. Figure 8.9 shows how much peak demand can be reduced when the number of peak pricing periods is restricted to the number indicated. Moving from six peak periods to five peak periods results in very little loss in peak reduction potential, while reducing from five periods to four periods has a considerably larger impact. It is interesting that having three peak periods leads to a slightly better peak reduction than having four peak periods. This oddity is due to the fact that solving the model (8.19)-(8.25) results in prices that most closely match the $\hat{x}$ given by model (8.3)-(8.7). The prices obtained when using four peak periods better match $\hat{x}$ than when there are three

peak periods, but do not do quite as well at lowering the peak demand. Figure 8.10 shows the system's energy consumption changes as the number of peak periods changes.

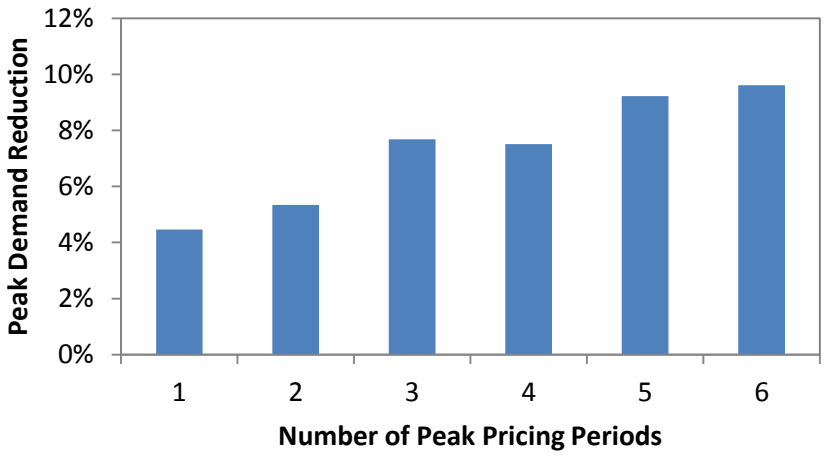

Figure 8.9: Peak demand reduction compared to the base case when the number of peak pricing periods is varied. One peak demand period is able to achieve nearly half the peak reduction of the six peak demand periods.

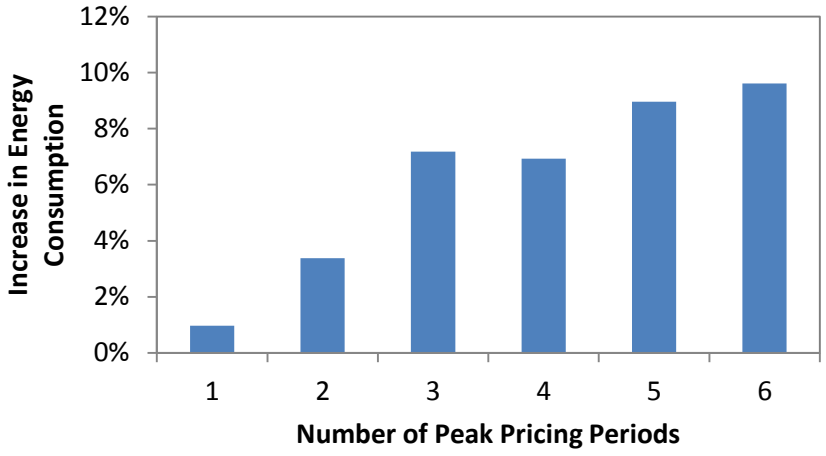

Figure 8.10: Increase in the total energy consumption for August 28, 2011 for the number peak periods indicated. Decreasing the number of peak periods leads to smaller increases in energy consumption.

When the peak electricity prices of the homes were compared to home efficiency metrics, it was found that the more efficient homes tended to have lower peak prices. For example, Figure 8.11 shows the peak electricity prices versus the model coefficient c_0 from equation (5.10). The coefficient c_0 indicates the change in energy consumption that occurs when the thermostat set point is raised by 1°C. Homes with a lower (more negative) value of c_0 are likely to be more efficient than those with higher values of c_0. In general, as homes become more efficient, the magnitude of the peak price need not be as high for the home to gain economic value by responding to the price. It also indicates that inefficient homes might require extreme prices before there is sufficient incentive to respond via thermostat set point changes.

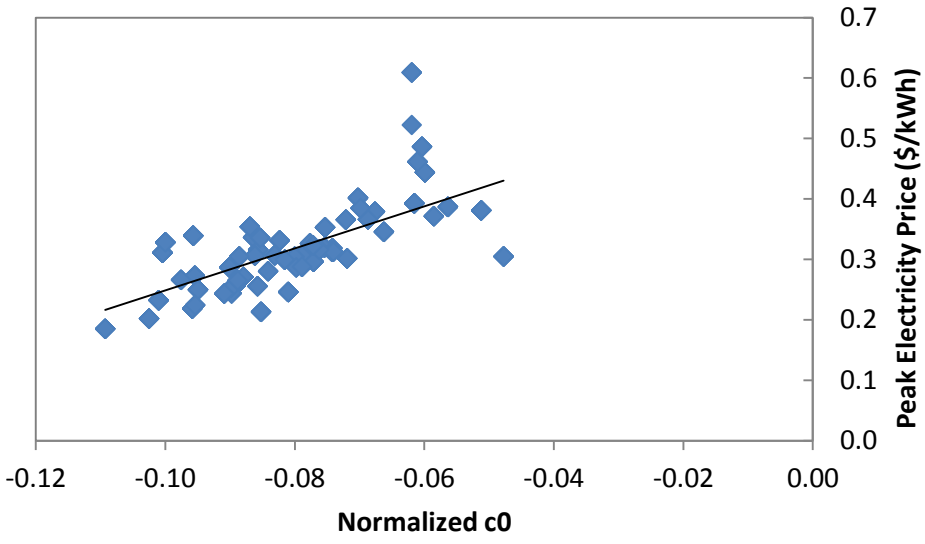

Figure 8.11: Peak electricity price versus the normalized c_0 coefficient in the home's ARX model (see equation (6.1)) for homes that were occupied during the entire day. The c_0 coefficient was normalized by dividing it by the air conditioner capacity (in kW). Homes with lower normalized values of c_0 are more efficient (i.e., home efficiency increases as normalized c_0 decreases). The positive correlation indicates that more efficient homes need lower peak electricity prices to respond optimally.

CONCLUSIONS

EMPC is a popular tool for managing building HVAC systems, as well as other energy systems. This work has shown that EMPC is not just useful for operating systems based on a variable pricing structure, but that EMPC is also a useful tool for determining the optimal variable prices for a given system. In this chapter, the system was a simulated community of residential homes where thermostat set points could be controlled. The community of homes was based on the physical homes in Austin, Texas, described in Chapter 6. By using ideas from inverse optimization, the primal-dual form of the EMPC was used to determine the optimal prices that would result in minimizing the peak electricity demand of the community.

For the system of homes presented here, the optimal pricing profiles for the homes were CPP-like pricing structures with relatively low prices for every hour except for one peak hour. One-hour peak periods occurred between 14:00 and 19:00, with most homes (~50%) experiencing peak pricing at 16:00-17:00. This pricing structure was able to reduce peak demand by 9.6% when implemented in a decentralized control, minimum cost EMPC formulation, compared to the 10% peak reduction with the centralized control, minimum peak demand formulation. The one-hour peak prices ranged from \$0.05-0.61/kWh with an average of \$0.31/kWh.

Reducing the number of peak pricing periods from six to five resulted in very little loss of peak reduction potential. Greater losses were found when the number of periods was reduced further. However, the amount of extra energy required to achieve the peak reduction decreased as the number of peak pricing periods decreased.

Although in this case the goal was to find prices that would minimize peak demand, the same method could easily be applied to other criteria. For example, the same methods could be used to find prices that would minimize the system's environmental

footprint or maximize the system's efficiency. However, the method does require that a model of the system be in place.

Future work includes adding stochastic elements to the system, both in how occupants behave as well as in how prices are assigned to the homes. Inclusion of these stochastic aspects will help provide bounds for the system estimates given in this chapter.

Chapter 9: Conclusions and Future Work

How we use energy will continue to be an area of major concern throughout the 21st century. Ensuring that we use energy in the most effective way is important both now and in developing future systems. This work has attempted to address some of the issues regarding energy use, especially as they relate to the electric grid.

The integration of energy systems can lead to improved system performance, but it is important that the systems are managed in such a way that the independent systems can work together synergistically. This work has integrated a number of systems, including

- Commercial buildings, chillers, and thermal energy storage (Chapter 3)
- Commercial buildings, chillers, a combined heat and power plant with turbine inlet cooling, and thermal energy storage (Chapter 4)
- A community of 900 residential homes (Chapters 6-8)
- Residential homes and solar PV (Chapter 7)

In each case a model predictive control framework was applied to manage the integrated system, and in each instance the integrated system (with the control) demonstrated superior energy management than the systems would have in isolation.

In all the examples provided, some form of thermal storage was utilized in order to shift energy consumption in time. In some cases the thermal storage was active, such as with the chilled water tanks. In other cases it was passive, such as with the residential homes that stored thermal energy in the building thermal mass. In all cases, the thermal storage increased the flexibility of the system and gave the controller more degrees of freedom in managing the system. The storage was useful in both reducing peak demand and in responding to time-of-use or market electricity prices. With the active thermal

storage, thermal storage can also be used to reduce energy consumption (see Chapter 3). The reason that the passive thermal storage in the homes cannot conserve energy is that when the homes are cooled, it increases the heat flux into the home, thus increasing the energy required to maintain the temperature. The active storage units, on the other hand, are very well insulated and have a lower surface-area-to-volume ratio, so heat losses are nearly the same for both a charged and discharged tank.

The smart grid is a necessary component of much of the work discussed here. Some level of information availability is necessary for the predictive controller to be able to have accurate forecasts and for system models to be accurate and efficient. How these data are shared and managed is an area of continual development, and it is important that appropriate standards are in place to both facilitate and safeguard the sharing of information.

FUTURE WORK

This dissertation has focused on integrated energy systems in a smart grid environment for the Austin, TX, climate. Extension of this work to other climate zones would be valuable because electricity markets, building codes, and resource availability vary considerably across the United States. New opportunities and challenges arise in other locations due to changing conditions.

This work has also only considered localized effects of implementing energy options such as thermal energy storage. However, if technologies such as thermal storage were deployed at a large scale, then they could affect other systems and change electricity markets [271]. Incorporating production cost models such as PLEXOS or GridView can account for these changes and provide insight into secondary or other effects.

There are a variety of energy systems that have not been considered in this work that would likely prove beneficial. The broader the technology base considered, the more likely synergies will be identified. Denholm *et al*. [272] has considered the integration thermal storage with nuclear power and renewable energy to provide benefit. Certainly improvements can be made as more types of systems are considered.

As an obvious first step, the work in the Chapter 3-4 can be combined with the work in Chapter 6-7 to consider how a system that incorporates residential and commercial buildings, active and passive thermal storage, and solar PV can provide benefit. An analysis of that kind of system can provide insight into which building types are best suited for managing electricity loads. Additionally, because the occupancy patterns of commercial and residential buildings are opposite of one another (we leave home to go to work and vice versa), it is likely that there is some combined benefit from treating the two building types together.

There is also considerable potential to couple the commercial and residential sectors with the industrial sector. Industrial facilities account for approximately 30% of the total primary energy consumption in the United States [273]. Of that input energy, 20-50% is lost in waste heat from hot exhaust gases, cooling water, and heat lost from hot surfaces and heated products [274]. Utilizing this waste heat is challenging because approximately 60% of waste heat is at relatively low temperatures (< 230°C) [274], which has limited use in an industrial facility. However, in regions with cooler climates, up to 50% of the total (not just industrial) energy consumption can be attributed to the production of low-grade heating services (<100°C) [275]. These low-grade heating services include space heating, water heating, and food-related activities in the commercial and residential sectors. Clearly, there is significant opportunity for synergies to occur between the

industrial sector, which has abundant low-grade heat, and the commercial and residential sectors, which consume sizeable amounts of energy to produce low-grade heat.

The final considerable to mention here is that of program implementation. One of the challenges in integrating energy systems is that the various energy systems are often owned and/or operated by different entities that often have different objectives. Designing policies or programs that allow the overall system to function in an optimal way is a challenging area that must be addressed in order to improve overall system efficiency. Research into developing new methods or business models might be just as important (and in many cases more important) than developing new algorithms, technologies, or control strategies.

Appendix

i	Variable					
	a	**b**	**c**	**d**	**f**	**h**
0	0.69162	0.015821	-0.38918	0.000301	-0.00064	0.058116
1		-0.0136	0.430079			0.049048
2		0.007389	-0.0421			0.15815
3						0.157133
4						0.198968
5						0.208215
6						0.242481
7						0.258064
8						0.264863
9						0.223903
10						0.180865
11						0.172919
12						0.055472
13						0.163932
14						0.103703
15						0.082195
16						0.0582
17						0.052892
18						0.064628
19						0.102631
20						0.086834
21						0.069853
22						0.110427
23						0.134044

Table A.1: Coefficients for (5.10) that are used in the MPC analysis.

Using the coefficients from Table A.1 and setting DBT = 30°C the model in (5.10) becomes

$$y(k) = 0.6916y(k-1) - 0.4084T(k) + 0.4301T(k-1) - 0.0421T(k-2) + \alpha \qquad \text{(A.1)}$$

where α is a term holding the constant values. Dropping the value α and applying the z-transform (see [226]) to (A.1) gives

$$Y(z) = 0.6916z^{-1}Y(z) - 0.4084T(z) + 0.4301z^{-1}T(z) - 0.0421z^{-2}T(z) \tag{A.2}$$

Solving for $Y(z)$ yields

$$Y(z) = \frac{-0.4084 + 0.4301z^{-1} - 0.0421z^{-2}}{1 - 0.6916z^{-1}} T(z) = H(z)T(z) \tag{A.3}$$

where $H(z)$ is the discrete transfer function given by

$$H(z) = \frac{-0.4084 + 0.4301z^{-1} - 0.0421z^{-2}}{1 - 0.6916z^{-1}} \tag{A.4}$$

The poles of $H(z)$ are determined by multiplying the denominator of (A.4) by z and setting it equal to zero

$$z - 0.6916 = 0 \tag{A.5}$$

A single pole exists at 0.6916. Because this pole lies inside the unit circle in the complex z-plane, it is a stable pole. Also, because the pole is real, there are no oscillations in the model response.

The zeros of $H(z)$ are determined by multiplying the numerator of (A.4) by z^2 and setting it equal to zero

$$-0.4084z^2 + 0.4301z - 0.0421 = 0 \tag{A.6}$$

This leads to zeros at 0.9438 and0.1092 which are both real and lie in the unit circle in the complex z-plane. Because the zeros are real, the model will not exhibit inverse response.

The steady-state response of the model is given by evaluating $H(1)$

$$H(1) = \frac{-0.4084 + 0.4301 - 0.0421}{1 - 0.6916} = -0.0663 \tag{A.7}$$

so a step of 1°C in T (ignoring α) will lead to a steady-state change in y of -0.0663.

References

[1] National Academy of Engineering, "Grand Challenges - Engineering Challenges," 2012. [Online]. Available: http://www.engineeringchallenges.org/cms/challenges.aspx. [Accessed: 18-Feb-2014].

[2] NY-BEST, "Energy Storage Incentives from ConEdison Announced," 2014. [Online]. Available: http://www.ny-best.org/page/energy-storage-incentives-conedison-announced. [Accessed: 17-Feb-2014].

[3] W. J. Cole, K. M. Powell, and T. F. Edgar, "Optimization and advanced control of thermal energy storage systems," *Reviews in Chemical Engineering*, vol. 28, no. 2–3, pp. 81–99, 2012.

[4] W. J. Cole, T. F. Edgar, and A. Novoselac, "Use of model predictive control to enhance the flexibility of thermal energy storage cooling systems," in *Proceedings of the 2012 American Control Conference*, Montreal, Canada, 2012, pp. 2788–2793.

[5] W. J. Cole, K. X. Perez, J. D. Rhodes, M. E. Webber, M. Baldea, and T. F. Edgar, "Community-scale air conditioning control for high penetrations of rooftop photovoltaics," in *Proceedings of the 2014 American Control Conference*, Portland, OR, USA, 2014.

[6] W. J. Cole, J. D. Rhodes, K. M. Powell, and T. F. Edgar, "Turbine inlet cooling with thermal energy storage," *International Journal of Energy Research*, vol. 38, no. 2, pp. 151–161, 2014.

[7] W. J. Cole, E. T. Hale, and T. F. Edgar, "Building energy model reduction for model predictive control using OpenStudio," in *Proceedings of the 2013 American Control Conference*, Washington, D.C., 2013, pp. 449–454.

[8] W. J. Cole, K. M. Powell, E. T. Hale, and T. F. Edgar, "Reduced-order residential home modeling for model predictive control," *Energy and Buildings*, vol. 74, pp. 69–77, 2014.

[9] W. J. Cole, J. D. Rhodes, W. Gorman, M. E. Webber, and T. F. Edgar, "Community-scale residential air conditioning control for effective grid management," *Applied Energy*, under review 2014.

[10] W. J. Cole, D. P. Morton, and T. F. Edgar, "Optimal electricity rate structures for peak demand reduction using economic model predictive control," *Journal of Process Control*, under review 2014.

[11] A. Gil, M. Medrano, I. Martorell, A. Lázaro, P. Dolado, B. Zalba, and L. F. Cabeza, "State of the art on high temperature thermal energy storage for power generation. Part 1--Concepts, materials and modellization," *Renewable and Sustainable Energy Reviews*, vol. 14, no. 1, pp. 31–55, Jan. 2010.

[12] K. M. Powell and T. F. Edgar, "Modeling and control of a solar thermal power plant with thermal energy storage.," *Chemical Engineering Science*, vol. 71, pp. 138–145, 2012.

[13] I. Dincer and M. A. Rosen, *Thermal Energy Storage: Systems and Applications*, 2nd ed. Chichester, West Sussex, UK: John Wiley & Sons, 2011.
[14] T. F. Edgar, D. M. Himmelblau, and L. S. Lasdon, *Optimization of Chemical Processes*, 2nd ed. New York, NY: McGraw-Hill, 2001.
[15] D. W. Wu and R. Z. Wang, "Combined cooling, heating and power: A review," *Progress in Energy and Combustion Science*, vol. 32, no. 5–6, pp. 459–495, 2006.
[16] Environmental Protection Agency, "Ethanol Fact Sheet | Combined Heat and Power Partnership | US EPA," 2007. [Online]. Available: http://www.epa.gov/chp/markets/ethanol_fs.html. [Accessed: 14-Oct-2011].
[17] Energy Information Administration (EIA), "Manufacturing Energy Consumption Survey, Tables 11.1 and 11.3," 1994.
[18] EIA, "Manufacturing Energy Consumption Survey, Tables 11.1 and 11.3," 2002.
[19] EIA, "Manufacturing Energy Consumption Survey, Tables 11.1 and 11.3," 2006.
[20] S. M. Lai and C. W. Hui, "Feasibility and flexibility for a trigeneration system," *Energy*, vol. 34, no. 10, pp. 1693–1704, Oct. 2009.
[21] G. Chicco and P. Mancarella, "Distributed multi-generation: A comprehensive view," *Renewable and Sustainable Energy Reviews*, vol. 13, no. 3, pp. 535–551, Apr. 2009.
[22] J. Wang, Z. Zhai, Y. Jing, and C. Zhang, "Particle swarm optimization for redundant building cooling heating and power system," *Applied Energy*, vol. 87, no. 12, pp. 3668–3679, Dec. 2010.
[23] L. R. Hinojosa, A. R. Day, G. G. Maidment, C. Dunham, and P. Kirk, "A comparison of combined heat and power feasibility models," *Applied Thermal Engineering*, vol. 27, no. 13, pp. 2166–2172, Sep. 2007.
[24] H. Zhao, J. Holst, and L. Arvastson, "Optimal operation of coproduction with storage," *Energy*, vol. 23, no. 10, pp. 859–866, Oct. 1998.
[25] D. Henning, "Cost minimization for a local utility through CHP, heat storage and load management," *International Journal of Energy Research*, vol. 22, no. 8, pp. 691–713, 1998.
[26] K. Ito, R. Yokoyama, and T. Shiba, "Optimal Operation of a Diesel Engine Cogeneration Plant Including a Heat Storage Tank," *J. Eng. Gas Turbines Power*, vol. 114, no. 4, pp. 687–694, Oct. 1992.
[27] R. Yokoyama and K. Ito, "Optimal Operational Planning of Cogeneration Systems With Thermal Storage by the Decomposition Method," *Journal of Energy Resources Technology*, vol. 117, no. 4, pp. 337–342, 1995.
[28] R. Yokoyama and K. Ito, "A novel decomposition method for MILP and its application to optimal operation of a thermal storage system," *Energy Conversion and Management*, vol. 41, no. 16, pp. 1781–1795, Nov. 2000.
[29] B. Rolfsman, "Combined heat-and-power plants and district heating in a deregulated electricity market," *Applied Energy*, vol. 78, no. 1, pp. 37–52, May 2004.
[30] M. Houwing, R. R. Negenborn, M. D. Ilic, and B. De Schutter, "Model predictive control of fuel cell micro cogeneration systems," presented at the International Conference on Networking, Sensing and Control, 2009, pp. 708–713.

[31] M. A. Lozano, J. C. Ramos, and L. M. Serra, “Cost optimization of the design of CHCP (combined heat, cooling and power) systems under legal constraints,” *Energy*, vol. 35, no. 2, pp. 794–805, Feb. 2010.
[32] B. Wille-Haussmann, T. Erge, and C. Wittwer, “Decentralised optimisation of cogeneration in virtual power plants,” *Solar Energy*, vol. 84, no. 4, pp. 604–611, Apr. 2010.
[33] J. Lee, C. Jung, and S. Lyu, “A daily operation scheduling of cogeneration systems using fuzzy linear programming,” presented at the IEEE Power Engineering Society Summer Meeting, 1999, vol. 2, pp. 983–988.
[34] R. Caldon, A. R. Patria, and R. Turri, “Optimisation algorithm for a virtual power plant operation,” presented at the 39th International Universities Power Engineering Conference, 2004. UPEC 2004., 2004, vol. 2, pp. 1058–1062.
[35] A. H. Azit and K. M. Nor, “Optimal Sizing for a Gas-Fired Grid-Connected Cogeneration System Planning,” *IEEE Transactions on Energy Conversion*, vol. 24, no. 4, pp. 950–958, Dec. 2009.
[36] F. Sancho-Bastos and H. Perez-Blanco, “Cogeneration System Simulation and Control to Meet Simultaneous Power, Heating, and Cooling Demands,” *J. Eng. Gas Turbines Power*, vol. 127, no. 2, pp. 404–409, 2005.
[37] G. Sandou, S. Font, S. Tebbani, A. Hiret, and C. Mondon, “Predictive Control of a Complex District Heating Network,” presented at the 44th IEEE Decision and Control, and European Control Conference, 2005, pp. 7372– 7377.
[38] M. Ristic, D. Brujic, and K. Thoma, “Economic dispatch of distributed combined heat and power systems participating in electricity spot markets,” *Proceedings of the Institution of Mechanical Engineers, Part A: Journal of Power and Energy*, vol. 222, no. 7, pp. 743 –752, Nov. 2008.
[39] A. Collazos, F. Maréchal, and C. Gähler, “Predictive optimal management method for the control of polygeneration systems,” *Computers & Chemical Engineering*, vol. 33, no. 10, pp. 1584–1592, Oct. 2009.
[40] Z. Bogdan and D. Kopjar, “Improvement of the cogeneration plant economy by using heat accumulator,” *Energy*, vol. 31, no. 13, pp. 2285–2292, Oct. 2006.
[41] L. L. Lai, J. T. Ma, and J. B. Lee, “Multitime-interval scheduling for daily operation of a two-cogeneration system with evolutionary programming,” *International Journal of Electrical Power & Energy Systems*, vol. 20, no. 5, pp. 305–311, Jun. 1998.
[42] S. Bruno, S. Lamonaca, M. La Scala, and U. Stecchi, “Optimal Design of Trigeneration and District Energy in the Presence of Energy Storage,” presented at the International Conference on Renewable Energies and Power Quality, Granada, Spain, 2010.
[43] A. Piacentino and F. Cardona, “EABOT - Energetic analysis as a basis for robust optimization of trigeneration systems by linear programming,” *Energy Conversion and Management*, vol. 49, no. 11, pp. 3006–3016, Nov. 2008.

[44] W. Kostowski and J. Skorek, “Thermodynamic and economic analysis of heat storage application in co-generation systems,” *International Journal of Energy Research*, vol. 29, no. 2, pp. 177–188, 2005.
[45] H. F. Ravn and J. M. Rygaard, “Optimal Scheduling of Coproduction with a Storage,” *Eng. Optimization*, vol. 22, no. 4, pp. 267–281, May 1994.
[46] C. Maifredi, L. Puzzi, and G. P. Beretta, “Optimal power production scheduling in a complex cogeneration system with heat storage,” presented at the 35th IECEC, 2000, vol. 2, pp. 1004–1012.
[47] E. Dotzauer, K. Holmström, and H. F. Ravn, “Optimal Unit Commitment And Economic Dispatch Of Cogeneration Systems With A Storage,” *Proceedings of the 13th PSCC conference*, pp. 738–744, 1999.
[48] J. Wang, Z. Zhai, Y. Jing, and C. Zhang, “Influence analysis of building types and climate zones on energetic, economic and environmental performances of BCHP systems,” *Applied Energy*, vol. 88, no. 9, pp. 3097–3112, Sep. 2011.
[49] D. Frankovic, A. Viskovic, and G. Gudac, “Optimization of trigeneration plant with heating and cooling energy storages operation,” in *Proceedings of the Fifteenth IASTED International Conference on Modelling and Simulation*, Calgary, Alberta, Canada, 2004, pp. 84–88.
[50] A. Antoniou and W. Lu, *Practical optimization: algorithms and engineering applications*. Springer, 2007.
[51] A. Fragaki, A. N. Andersen, and D. Toke, “Exploration of economical sizing of gas engine and thermal store for combined heat and power plants in the UK,” *Energy*, vol. 33, no. 11, pp. 1659–1670, Nov. 2008.
[52] G. Streckiene, V. Martinaitis, A. N. Andersen, and J. Katz, “Feasibility of CHP-plants with thermal stores in the German spot market,” *Applied Energy*, vol. 86, no. 11, pp. 2308–2316, Nov. 2009.
[53] L. M. Serra, M. Lozano, F. Ramos, A. V. Ensinas, and S. A. Nebra, “Polygeneration and efficient use of natural resources,” *Energy*, vol. 34, no. 5, pp. 575–586, May 2009.
[54] G. Pagliarini and S. Rainieri, “Modeling of a thermal energy storage system coupled with combined heat and power generation for the heating requirements of a University Campus,” *Applied Thermal Engineering*, vol. 30, no. 10, pp. 1255–1261, Jul. 2010.
[55] F. Lin and J. Yi, “Optimal operation of a CHP plant for space heating as a peak load regulating plant,” *Energy*, vol. 25, no. 3, pp. 283–298, Mar. 2000.
[56] H. Lund and A. N. Andersen, “Optimal designs of small CHP plants in a market with fluctuating electricity prices,” *Energy Conversion and Management*, vol. 46, no. 6, pp. 893–904, Apr. 2005.
[57] V. Verda and F. Colella, “Primary energy savings through thermal storage in district heating networks,” *Energy*, vol. 36, no. 7, pp. 4278–4286, Jul. 2011.
[58] T. Urbaneck, U. Schirmer, B. Platzer, U. Uhlig, T. Göschel, and D. Zimmermann, “Optimal design of chiller units and cold water storages for district cooling,”

presented at the Ecostock, 10th International Conference on Thermal Energy Storage, Stockton, New Jersey, USA, 2006.
[59] T. Urbaneck, U. Barthel, U. Uhlig, and T. Göschel, "Only cold water?! - The success with the First Large-Scale Cold Water Store in Germany," presented at the Effstock, 11th International Conference on Thermal Energy Storage, Stockholm, Sweden, 2009.
[60] T. Urbaneck, J. Gehrmann, and V. Lottner, "First large-scale Chilled Water Stores in Germany," presented at the Effstock, 11th International Conference on Thermal Energy Storage, Stockholm, Sweden, 2009.
[61] W. Wang, Y. Hu, J. Yan, J. Nyström, and E. Dahlquist, "Combined heat and power plant integrated with mobilized thermal energy storage (M-TES) system," *Frontiers of Energy and Power Engineering in China*, vol. 4, no. 4, pp. 469–474, Dec. 2010.
[62] K. Alanne and J. Paatero, "Seasonal Heat Storages and Residential Micro-cogeneration," presented at the 1st International Conference on Micro-Generation and Application, Ottawa, Canada, 2008.
[63] M. Domínguez, C. García, and J. M. Arias, "Free Cooling with Phase Change Materials (PCM)," *Advanced Materials Research*, vol. 107, pp. 49–54, 2010.
[64] K. Gaine and A. Duffy, "A life cycle cost analysis of large-scale thermal energy storage technologies for buildings using combined heat and power," presented at the Renewable Energy Research Conference 2010 Zero Emission Buildings, Trondheim, Norway, 2010.
[65] M. A. Ehyaei, A. Mozafari, A. Ahmadi, P. Esmaili, M. Shayesteh, M. Sarkhosh, and I. Dincer, "Potential use of cold thermal energy storage systems for better efficiency and cost effectiveness," *Energy and Buildings*, vol. 42, no. 12, pp. 2296–2303, Dec. 2010.
[66] X. H. Liu, K. C. Geng, B. R. Lin, and Y. Jiang, "Combined cogeneration and liquid-desiccant system applied in a demonstration building," *Energy and Buildings*, vol. 36, no. 9, pp. 945–953, Sep. 2004.
[67] W. Somcharoenwattana, C. Menke, D. Kamolpus, and D. Gvozdenac, "Study of operational parameters improvement of natural-gas cogeneration plant in public buildings in Thailand," *Energy and Buildings*, vol. 43, no. 4, pp. 925–934, Apr. 2011.
[68] D. Ziher and A. Poredos, "Economics of a trigeneration system in a hospital," *Applied Thermal Engineering*, vol. 26, no. 7, pp. 680–687, May 2006.
[69] K. H. Khan, M. G. Rasul, and M. M. K. Khan, "Energy conservation in buildings: cogeneration and cogeneration coupled with thermal energy storage," *Applied Energy*, vol. 77, no. 1, pp. 15–34, Jan. 2004.
[70] J. McNeill, J. Previtali, and M. Krarti, "A Simplified Method to Predict Energy Cost Savings in Office Buildings Using a Hybrid Desiccant, Absorption Chiller, and Natural Gas Turbine Cogeneration System With Thermal Storage," *ASME Conference Proceedings*, vol. 2007, no. 47977, pp. 787–795, 2007.
[71] D. Haeseldonckx, L. Peeters, L. Helsen, and W. D'haeseleer, "The impact of thermal storage on the operational behaviour of residential CHP facilities and the

overall CO2 emissions," *Renewable and Sustainable Energy Reviews*, vol. 11, no. 6, pp. 1227–1243, Aug. 2007.
[72] A. Campos Celador, M. Odriozola, and J. M. Sala, "Implications of the modelling of stratified hot water storage tanks in the simulation of CHP plants," *Energy Conversion and Management*, vol. 52, no. 8–9, pp. 3018–3026, Aug. 2011.
[73] A. N. Andersen and H. Lund, "New CHP partnerships offering balancing of fluctuating renewable electricity productions," *Journal of Cleaner Production*, vol. 15, no. 3, pp. 288–293, 2007.
[74] R. M. Dell and D. A. J. Rand, "Energy storage -- a key technology for global energy sustainability," *Journal of Power Sources*, vol. 100, no. 1–2, pp. 2–17, Nov. 2001.
[75] J. K. Kaldellis and D. Zafirakis, "Optimum energy storage techniques for the improvement of renewable energy sources-based electricity generation economic efficiency," *Energy*, vol. 32, no. 12, pp. 2295–2305, Dec. 2007.
[76] H. Ibrahim, A. Ilinca, and J. Perron, "Energy storage systems--Characteristics and comparisons," *Renewable and Sustainable Energy Reviews*, vol. 12, no. 5, pp. 1221–1250, Jun. 2008.
[77] J. Taneja, D. Culler, and P. Dutta, "Towards Cooperative Grids: Sensor/Actuator Networks for Renewables Integration," presented at the First IEEE International Conference on Smart Grid Communications, 2010, pp. 531–536.
[78] M. B. Blarke and H. Lund, "The effectiveness of storage and relocation options in renewable energy systems," *Renewable Energy*, vol. 33, no. 7, pp. 1499–1507, Jul. 2008.
[79] I. Stadler, "Power grid balancing of energy systems with high renewable energy penetration by demand response," *Utilities Policy*, vol. 16, no. 2, pp. 90–98, Jun. 2008.
[80] C. Ryu, A. Srinivasan, D. R. Tiffany, J. F. Crittenden, W. E. Lear, and S. A. Sherif, "Dynamic Modeling of a Novel Cooling, Heat, Power, and Water Microturbine Combined Cycle," *ASME Conf. Proc.*, vol. 2008, no. 43192, pp. 735–746, Jan. 2008.
[81] J. Porteiro, J. L. Míguez, S. Murillo, and L. M. López, "Feasibility of a new domestic CHP trigeneration with heat pump: II. Availability analysis," *Applied Thermal Engineering*, vol. 24, no. 10, pp. 1421–1429, Jul. 2004.
[82] H. Lund, "Large-scale integration of wind power into different energy systems," *Energy*, vol. 30, no. 13, pp. 2402–2412, Oct. 2005.
[83] O. Linkevics and A. Sauhats, "Formulation of the objective function for economic dispatch optimisation of steam cycle CHP plants," presented at the Power Tech, IEEE Russia, 2005, pp. 1–6.
[84] C. Schulz, G. Roder, and M. Kurrat, "Virtual power plants with combined heat and power micro-units," presented at the International Conference on Future Power Systems, 2005, pp. 1–5.
[85] E. Handschin, F. Neise, H. Neumann, and R. Schultz, "Optimal operation of dispersed generation under uncertainty using mathematical programming,"

International Journal of Electrical Power & Energy Systems, vol. 28, no. 9, pp. 618–626, Nov. 2006.
[86] M. Hollmann, "System Dynamics Modeling and Simulation of Distributed Generation for the Analysis of a Future Energy Supply," presented at the The 24th International Conference of the System Dynamics Society, Nijmegen, The Netherlands, 2006.
[87] J. Kalina and J. Skorek, "Small-scale co-generation for building applications - energy demand analysis at demonstration site and optimal sizing of the CHP plant," *Journal of Civil Engineering and Management*, vol. 12, no. 1, pp. 5–13, 2006.
[88] R. Kuhi-Thalfeldt and J. Valtin, "Economic analysis of a biogas-fuelled cogeneration power plant," in *4th International Symposium*, Kuressaare , Estonia, 2007, pp. 164–168.
[89] R. Kuhi-Thalfeldt and J. Valtin, "Combined heat and power plants balancing wind power," *Oil Shale*, vol. 26, no. 3 Special, pp. 294–308, 2009.
[90] A. Hawkes, I. Staffell, D. Brett, and N. Brandon, "Fuel cells for micro-combined heat and power generation," *Energy Environ. Sci.*, vol. 2, no. 7, pp. 729–744, 2009.
[91] V. Dorer and A. Weber, "Energy and CO2 emissions performance assessment of residential micro-cogeneration systems with dynamic whole-building simulation programs," *Energy Conversion and Management*, vol. 50, no. 3, pp. 648–657, Mar. 2009.
[92] Energy Information Administration, "Manufacturing Energy Consumption Survey, Tables 11.1 and 11.3," 2006.
[93] Energy Information Administration, "Annual Energy Outlook 2011 Early Release," Dec. 2010.
[94] Energy Information Administration, "State Energy Data 2008 Consumption," Jun. 2010.
[95] K. Liu, H. Güven, A. Beyene, and P. Lowrey, "A comparison of the field performance of thermal energy storage (TES) and conventional chiller systems," *Energy*, vol. 19, no. 8, pp. 889–900, Aug. 1994.
[96] J. E. Braun, "Load Control Using Building Thermal Mass," *Journal of Solar Energy Engineering*, vol. 125, no. 3, pp. 292–301, 2003.
[97] I. Dincer and M. A. Rosen, "Exergetically efficient thermal energy storage systems for sustainable buildings," *ASHRAE Transactions*, vol. 114, pp. 98–107, 2008.
[98] L. F. Cabeza, A. Castell, C. Barreneche, A. de Gracia, and A. I. Fernandez, "Materials used as PCM in thermal energy storage in buildings: A review," *Renewable & Sustainable Energy Reviews*, vol. 15, no. 3, pp. 1675–1695, Apr. 2011.
[99] J. S. Andrepont, "Reducing Energy Costs And Minimizing Capital Requirements: Case Studies of Thermal Energy Storage (TES)," presented at the 29th Industrial Energy Technology Conference, New Orleans, LA, 2007.
[100] J. E. Braun, "A Near-Optimal Control Strategy for Cool Storage Systems with Dynamic Electric Rates (RP-1252).," *HVACR Research*, vol. 13, no. 4, pp. 557–580, 2007.

[101] C. E. Dorgan and J. S. Elleson, *Design guide for cool thermal storage*. ASHRAE, 1993.
[102] G. P. Henze, R. H. Dodier, and M. Krarti, "Development of a Predictive Optimal Controller for Thermal Energy Storage Systems," *HVAC&R Research*, vol. 3, no. 3, pp. 233 – 264, 1997.
[103] G. P. Henze, "An overview of optimal control for central cooling plants with ice thermal energy storage," *Journal of Solar Energy Engineering*, vol. 125, no. 3, pp. 302–309, Aug. 2003.
[104] V. Lemort, "A numerical comparison of control strategies applied to an existing ice storage system," *Energy Conversion and Management*, vol. 47, no. 20, pp. 3619–3631, Dec. 2006.
[105] C. Beggs, *Energy: Management, Supply and Conservation*. Woburn, MA: Butterworth-Heinemann, 2009.
[106] I. Dincer, "On thermal energy storage systems and applications in buildings," *Energy and Buildings*, vol. 34, no. 4, pp. 377–388, May 2002.
[107] G. P. Henze, C. Felsmann, A. R. Florita, M. J. Brandemuehl, H. K. Cheng, and C. E. Waters, "Optimization of Building Thermal Mass Control in the Presence of Energy and Demand Charges," *ASHRAE Transactions*, vol. 114, pp. 75–84, 2008.
[108] T. X. Nghiem and G. J. Pappas, "Receding-horizon Supervisory Control of Green Buildings," presented at the American Control Conference, San Francisco, CA, USA, 2011, pp. 4416–4421.
[109] J. Široký, F. Oldewurtel, J. Cigler, and S. Prívara, "Experimental analysis of model predictive control for an energy efficient building heating system," *Applied Energy*, vol. 88, no. 9, pp. 3079–3087, Sep. 2011.
[110] G. P. Henze, D. E. Kalz, S. M. Liu, and C. Felsmann, "Experimental analysis of model-based predictive optimal control for active and passive building thermal storage inventory," *HVAC&R Research*, vol. 11, no. 2, pp. 189–213, Apr. 2005.
[111] Y. Ma, F. Borrelli, B. Hencey, B. Coffey, S. Bengea, and P. Haves, "Model predictive control for the operation of building cooling systems," presented at the American Control Conference, Baltimore, Maryland, USA, 2010, pp. 5106–5111.
[112] G. P. Henze, D. E. Kalz, C. Felsmann, and G. Knabe, "Impact of forecasting accuracy on predictive optimal control of active and passive building thermal storage inventory," *HVAC&R Research*, vol. 10, no. 2, pp. 153–178, Apr. 2004.
[113] Y. Ma, F. Borrelli, B. Hencey, A. Packard, and S. Bortoff, "Model predictive control of thermal energy storage in building cooling systems," presented at the Decision and Control, held jointly with the 2009 28th Chinese Control Conference, 2009, pp. 392–397.
[114] G. Zhou, M. Krarti, and G. P. Henze, "Parametric analysis of active and passive building thermal storage utilization," *Journal of Solar Energy Engineering*, vol. 127, no. 1, pp. 37–46, Feb. 2005.
[115] J. Cigler and S. Prívara, "Subspace identification and model predictive control for buildings," presented at the 2010 11th International Conference on Control Automation Robotics & Vision (ICARCV), 2010, pp. 750–755.

[116] F. Oldewurtel, A. Ulbig, A. Parisio, G. Andersson, and M. Morari, "Reducing peak electricity demand in building climate control using real-time pricing and model predictive control," presented at the 49th IEEE Conference on Decision and Control, 2010, pp. 1927–1932.
[117] G. P. Henze, A. R. Florita, M. J. Brandemuehl, C. Felsmann, and H. Cheng, "Advances in Near-Optimal Control of Passive Building Thermal Storage," *Journal of Solar Energy Engineering*, vol. 132, no. 2, p. (9 pages), May 2010.
[118] J. J. Zhou, G. H. Wei, W. D. Turner, S. Deng, D. E. Claridge, and O. Contreras, "Control optimization for chilled water thermal storage system under complicated time-of-use electricity rate schedule," *ASHRAE Transactions*, vol. 111, pp. 184–195, 2005.
[119] G. P. Henze, C. Felsmann, and G. Knabe, "Evaluation of optimal control for active and passive building thermal storage," *International Journal of Thermal Sciences*, vol. 43, no. 2, pp. 173–183, Feb. 2004.
[120] S. Liu and G. P. Henze, "Impact of Modeling Accuracy on Predictive Optimal Control of Active and Passive Building Thermal Storage Inventory," *ASHRAE Transactions*, vol. 110, no. 1, pp. 151–163, 2004.
[121] H. Cheng, M. J. Brandemuehl, G. P. Henze, A. R. Florita, and C. Felsmann, "Evaluation of the Primary Factors Impacting the Optimal Control of Passive Thermal Storage.," *ASHRAE Transactions*, vol. 114, no. 2, pp. 57–64, Oct. 2008.
[122] S. P. Corgnati, A. Kindinis, and M. Perino, "Thermal mass activation by means of night cooling: comparison of different techniques and strategies," presented at the The Fifth International Workshop on Energy and Environment of Residential Buildings, Guilin, Guangxi, China, 2009, pp. 685–693.
[123] C. R. Touretzky and M. Baldea, "Nonlinear model reduction and model predictive control of residential buildings with energy recovery," *Journal of Process Control*.
[124] D. H. Seo and M. Krarti, "Evaluation of energy savings by optimization control in thermal energy storage system," *Proceedings of the ASME International Solar Energy Conference*, pp. 433–440, 2007.
[125] S. Liu and G. P. Henze, "Evaluation of Reinforcement Learning for Optimal Control of Building Active and Passive Thermal Storage Inventory," *J. Sol. Energy Eng.*, vol. 129, no. 2, pp. 215–225, May 2007.
[126] Z. Yu and A. Dexter, "Hierarchical fuzzy control of low-energy building systems," *Solar Energy*, vol. 84, no. 4, pp. 538–548, Apr. 2010.
[127] H. Dasi, F. Xiaowei, and C. Wenjian, "A near-optimal operation strategy for ice storage air-conditioning systems," presented at the 3rd IEEE Conference on Industrial Electronics and Applications, Singapore, 2008, pp. 1287–1290.
[128] G. P. Henze, B. Biffar, M. Wienecke, and M. P. Becker, "Analysis of Thermal Energy Storage for a Pharmaceutical Company," *at-Automatisierungstechnik*, vol. 57, no. 9, pp. 443–451, 2009.
[129] G. Ghatikar and R. Bienert, "Smart Grid Standards and Systems Interoperability: A Precedent with OpenADR," in *Grid-Interop*, Phoenix, AZ, 2011, vol. LBNL-5273E.

[130] T. X. Nghiem and G. J. Pappas, “Receding-horizon Supervisory Control of Green Buildings,” presented at the ACC, San Francisco, CA, USA, 2011, pp. 4416–4421.
[131] K. M. Powell and T. F. Edgar, “Control of a Large Scale Solar Thermal Energy Storage System,” presented at the ACC, San Francisco, CA, USA, 2011, pp. 1530–1535.
[132] S. M. Lai and C. W. Hui, “Feasibility and flexibility for a trigeneration system,” *Energy*, vol. 34, no. 10, pp. 1693–1704, Oct. 2009.
[133] Y. Ma, F. Borrelli, B. Hencey, B. Coffey, S. Bengea, and P. Haves, “Model predictive control for the operation of building cooling systems,” in *ACC*, 2010, pp. 5106–5111.
[134] K. M. Powell, W. Cole, U. F. Ekarika, and T. F. Edgar, “Dynamic optimization of a campus cooling system with thermal storage,” in *Proceedings of the 2013 European Control Conference*, Zurich, Switzerland, 2013, pp. 4077–4082.
[135] K. M. Powell, W. J. Cole, U. F. Ekarika, and T. F. Edgar, “Optimal chiller loading in a district cooling system with thermal energy storage,” *Energy*, vol. 50, pp. 445–453, Feb. 2013.
[136] G. Henze, “Energy and cost minimal control of active and passive building thermal storage inventory,” *J. Sol. Energ. Eng.*, vol. 127, no. 3, pp. 343–351, 2005.
[137] G. Zhou, M. Krarti, and G. Henze, “Parametric analysis of active and passive building thermal storage utilization,” *J. Sol. Energ. Eng.*, vol. 127, no. 1, pp. 37–46, 2005.
[138] V. Lemort, “A numerical comparison of control strategies applied to an existing ice storage system,” *Energ. Convers. Manage.*, vol. 47, no. 20, pp. 3619–3631, 2006.
[139] J. E. Braun, “A near-optimal control strategy for cool storage systems with dynamic electric rates,” *HVAC&R Research*, vol. 13, no. 4, pp. 557–580, 2007.
[140] G. Henze, C. Felsmann, A. Florita, M. Brandemuehl, H. Cheng, and C. Waters, “Optimization of Building Thermal Mass Control in the Presence of Energy and Demand Charges,” *ASHRAE Transactions*, vol. 114, pp. 75–84, 2008.
[141] F. Oldewurtel, A. Ulbig, A. Parisio, G. Andersson, and M. Morari, “Reducing peak electricity demand in building climate control using real-time pricing and model predictive control,” in *49th IEEE CDC*, 2010, pp. 1927–1932.
[142] J. Cigler and S. Prívara, “Subspace identification and model predictive control for buildings,” in *11th ICARCV*, 2010, pp. 750–755.
[143] G. Henze, A. Florita, M. Brandemuehl, C. Felsmann, and H. Cheng, “Advances in Near-Optimal Control of Passive Building Thermal Storage,” *J. Sol. Energ. Eng.*, vol. 132, no. 2, 2010.
[144] J. Siroký, F. Oldewurtel, J. Cigler, and S. Prívara, “Experimental analysis of model predictive control for an energy efficient building heating system,” *Appl. Energ.*, vol. 88, no. 9, pp. 3079–3087, 2011.
[145] J. Asrael, P. E. Phelan, and B. D. Wood, “Feasibility of lowering the condenser’s inlet water temperature of a chiller using thermal water storage,” *Appl. Energ.*, vol. 66, no. 4, pp. 339–356, 2000.

[146] V. Gadhamshetty, N. Nirmalakhandan, M. Myint, and C. Ricketts, “Improving air-cooled condenser performance in combined cycle power plants,” *J. Energ. Eng.*, vol. 132, no. 2, pp. 81–88, 2006.
[147] W. Liu, X. Miao, J. Wang, X. Ma, G. Peng, and Z. Pan, “Applying ‘Thermal Storage Cooling Tower’ to Shift On-Peak Electric Energy Demand of Underground Commercial Building,” in *APPEEC*, 2009, pp. 1–4.
[148] DOE, “Building Technologies Office: EnergyPlus Energy Simulation Software,” 2013. [Online]. Available: http://apps1.eere.energy.gov/buildings/energyplus/. [Accessed: 13-Sep-2013].
[149] M. Hydeman, N. Webb, P. Sreedharan, and S. Blanc, “Development and testing of a reformulated regression-based electric chiller model,” *ASHRAE Transactions*, vol. 108, no. 2, pp. 1118–1127, 2002.
[150] H. W. Stanford, *HVAC water chillers and cooling towers: fundamentals, application, and operation*. CRC Press, 2003.
[151] M. A. Rosen, I. Dincer, and N. Pedinelli, “Thermodynamic Performance of Ice Thermal Energy Storage Systems,” *J. Energy Resour. Technol.*, vol. 122, no. 4, pp. 205–211, Dec. 2000.
[152] G. Henze and J. Schoenmann, “Evaluation of reinforcement learning control for thermal energy storage systems,” *HVAC&R Research*, vol. 9, no. 3, pp. 259–275, 2003.
[153] B. Kilkis, “Net-zero energy cities: A hub for decentralized energy for better environment,” *International Journal of Energy Research*, vol. 36, no. 15, pp. 1358–1365, 2012.
[154] IEA, “Key World Energy Statistics,” International Energy Agencey, 9 rue de la Fédération, 75739 Paris Cedex 15, France, 2010.
[155] S. M. Hasnain, “Review on sustainable thermal energy storage technologies, part II: Cool thermal storage,” *Energy Conversion and Management*, vol. 39, no. 11, pp. 1139–1153, 1998.
[156] M. Ameri and S. H. Hejazi, “The study of capacity enhancement of the Chabahar gas turbine installation using an absorption chiller,” *Applied Thermal Engineering*, vol. 24, no. 1, pp. 59–68, Jan. 2004.
[157] M. Ameri, S. H. Hejazi, and K. Montaser, “Performance and economic of the thermal energy storage systems to enhance the peaking capacity of the gas turbines,” *Applied Thermal Engineering*, vol. 25, no. 2–3, pp. 241–251, Feb. 2005.
[158] M. Chaker and C. B. Meher-Homji, “Inlet Fogging of Gas Turbine Engines: Climatic Analysis of Gas Turbine Evaporative Cooling Potential of International Locations,” *Journal of Engineering for Gas Turbines and Power*, vol. 128, no. 4, pp. 815–825, Oct. 2006.
[159] A. D. Hall, J. C. Stover, and R. L. Breisch, “Gas turbine inlet-air chilling at a cogeneration facility,” *ASHRAE Transactions*, vol. 100, no. 1, pp. 595–600, 1994.
[160] A. M. Al-Ibrahim and A. Varnham, “A review of inlet air-cooling technologies for enhancing the performance of combustion turbines in Saudi Arabia,” *Applied Thermal Engineering*, vol. 30, no. 14–15, pp. 1879–1888, Oct. 2010.

[161] M. Bianchi, L. Branchini, A. De Pascale, F. Melino, A. Peretto, R. K. Bhargava, and M. A. Chaker, "Gas Turbine Power Augmentation Technologies: A Systematic Comparative Evaluation Approach," in *ASME Conference Proceedings*, Glasgow, UK, 2010, pp. 99–107.
[162] M. Ameri, H. R. Shahbazian, and M. Nabizadeh, "Comparison of evaporative inlet air cooling systems to enhance the gas turbine generated power," *International Journal of Energy Research*, vol. 31, no. 15, pp. 1483–1503, 2007.
[163] M. M. Alhazmy, R. K. Jassim, and G. M. Zaki, "Performance enhancement of gas turbines by inlet air-cooling in hot and humid climates," *International Journal of Energy Research*, vol. 30, no. 10, pp. 777–797, 2006.
[164] E. I. Mackie, "Inlet Air Cooling for a Combustion Turbine Using Thermal Storage," in *ASHRAE Transactions: Symposia*, 1994, vol. 100, pp. 572–582.
[165] A. A. Amell and F. J. Cadavid, "Influence of the relative humidity on the air cooling thermal load in gas turbine power plant," *Applied Thermal Engineering*, vol. 22, no. 13, pp. 1529–1533, Sep. 2002.
[166] M. Farzaneh-Gord and M. Deymi-Dashtebayaz, "Effect of various inlet air cooling methods on gas turbine performance," *Energy*, vol. 36, no. 2, pp. 1196–1205, Feb. 2011.
[167] D. R. Brown, S. Katipamula, and J. H. Koynenbelt, "A Comparative Assessment of Alternative Combustion Turbine Cooling Systems," PNNL-10966, 1996.
[168] S. F. Al-Fahed, F. N. Alasfour, and H. K. Abdulrahim, "The effect of elevated inlet air temperature and relative humidity on cogeneration system," *International Journal of Energy Research*, vol. 33, no. 15, pp. 1384–1394, 2009.
[169] J. S. Andrepont, "Demand-Side and Supply-Side Load Management: Optimizing with Thermal Energy Storage (TES) for the Restructuring Energy Marketplace," in *Industrial Energy Technology Conference*, Texas A&M University, 2002, pp. 301–305.
[170] K. M. Liebendorfer and J. S. Andrepont, "Cooling the hot desert wind: Turbine inlet cooling with thermal energy storage (TES) increases net power plant output 30%," in *ASHRAE Transactions*, Atlanta, Georgia, USA, 2005, vol. 111, pp. 545–550.
[171] J. Bédécarrats and F. Strub, "Gas turbine performance increase using an air cooler with a phase change energy storage," *Applied Thermal Engineering*, vol. 29, no. 5–6, pp. 1166–1172, Apr. 2009.
[172] Y. H. Zurigat, B. Dawoud, and J. Bortmany, "On the technical feasibility of gas turbine inlet air cooling utilizing thermal energy storage," *International Journal of Energy Research*, vol. 30, no. 5, pp. 291–305, 2006.
[173] S. Boonnasa, P. Namprakai, and T. Muangnapoh, "Performance improvement of the combined cycle power plant by intake air cooling using an absorption chiller," *Energy*, vol. 31, no. 12, pp. 2036–2046, Sep. 2006.
[174] S. Somasundaram, M. K. Drost, D. R. Brown, and Z. I. Antoniak, "Coadunation of Technologies: Cogeneration and Thermal Energy Storage," *Journal of Engineering for Gas Turbines and Power*, vol. 118, no. 1, pp. 32–37, Jan. 1996.

[175] F. Behafarid and M. N. Bahadori, “Performance Evaluation of a Gas Turbine Operating Noncontinuously with its Inlet Air Cooled Through an Aquifer Thermal Energy Storage,” *Journal of Energy Resources Technology*, vol. 129, no. 2, pp. 117–124, Jun. 2007.
[176] J. K. Cross, W. A. Beckman, J. W. Mitchell, D. T. Reindl, and D. E. Knebel, “Modeling of hybrid combustion turbine inlet air cooling systems,” in *ASHRAE Transactions*, Atlanta, Georgia, USA, 1995, vol. 101, pp. 1335–1341.
[177] N. Palestra, G. Barigozzi, and A. Perdichizzi, “Inlet Air Cooling Applied to Combined Cycle Power Plants: Influence of Site Climate and Thermal Storage Systems,” *Journal of Engineering for Gas Turbines and Power*, vol. 130, no. 2, p. 022002, Mar. 2008.
[178] S. Boonnasa and P. Namprakai, “Sensitivity analysis for the capacity improvement of a combined cycle power plant (100-600 MW),” *Applied Thermal Engineering*, vol. 28, no. 14–15, pp. 1865–1874, Oct. 2008.
[179] N. Palestra, G. Barigozzi, and A. Perdichizzi, “GT Inlet Air Boosting and Cooling Coupled With Cold Thermal Storage in Combined Cycle Power Plants,” in *ASME Conference Proceedings*, Berlin, Germany, 2008, pp. 273–283.
[180] R. Chacartegui, F. Jiménez-Espadafor, D. Sánchez, and T. Sánchez, “Analysis of combustion turbine inlet air cooling systems applied to an operating cogeneration power plant,” *Energy Conversion and Management*, vol. 49, no. 8, pp. 2130–2141, Aug. 2008.
[181] A. Al Bassam and Y. M. Al Said, “Qassim Central Power Plant Inlet Air Cooling System,” in *Proceedings of the ASME Turbo Expo*, New Orleans, LA, 2001.
[182] S. Sanaye, A. Fardad, and M. Mostakhdemi, “Thermoeconomic optimization of an ice thermal storage system for gas turbine inlet cooling,” *Energy*, vol. 36, no. 2, pp. 1057–1067, Feb. 2011.
[183] G. L. Arnulfi, G. Croce, and M. Marini, “Parametric Analysis of Thermal Energy Storage for Gas Turbine Inlet Air Cooling,” in *ASME Conference Proceedings*, Montreal, Canada, 2007, pp. 231–238.
[184] R. Yokoyama and K. Ito, “Effect of Inlet Air Cooling by Ice Storage on Unit Sizing of a Gas Turbine Cogeneration Plant,” *Journal of Engineering for Gas Turbines and Power*, vol. 126, no. 2, pp. 351–357, 2004.
[185] U. C. Colpier and D. Cornland, “The economics of the combined cycle gas turbine—an experience curve analysis,” *Energy Policy*, vol. 30, no. 4, pp. 309–316, Mar. 2002.
[186] B. H. Bakenhus, “Ice storage project,” *ASHRAE Journal*, vol. 42, no. 5, pp. 64–66, 2000.
[187] Anon., “Ice Maker Adds Low-Cost Kilowatts to Peaking Unit,” *Power*, vol. 136, no. 1, 1992.
[188] Department of Energy, “eQUEST,” 2010. [Online]. Available: http://www.doe2.com/equest/. [Accessed: 09-May-2012].
[189] Google, “Google SketchUp,” 2012. [Online]. Available: http://sketchup.google.com/. [Accessed: 09-May-2012].

[190] Google, “Google Building Maker,” 2012. [Online]. Available: http://sketchup.google.com/3dwh/buildingmaker.html. [Accessed: 09-May-2012].
[191] K. M. Knight, S. A. Klein, and J. A. Duffie, “A methodology for the synthesis of hourly weather data,” *Solar Energy*, vol. 46, no. 2, pp. 109–120, 1991.
[192] J. Haberl, D. Bronson, and D. O’Neal, “Impact of Using Measured Weather Data vs. TMY Weather Data in a DOE-2 Simulation,” *ASHRAE Transactions*, vol. 101, no. 2, pp. 558–576, 1995.
[193] D. E. Seborg, D. A. Mellichamp, T. F. Edgar, and F. J. D. Doyle, *Process Dynamics and Control*, 3rd ed. Wiley, 2011.
[194] A. Campos Celador, M. Odriozola, and J. M. Sala, “Implications of the modelling of stratified hot water storage tanks in the simulation of CHP plants,” *Energy Conversion and Management*, vol. 52, no. 8–9, pp. 3018–3026, Aug. 2011.
[195] US Census Bureau, “USA QuickFacts from the US Census Bureau,” *USA QuickFacts from the US Census Bureau*, 2013. [Online]. Available: http://quickfacts.census.gov/qfd/states/00000.html. [Accessed: 01-Feb-2013].
[196] B. McNary and C. Berry, “How Americans are using energy in homes today,” in *Proceedings of the 2012 ACEEE Summer Study on Energy Efficiency in Buildings*, Pacific Grove, CA, 2012, vol. 1, pp. 1 – 204–215.
[197] P. Wattles, “ERCOT demand response overview & status report,” *AMIT-DSWG Workshop “AMI’s Next Frontier: Demand Response,”* 30-Aug-2011. [Online]. Available: http://www.ercot.com/content/meetings/dswg/keydocs/2011/0830/3_ERCOT_presentation_workshop_083011.pdf. [Accessed: 29-Mar-2013].
[198] S. Prívara, J. Cigler, Z. Váňa, F. Oldewurtel, C. Sagerschnig, and E. Žáčeková, “Building modeling as a crucial part for building predictive control,” *Energy and Buildings*, vol. 56, pp. 8–22, Jan. 2013.
[199] J. Cigler, P. Tomáško, and J. Široký, “BuildingLAB: A tool to analyze performance of model predictive controllers for buildings,” *Energy and Buildings*, vol. 57, pp. 34–41, Feb. 2013.
[200] I. Hazyuk, C. Ghiaus, and D. Penhouet, “Optimal temperature control of intermittently heated buildings using Model Predictive Control: Part I – Building modeling,” *Building and Environment*, vol. 51, pp. 379–387, May 2012.
[201] S. Goyal and P. Barooah, “A method for model-reduction of non-linear thermal dynamics of multi-zone buildings,” *Energy and Buildings*, vol. 47, pp. 332–340, Apr. 2012.
[202] S. Karmacharya, G. Putrus, C. Underwood, and K. Mahkamov, “Thermal modelling of the building and its HVAC system using Matlab/Simulink,” in *2012 2nd International Symposium on Environment Friendly Energies and Applications (EFEA)*, 2012, pp. 202 –206.
[203] M. M. Gouda, S. Danaher, and C. P. Underwood, “Building thermal model reduction using nonlinear constrained optimization,” *Building and Environment*, vol. 37, no. 12, pp. 1255–1265, Dec. 2002.

[204] P. Malisani, F. Chaplais, N. Petit, and D. Feldmann, “Thermal building model identification using time-scaled identification methods,” in *2010 49th IEEE Conference on Decision and Control (CDC)*, 2010, pp. 308 –315.
[205] A. Kelman and F. Borrelli, “Bilinear model predictive control of a HVAC system using sequential quadratic programming,” in *IFAC World Congress*, 2011.
[206] W. Surles and G. P. Henze, “Evaluation of automatic priced based thermostat control for peak energy reduction under residential time-of-use utility tariffs,” *Energy and Buildings*, vol. 49, no. 0, pp. 99–108, Jun. 2012.
[207] R. Yin, P. Xu, M. A. Piette, and S. Kiliccote, “Study on Auto-DR and pre-cooling of commercial buildings with thermal mass in California,” *Energy and Buildings*, vol. 42, no. 7, pp. 967–975, Jul. 2010.
[208] H. Cheng, M. J. Brandemuehl, G. P. Henze, A. R. Florita, and C. Felsmann, “Evaluation of the Primary Factors Impacting the Optimal Control of Passive Thermal Storage.,” *ASHRAE Transactions*, vol. 114, no. 2, pp. 57–64, Oct. 2008.
[209] J. E. Braun, “Load Control Using Building Thermal Mass,” *J. Sol. Energ. Eng.*, vol. 125, no. 3, pp. 292–301, 2003.
[210] M. Klos, J. Erickson, E. Bryant, and L. Ringhof, “Communicating Thermostats for Residential Time-of-Use Rates: They Do Make a Difference,” in *Proceedings of the ACEEE Summer Study*, 2008, pp. 7–(179–190).
[211] A. Brissette, A. Hoke, D. Maksimovic, and A. Pratt, “A microgrid modeling and simulation platform for system evaluation on a range of time scales,” in *2011 IEEE Energy Conversion Congress and Exposition (ECCE)*, 2011, pp. 968–976.
[212] D. O’Neill, M. Levorato, A. Goldsmith, and U. Mitra, “Residential Demand Response Using Reinforcement Learning,” in *2010 First IEEE International Conference on Smart Grid Communications (SmartGridComm)*, 2010, pp. 409–414.
[213] Google, “Google Building Maker,” 2012. [Online]. Available: http://sketchup.google.com/3dwh/buildingmaker.html. [Accessed: 09-May-2012].
[214] C. Christensen, R. Anderson, S. Horowitz, A. Courtney, and J. Spencer, “BEopt™ Software for Building Energy Optimization: Features and Capabilities,” National Renewable Energy Laboratory, Golden, CO, NREL/TP-550-39929, 2006.
[215] National Renewable Energy Laboratory, “BEopt,” 2012. [Online]. Available: http://beopt.nrel.gov/. [Accessed: 03-Dec-2012].
[216] J. D. Rhodes, B. Stephens, and M. E. Webber, “Using energy audits to investigate the impacts of common air-conditioning design and installation issues on peak power demand and energy consumption in Austin, Texas,” *Energy and Buildings*, vol. 43, no. 11, pp. 3271–3278, Nov. 2011.
[217] J. D. Rhodes, B. Stephens, and M. E. Webber, “Energy audit analysis of residential air-conditioning systems in Austin, Texas,” *ASHRAE Transactions*, vol. 118, no. 1, pp. 143–150, 2012.
[218] E. T. Hale, D. L. Macumber, K. S. Benne, and D. Goldwasser, “Scripted Building Energy Modeling and Analysis,” presented at the 5th National Conference of IBPSA-USA, Madison, WI, 2012, pp. 369–376.

[219] E. T. Hale, D. L. Macumber, E. Weaver, and D. Shekhar, "A Flexible Framework for Building Energy Analysis," in *Proceedings of the 2012 ACEEE Summer Study on Energy Efficiency in Buildings*, Pacific Grove, CA, 2012, pp. 12– 120–132.
[220] R. Stull, "Wet-Bulb Temperature from Relative Humidity and Air Temperature," *Journal of Applied Meteorology and Climatology*, vol. 50, no. 11, pp. 2267–2269, Nov. 2011.
[221] R. Bălan, J. Cooper, K.-M. Chao, S. Stan, and R. Donca, "Parameter identification and model based predictive control of temperature inside a house," *Energy and Buildings*, vol. 43, no. 2–3, pp. 748–758, Feb. 2011.
[222] M. Avci, M. Erkoc, A. Rahmani, and S. Asfour, "Model predictive HVAC load control in buildings using real-time electricity pricing," *Energy and Buildings*, vol. 60, pp. 199–209, May 2013.
[223] Y. Zhu, "Chapter 9 - Nonlinear Process Identification," in in *Multivariable System Identification For Process Control*, Oxford: Pergamon, 2001, pp. 217–250.
[224] D. E. Rivera and K. S. Jun, "An integrated identification and control design methodology for multivariable process system applications," *IEEE Control Systems*, vol. 20, no. 3, pp. 25–37, 2000.
[225] M. D. McKay, R. J. Beckman, and W. J. Conover, "A comparison of three methods for selecting values of input variables in the analysis of output from a computer code," *Technometrics*, vol. 21, pp. 239–245, 1979.
[226] D. E. Seborg, D. A. Mellichamp, T. F. Edgar, and F. J. Doyle III, "Chapter 17 - Digital Sampling, Filtering, and Control," in in *Process Dynamics and Control*, Wiley, 2011.
[227] R. K. Pearson, *Discrete-time Dynamic Models*. New York, NY: Oxford University Press, 1999.
[228] D. S. Callaway and I. A. Hiskens, "Achieving Controllability of Electric Loads," *Proceedings of the IEEE*, vol. 99, no. 1, pp. 184–199, 2011.
[229] S. Koch, J. L. Mathieu, and D. S. Callaway, "Modeling and control of aggregated heterogeneous thermostatically controlled loads for ancillary services," in *Proceedings of the Power Systems Computation Conference*, 2011, pp. 1–7.
[230] M. M. Rahman, M. G. Rasul, and M. M. K. Khan, "Energy conservation measures in an institutional building in sub-tropical climate in Australia," *Applied Energy*, vol. 87, no. 10, pp. 2994–3004, Oct. 2010.
[231] Y. Huang, J. Niu, and T. Chung, "Study on performance of energy-efficient retrofitting measures on commercial building external walls in cooling-dominant cities," *Applied Energy*, vol. 103, pp. 97–108, Mar. 2013.
[232] A. L. S. Chan, "Effect of adjacent shading on the thermal performance of residential buildings in a subtropical region," *Applied Energy*, vol. 92, pp. 516–522, Apr. 2012.
[233] P. Palensky and D. Dietrich, "Demand Side Management: Demand Response, Intelligent Energy Systems, and Smart Loads," *IEEE Transactions on Industrial Informatics*, vol. 7, no. 3, pp. 381–388, 2011.

[234] S. Borenstein, M. Jaske, and A. Rosenfeld, “Dynamic Pricing, Advanced Metering, and Demand Response in Electricity Markets,” Center for the Study of Energy Markets, University of California Energy Institute, UC Berkeley, CSEM WP 105, Oct. 2002.
[235] D. P. Chassin and J. C. Fuller, “On the Equilibrium Dynamics of Demand Response in Thermostatic Loads,” in *2011 44th Hawaii International Conference on System Sciences (HICSS)*, 2011, pp. 1–6.
[236] D. P. Chassin, P. Du, and J. C. Fuller, “The potential and limits of residential demand response control strategies,” in *2011 IEEE Power and Energy Society General Meeting*, 2011, pp. 1–6.
[237] S. Katipamula and N. Lu, “Evaluation of residential HVAC control strategies for demand response programs,” in *ASHRAE transactions*, pp. 535–546.
[238] C. Bartusch, F. Wallin, M. Odlare, I. Vassileva, and L. Wester, “Introducing a demand-based electricity distribution tariff in the residential sector: Demand response and customer perception,” *Energy Policy*, vol. 39, no. 9, pp. 5008–5025, Sep. 2011.
[239] J. L. Bode, M. J. Sullivan, D. Berghman, and J. H. Eto, “Incorporating residential AC load control into ancillary service markets: Measurement and settlement,” *Energy Policy*, vol. 56, pp. 175–185, May 2013.
[240] W. Chung, “Review of building energy-use performance benchmarking methodologies,” *Applied Energy*, vol. 88, no. 5, pp. 1470–1479, May 2011.
[241] D. S. Callaway, “Tapping the energy storage potential in electric loads to deliver load following and regulation, with application to wind energy,” *Energ. Convers. Manage.*, vol. 50, no. 5, pp. 1389–1400, May 2009.
[242] S. Bashash and H. K. Fathy, “Modeling and Control of Aggregate Air Conditioning Loads for Robust Renewable Power Management,” *IEEE Transactions on Control Systems Technology*, vol. 21, no. 4, pp. 1318–1327, 2013.
[243] N. A. Sinitsyn, S. Kundu, and S. Backhaus, “Safe protocols for generating power pulses with heterogeneous populations of thermostatically controlled loads,” *Energy Conversion and Management*, vol. 67, pp. 297–308, Mar. 2013.
[244] N. Lu, “An Evaluation of the HVAC Load Potential for Providing Load Balancing Service,” *IEEE Transactions on Smart Grid*, vol. 3, no. 3, pp. 1263–1270, 2012.
[245] C.-Y. Chang, W. Zhang, J. Lian, and K. Kalsi, “Modeling and control of aggregated air conditioning loads under realistic conditions,” in *Innovative Smart Grid Technologies (ISGT), 2013 IEEE PES*, 2013, pp. 1–6.
[246] C. Perfumo, E. Kofman, J. H. Braslavsky, and J. K. Ward, “Load management: Model-based control of aggregate power for populations of thermostatically controlled loads,” *Energy Conversion and Management*, vol. 55, pp. 36–48, Mar. 2012.
[247] T. Hong, W.-K. Chang, and H.-W. Lin, “A fresh look at weather impact on peak electricity demand and energy use of buildings using 30-year actual weather data,” *Applied Energy*, vol. 111, pp. 333–350, Nov. 2013.

[248] J. D. Rhodes, C. R. Upshaw, C. B. Harris, C. M. Meehan, D. A. Walling, P. A. Navrátil, A. L. Beck, K. Nagasawa, R. L. Fares, W. J. Cole, H. Kumar, R. D. Duncan, C. L. Holcomb, T. F. Edgar, A. Kwasinski, and M. E. Webber, "Experimental and data collection methods for a large-scale smart grid deployment: Methods and first results," *Energy*, vol. 65, pp. 462–471, Feb. 2014.
[249] J. D. Rhodes, W. J. Cole, C. R. Upshaw, and M. E. Webber, "Clustering analysis of residential electricity demand profiles," *Energy Policy*, under review 2014.
[250] D. Feldman, G. Barbose, R. Margolis, R. Wiser, N. Darghouth, and A. Goodrich, "Photovoltaic (PV) Pricing Trends: Historical, Recent, and Near-Term Projections," National Renewable Energy Laboratory (NREL), Golden, CO, DOE/GO-102012-3839, 2012.
[251] R. Perez, T. Hoff, C. Herig, and J. Shah, "Maximizing PV peak shaving with solar load control: validation of a web-based economic evaluation tool," *Solar Energy*, vol. 74, pp. 409–415, Apr. 2003.
[252] K. R. Keeney and J. E. Braun, "Application of Building Precooling to Reduce Peak Cooling Requirements," *ASHRAE Transactions*, vol. 103, pp. 463–469, 1997.
[253] F. B. Morris, J. E. Braun, and S. J. Treado, "Experimental and simulated performance of optimal control of building thermal storage," *ASHRAE Transactions*, vol. 100, pp. 402–414, 1994.
[254] A. Rabl and L. K. Norford, "Peak Load Reduction by Preconditioning Buildings at Night," *Int. J. Energy Res.*, vol. 15, pp. 781–798, 1991.
[255] P. Xu and P. Haves, "Case study of demand shifting with thermal mass in two large commercial buildings," *ASHRAE Transactions*, vol. 112, pp. 875–888, 2005.
[256] J. Ma, S. J. Qin, and T. Salsbury, "Experimental study of economic model predictive control in building energy systems," in *American Control Conference (ACC), 2013*, 2013, pp. 3753–3758.
[257] J. B. Rawlings, D. Angeli, and C. N. Bates, "Fundamentals of economic model predictive control," in *2012 IEEE 51st Annual Conference on Decision and Control (CDC)*, 2012, pp. 3851–3861.
[258] R. Halvgaard, N. K. Poulsen, H. Madsen, J. B. Jorgensen, F. Marra, and D. E. M. Bondy, "Electric vehicle charge planning using economic model predictive control," in *Electric Vehicle Conference (IEVC), 2012 IEEE International*, 2012, pp. 1–6.
[259] K. Kapoor, K. Powell, W. Cole, J. Kim, and T. Edgar, "Improved large-scale process cooling operation through energy optimization," *Processes*, vol. 1, no. 3, pp. 312–329, Nov. 2013.
[260] B. P. Omell and D. J. Chmielewski, "IGCC power plant dispatch using infinite-horizon economic model predictive control," *Ind. Eng. Chem. Res.*, vol. 52, no. 9, pp. 3151–3164, Mar. 2013.
[261] City of Austin, "City of Austin residential rate schedules," 2013. [Online]. Available: http://www.austinenergy.com/about%20us/rates/pdfs/Residential/ResidentialAustin.pdf. [Accessed: 08-Jan-2014].

[262] G. R. Newsham and B. G. Bowker, “The effect of utility time-varying pricing and load control strategies on residential summer peak electricity use: A review,” *Energy Policy*, vol. 38, no. 7, pp. 3289–3296, Jul. 2010.
[263] We Energies, “Critical-Peak Pricing Program,” 2014. [Online]. Available: http://www.we-energies.com/residential/acctoptions/cpp.htm. [Accessed: 14-Jan-2014].
[264] Jingran Ma, S. J. Qin, Bo Li, and T. Salsbury, “Economic model predictive control for building energy systems,” in *Innovative Smart Grid Technologies (ISGT), 2011 IEEE PES*, 2011, pp. 1–6.
[265] G. P. Henze, C. Felsmann, and G. Knabe, “Evaluation of optimal control for active and passive building thermal storage,” *International Journal of Thermal Sciences*, vol. 43, no. 2, pp. 173–183, Feb. 2004.
[266] F. Oldewurtel, A. Parisio, C. N. Jones, D. Gyalistras, M. Gwerder, V. Stauch, B. Lehmann, and M. Morari, “Use of model predictive control and weather forecasts for energy efficient building climate control,” *Energy and Buildings*, vol. 45, pp. 15–27, Feb. 2012.
[267] R. Halvgaard, N. K. Poulsen, H. Madsen, and J. B. Jorgensen, “Economic model predictive control for building climate control in a smart grid,” in *Innovative Smart Grid Technologies (ISGT), 2012 IEEE PES*, 2012, pp. 1–6.
[268] R. E. Bohn, M. C. Caramanis, and F. C. Schweppe, “Optimal pricing in electrical networks over space and time,” *The RAND Journal of Economics*, vol. 15, no. 3, pp. 360–376, Oct. 1984.
[269] R. K. Ahuja and J. B. Orlin, “Inverse optimization,” *Operations Research*, vol. 49, no. 5, pp. 771–783, 2001.
[270] J. Currie and D. I. Wilson, “OPTI: Lowering the barrier between open source optimizers and the industrial MATLAB user,” in *Foundations of Computer-Aided Process Operations*, Savannah, Georgia, USA, 2012.
[271] P. Denholm and M. Hummon, “Simulating the Value of Concentrating Solar Power with Thermal Energy Storage in a Production Cost Model,” National Renewable Energy Laboratory, Golden, CO, TP-6A20-56731, 2012.
[272] P. Denholm, J. C. King, C. F. Kutcher, and P. P. H. Wilson, “Decarbonizing the electric sector: Combining renewable and nuclear energy using thermal storage,” *Energy Policy*, vol. 44, pp. 301–311, May 2012.
[273] U.S. Energy Information Administration, “Annual Energy Review 2011,” Sep. 2012.
[274] BCS, Incorporated, “Waste Heat Recovery: Technology and Opportunities in U.S. Industry,” Report for the U.S. Department of Energy, 2008.
[275] F. Maréchal, C. Weber, and D. Favrat, “Chapter 2: Multiobjective Design and Optimization of Urban Energy Systems,” in in *Process Systems Engineering*, M. C. Georgiadis, E. S. Kikkinides, and E. N. Pistikopoulos, Eds. Wiley-VCH Verlag GmbH & Co. KGaA, 2008, pp. 39–83.